

GENERAL STATEMENT OF RESEARCH ACHIEVEMENTS

Oxygen-17 NMR Studies of Molecules of Biological Interest

The ^{17}O isotope is one of the most difficult to observe by NMR spectroscopy due to extremely low absolute sensitivity compared to that of ^1H ($\approx 1.1 \times 10^{-5}$) and the breadth of the resonances. It is, however, of great interest to use a nucleus, such as oxygen, that is located at strategic molecular sites and is directly involved in inter- and intra- molecular interactions.

The objective of this research project was:

- (i) to introduce ^{17}O shieldings as a new method to investigate for the first time hydration phenomena and solvation differences of the amide oxygens of the cis/trans isomers of amides, the effects of a γ -turn intramolecular hydrogen bond and β -turn structures of model peptides and peptide hormones. (publications 10a, 13a, 16a, 18a, 19a, 20a, 22a, 23a, 24a, 25a, 26a, 27a, 33a, 35a, 36a, 37a). It was demonstrated that ^{17}O NMR shieldings are a promising tool for studying hydration phenomena and inter- and inter-molecular hydrogen bonding effects in amides, model peptides and peptide hormones due to the large shielding range ($\sim 100\text{ppm}$) and the large and specific effect of hydrogen bonding and long range dipole-dipole interactions.

This research project was initiated in the period 1981-1983 in collaboration with As. Professor J. Lauterwein, University of Lausanne, in the period 1984-1989 in collaboration with Prof. C. Sakarellos, University of Ioannina who was responsible for the synthesis of the isotope enriched ^{17}O compounds. Part of this research was the subject of two PhD students (Dr. C. Vakka and C. Tsanaktsidis) who completed their PhD thesis under my supervision (publications 22a, 23a, 24a, 25a, 34a).

- (ii) To introduce ^{17}O NMR shieldings as a novel tool to investigate dioxygen and carbonmonoxide binding to heme model compounds. After several unsuccessful attempts on the literature [C. Maricic et al., Nature 214, 462-466 (1967); C.S. Irving & a Lapidot, Nature 230, 224 (1971)] two signals at ~ 1750 and 2500ppm were observed for the FeO_2 linkage in which the electrons are totally paired (publications 9a, 11a, 17a, 21a, 31a, 32a). This research project was initiated in collaboration with the late Dr. M. Momenteau (Institute Cure, Section de Biologie, Orsay, France) who performed the synthesis of the model compounds.

Multinuclear NMR investigation of Heme Proteins and Synthetic Models

Heme models have been widely used to understand the bonding of small molecules such as dioxygen and carbon monoxide to hemoproteins. The objective of this research project was to apply new NMR methods for the structural investigation of heme proteins and superstructured synthetic model compounds in solution and in the solid state. Particular emphasis has been given to:

- (i) ^{13}C cross-polarization magic-angle-spinning (CP/MRS) NMR which was reported as a novel tool for investigating whether the iron-carbon-oxygen moiety is linear or bent (publications 11b, 12b,

13b, 14b). Furthermore ^{13}C shielding of the meso carbons of several carbon monoxide hexa coordinated super structured hemoprotein models were shown to be sensitive novel method for estimating porphyrin ruffling (publications 15b, 16b).

- (ii) ^{57}Fe NMR chemical shifts of super structured heme models which have been found to be extremely sensitive to atropisomerism and deformation (ruffling) of porphyrin geometry (publications 17b, 18b, 19b) and increased shielding by more than 800 ppm with increased ruffling was observed. Furthermore, the great variation of $\delta(^{57}\text{Fe})$ as a function of the average displacement of the meso carbo atom ($\sim 140 \text{ ppm} / 0.1\text{\AA}$) demonstrates that ^{57}Fe shielding can be used in structure refinement protocols.

This project was initiated in my research group in collaboration with Dr. G. Hawkes (QMN, England) for recording the ^{57}Fe NMR spectra and Dr. P.J. Barrie for recording CP MAS spectra due to lack of the appropriate NMR instrumentation in our University. A significant part of this research was the subject of a PhD student (Dr. C.G. Kalodimos) who completed his thesis under my supervision (publications 14b, 15b, 16b, 17b, 18b, 19b)

NMR and Computational Studies of Angiotensin II, Angiotensin Converting Enzyme (ACE) and ACE Inhibitors

Angiotensin II (AII), the main effector octapeptide hormone of the rennin-angiotensin system exerts a variety of actions via specific receptors designated AT_1 and AT_2 . AII has been extensively investigated in solution during the last 40 years with a variety of techniques. The results have been interpreted in terms of various models such as an α -helix, β -turn, cross- β -forms I, γ -turn, random coil side chain ring cluster etc. It is evident that several of the reported models are not consistent with each other and that there is no general consensus on the solution conformation of AII. The high resolution 3D NMR structures of the octapeptide hormone angiotensin II (AII) in aqueous solution have been obtained (publications 22b, 24b). These data were interpreted in terms of a biological ‘nucleus’ conformation of the hormone in solution which requires a limited number of structural rearrangements for receptor-antigen recognition and binding. The 3D structure of angiotensin-converting enzyme (tACE), ACE_N was modeled for the first time (publication 23b). Putative structural models have been generated for the interactions of several ACE inhibitors with both the ACE_C and the ACE_N domains which might provide an improved basis for structure-base rational design, domain selective inhibitors (publication 25b). Further, in order to shed light on the recognition process in the case of human angiotensin I converting enzyme (hACE) and its inhibitor captopril, we have established a novel combinatorial approach exploiting solution NMR, flexible docking calculations mutagenesis, and enzymatic studies (publication 26b).

This research project was the subject of a PhD student (Dr. A. Tzakos) who completed his thesis under my supervision.

NMR Analytical Applications of Complex Natural Extracts

Analysis of natural products is an attractive research area which is based on tedious and time-consuming techniques. Typically, their study includes fractionation of the complex mixture, separation and isolation of the individual components with liquid chromatography, and structure elucidation using various spectroscopic methods (UV, IR, MS and NMR). The traditional use of NMR spectroscopy in natural products analysis, therefore, is the determination of the structure of various components isolated from plant extracts. The objective of this research project was two-fold:

- (i) The development of NMR methodologies that can be successfully applied for the analysis of various constituents of complex plant extracts without any previous separation and isolation of the individual components. For the analysis of the extremely complex ^1H NMR spectra, particular emphasis has been given: (a) to two dimensional (2D) homonuclear NMR (COSY, TOCSY) and variable temperature heteronuclear ^1H - ^{13}C HSQC and HMBC NMR experiments (publications 1c, 2c, 9c, 13c) and to the use of the strongly deshielded OH protons in the region of 8-15 ppm (publications 3c, 4c, 5c, 11c). The use of the significantly enhanced resolution of the “forgotten” –OH NMR spectral region and the application of 2D ^1H - ^{13}C HMBC techniques (publication 15c) will open new avenues in structure analysis of complex natural extracts with phenol type –OH groups.
- (ii) The development, for the first time, of coupled on-line solid-phase extraction (SPE) in LC-NMR for peak storage after the liquid chromatography (LC) separation prior to NMR analysis (publications 6c and 7c) and application to several extracts from natural plants (publications 8c, 10c, 12c 14c).

This project was initiated in my research group in collaboration with two specialists in the field of Food Chemistry, Prof. D. Boskou and As. Prof. M. Tsimidou, Aristotle University of Thessaloniki, and was the subject of four PhD students (Dr. V. Exarchou, Dr. E. Tatsis, Dr. V. Kontogianni and Dr. V. Goulas) who completed their PhD thesis under my supervision. The only exception is publication 6c which describes the development, for the first time, of coupled HPLC-DAD-SPE-NMR and was mainly due to the efforts of my former PhD student Dr. V. Exarchou.

**THEMATIC CLASSIFICATION AND ANALYSIS OF PUBLICATIONS IN
INTERNATIONAL JOURNALS**

¹⁷O NMR SPECTROSCOPY

(in bold is indicated the principal author)

Development of Experimental Methods

- 1a. “Acquisition Times, Relaxation rates and Solvent and Temperature Effects as Sensitivity Parameters for Quadrupolar Nuclei”.
I.P. Gerothanassis, *Org. Magn. Reson.* 21, 719-722 (1983). University of East Anglia.
- 2a. Application of a Steady-State Pulse Sequence for Solvent Elimination in ¹⁷O NMR”.
J. Lauterwein* and I.P. Gerothanassis, *J. Magn. Reson.* 51, 153-156 (1983). University of Lausanne.
- 3a. “¹⁷O NMR Spectroscopy: Referencing in Diamagnetic and Paramagnetic Solutions”. University of Lausanne.
I.P. Gerothanassis and J. Lauterwein*, *Magn. Reson. Chem.* 24, 1034-1038 (1986).
- 4a. “Simple Reference Baseline Subtraction-90° Pulse Sequence for Acoustic Ringing Elimination in Pulsed Fourier Transform NMR Spectroscopy”. University of Ioannina.
I.P. Gerothanassis, *Magn. Reson. Chem.*, 24, 428-433 (1986).
- 5a. “Methods of Avoiding the Effects of Acoustic Ringing in Pulsed FT NMR Spectroscopy”.
I.P. Gerothanassis, *Progr. NMR Spectrosc.* 19, 267-329 (1987). University of Ioannina.
- 6a. “Effectiveness of Pulse Sequences for Suppression of Acoustic Ringing in FT NMR”
I.P. Gerothanassis*, *J. Magn. Reson.* 75, 361-363 (1987). University of Ioannina.

¹⁷O NMR Applications to Molecules of Biological Interest

- 7a. “A Study of the *cis/trans* Isomerism of *N*-acetyl-L-proline in Aqueous Solution by ¹⁷O N.M.R. Spectroscopy”.
J. Lauterwein*, I.P. Gerothanassis and R.N. Hunston, *J. Chem. Soc., Chem. Commun.*, 367-369 (1984). University of Lausanne.
- 8a. “A study of L-proline, Sarcosine, and the *cis-trans* Isomers of *N*-acetyl-L-proline and *N*-acetylsarcosine in Aqueous and Organic Solution by Oxygen-17 NMR”
R.N. Hunston, I.P. Gerothanassis, and J. Lauterwein*, *J. Am. Chem. Soc.*, 107, 2654-2661 (1985). University of Lausanne.
- 9a. “¹⁷O-NMR Spectroscopy as a Tool for Studying Synthetic Oxygen Carriers Related to Biological Systems: Application to a Synthetic Single-face Hindered Iron Porphyrin-dioxygen Complex in Solution”.
I.P. Gerothanassis* and M. Momenteau, *J. Am. Chem. Soc.* 109, 6944-6947 (1987). University

of Ioannina.

- 10a. “¹⁷O-NMR Studies of the Conformational and Dynamic Properties of Enkephalins in Aqueous and Organic Solutions Using Selectively Labeled Analogues”.
C. Sakarellos, **I.P. Gerothanassis**, N. Birlirakis, T. Karayannis, M. Sakarellos-Daitsiotis and M. Marraud, *Biopolymers* 28, 15-26 (1989). University of Ioannina.
- 11a. “Hydrogen-Bond Stabilization of Dioxygen, Conformation Excitation, and Autoxidation Mechanism in Hemoprotein Models as Revealed by ¹⁷O-NMR Spectroscopy”.
I.P. Gerothanassis*, M. Momenteau* and B. Loock, *J. Am. Chem. Soc.* 111, 7006-7012 (1989). University of Ioannina.
- 12a. “¹⁷O-NMR Spectroscopy as a Novel Tool of Investigating, β -turns in Model Peptides”.
N. Birlirakis, I.P. Gerothanassis, C. Sakarellos* and M. Marraud, *J. Chem. Soc., Chem. Commun.* 1122-1123 (1989). University of Ioannina.
- 13a. “¹⁷O- and ¹⁴N-nmr Studies of Leu-enkephalin and Enkephalin-related Fragments in Aqueous Solution”.
T. Karayannis, **I.P. Gerothanassis***, M. Sakarellos-Daitsiotis, C. Sakarellos and M. Marraud, *Biopolymers* 29, 423-439 (1990). University of Ioannina.
- 14a. “Does a 2 \leftarrow 5 β -turn Structure Exist in Enkephalins?: Study of a Fully Protected Leu-enkephalin in Organic Solution by ¹⁷O-NMR”.
E. Moret, I.P. Gerothanassis, R.N. Hunston and J. Lauterwein*, *FEBS Letters* 262, 173-175 (1990). University of Lausanne.
- 15a. “Oxygen-17 NMR Relaxation Times of the Protein Amino Acids in Aqueous Solution: Estimation of the Relative Hydration Numbers in the Cationic, Anionic, and Zwitterionic forms”.
J. Lauterwein*, I.P. Gerothanassis, R.N. Hunston, M. Schumacher, *J. Phys. Chem.* 95, 3804-3811 (1991). University of Lausanne.
- 16a. “¹⁷O-NMR and FT-IR Study of the Ionization State of Peptides in Aprotic Solvents. Application to Leu-enkephalin”.
I.P. Gerothanassis*, N. Birlirakis, T. Karayannis, V. Tsikaris, M. Sakarellos-Daitsiotis, C. Sakarellos, B. Vitoux and M. Marraud, *FEBS Letters* 298, 188-190 (1992). University of Ioannina.
- 17a. “Structural Differences of the Iron-Dioxygen Moiety of Haemoprotein Models with and without Axial Hindered Base as Revealed by ¹⁷O NMR and FTIR Spectroscopy in Solution”.
I.P. Gerothanassis*, B. Loock and M. Momenteau*, *J. Chem. Soc., Chem. Commun.* 598-600 (1992). University of Ioannina.
- 18a. “Hydration of Gly-2 and Gly-3 Peptide Oxygens of Leu-5-enkephalin in Aqueous Solution as Revealed by the Combined Use of ¹⁷O-NMR and Fourier- Transform Infrared Spectroscopy”.
I.P. Gerothanassis*, N. Birlirakis, T. Karayannis, M. Sakarellos-Daitsiotis, C. Sakarellos*, B. Vitoux and M. Marraud, *Eur. J. Biochem.* 210, 693-698 (1992). University of Ioannina.

- 19a. "Solvation State of the Tyr Side-chain in Peptides. An FT-IR and ^{17}O -NMR Approach".
I.P. Gerothanassis*, N. Birlirakis, C. Sakarellos* and M. Marraud, *J. Am. Chem. Soc.* 114, 9043-9047 (1992). University of Ioannina.
- 20a. "Multinuclear and Multidimensional NMR Methodology for Studying Individual Water Molecules Bound to Peptides and Proteins in Solution: Principles and Applications".
I.P. Gerothanassis, *Progr. NMR Spectrosc.* 26, 171-237 (1994). University of Ioannina.
- 21a. " ^{17}O NMR Studies of Hemoproteins and Synthetic Model Compounds in the Solution and Solid State".
I.P. Gerothanassis, *Progr. NMR Spectrosc.* 26, 239-292 (1994). University of Ioannina.
- 22a. " ^{17}O NMR Chemical Shifts as a Tool to Study Specific Hydration Sites of Amides and Peptides - Correlation with the IR Amide I Stretching Vibration".
I.P. Gerothanassis* and C. Vakka, *J. Org. Chem.* 59, 2341-2348 (1994). University of Ioannina.
- 23a. "Hydration of Cis and Trans N-Methylformamide as Revealed by the Use of ^{17}O NMR, Molecular Mechanics and Ab Initio Calculations".
I.P. Gerothanassis*, I.N. Demetropoulos* and C. Vakka, *Biopolymers*, 36, 415-428 (1995). University of Ioannina.
- 24a. " ^{17}O and ^1H - ^{15}N Heteronuclear Multiple Quantum Coherence (^1H - ^{15}N HMQC) NMR of Linear Amides: Evidence of an Out-of-Plane (Torsion Angle) Deformation of the Amide Bond and Pyramidicity at the Amide Nitrogen".
I.P. Gerothanassis*, A. Troganis and C. Vakka, *Tetrahedron*, 51, 9493-9500 (1995). University of Ioannina.
- 25a. " ^{17}O NMR Studies of the Solvation State of Cis/Trans Isomers of Amides and Model Protected Peptides".
I.P. Gerothanassis*, C. Vakka and A. Troganis, *J. Magn. Reson. B* 111, 220-229 (1996). University of Ioannina.
- 26a. " ^{17}O and ^{14}N NMR Studies of Quinoxaline-2(1H), 3(4H)-diones and N,N'-Substituted Oxamides: The First Experimental Evidence of Torsion Angle Deformation Resulting from an Unprecedented Through Six-bond Substituent Effect on the Diamide Group of Quinoxaline-2(1H),3(4H)-diones".
I.P. Gerothanassis*, J. Cobb, A. Kimbaris, J.A.S. Smith and G. Varvounis, *Tetrahedron Lett.* 37, 3191-3194 (1996). University of Ioannina.
- 27a. " ^{17}O NMR studies of Electronic and Steric Interactions of Substituted Quinoxaline-2(1H), 3(4H)-diones".
I.P. Gerothanassis* and G. Varvounis, *J. Heterocyclic Chem.* 33, 643-646 (1996). University of Ioannina.
- 28a. "NMR Shielding and the Periodic Table".

- I.P. Gerothanassis*** and C. G. Kalodimos, *J. Chem. Educ.* 73, 801-804 (1996). University of Ioannina.
- 29a. "Solvent Effects on Oxygen-17 Chemical Shifts in Amides. Quantitative Linear Solvation Shift Relationships".
E. Diez*, J. San Fabian, I.P. Gerothanassis, A.L. Esteban, J-L.M. Abboud, R.H. Contreras, D. G. De Kowalewski, *J. Magn. Reson.* 124, 8-19 (1997). University of Ioannina.
- 30a. "(2+4)-Cycloaddition with Singlet Oxygen. ¹⁷O-Investigation of the Reactivity of Furfuryl Alcohol Endoperoxide".
A. M. Braun*, H. Dahn, E. Gassmann, I. Gerothanassis, L. Jakob, J. Kateva, C.G. Martinez, E. Oliveros, *Photochem. Photobiol.* 70, 868-874 (1999). University of Ioannina.
- 31a. "Carbon-13 and Oxygen-17 Chemical Shifts, (¹⁶O/¹⁸O) Isotope Effects on ¹³C Chemical Shifts, and Vibrational Frequencies of Carbon Monoxide in Various Solvents and of the Fe-C-O Unit in Carbonmonoxy Heme Proteins and Synthetic Model Compounds".
C.G. Kalodimos, **I.P. Gerothanassis***, R. Pierattelli and B. Ancian, *Inorg. Chem.* 38, 4283-4293 (1999). University of Ioannina.
- 32a. "Multinuclear (¹³C, ¹⁷O, ⁵⁷Fe) NMR Studies of Carbonmonoxy Heme Proteins and Synthetic Model Compounds".
C.G. Kalodimos, **I.P. Gerothanassis***, R. Pierattelli and A. Troganis *J. Inorg. Biochem.* 79, 371-380 (2000). University of Ioannina.
- 33a. "The ¹⁷O-NMR Shielding Range and Shielding Time Scale and Detection of Discrete Hydrogen-Bonded Conformational States in Peptides".
I.P. Gerothanassis, *Biopolymers* 59, 125-130 (2001). University of Ioannina.
- 34a. "¹⁴N NMR Relaxation Times of Several Protein Amino Acids in Aqueous Solution-Comparison with ¹⁷O NMR Data and Estimation of the Relative Hydration Numbers in the Cationic and Zwitterionic Forms".
A.N. Troganis*, C. Tsanaktsidis, and I.P. Gerothanassis, *J. Magn. Reson.* 164, 294-303 (2003). University of Ioannina
- 35a. "On the Detection of Both Carbonyl and Hydroxyl Oxygens in Amino Acid Derivatives: a ¹⁷O NMR Reinvestigation".
V. Theodorou, A.N. Troganis and **I.P. Gerothanassis***, *Tetrahedron Lett.* 45, 2243-2245 (2004). University of Ioannina.
- 36a. "Oxygen - 17 NMR Spectroscopy: Basic Principles and Applications (Part I)"
I.P. Gerothanassis, *Progr. NMR Spectrosc.* 56, 95-197 (2010). University of Ioannina.
- 37a. "Oxygen - 17 NMR Spectroscopy: Basic Principles and Applications (Part II)"
I.P. Gerothanassis, *Progr. NMR Spectrosc.* 57, 1-110 (2010). University of Ioannina.

OXYGEN-17 NMR SPECTROSCOPY

(in bold is indicated the principal author)

Development of Experimental Methods of ^{17}O NMR Spectroscopy

Relationship between signal-to-noise ratio and T_2 and the line width of a ^{17}O resonance.

For the broad resonances from ^{17}O nuclei, $T_2^* = T_2$, therefore, a value of $T_{\text{acq}} = 4T_2$ will allow the recovery of more than 98% of the total signal intensity, therefore, if T_{acq} is chosen to be a constant multiple, x , of T_2 , then, [**I.P. Gerothanassis**, *Org. Magn. Reson.* 21, 719-722 (1983)]:

$$(S/N)_{\text{FID}} = x^{-1/2} M_0 T_2^{1/2} \bar{v}^{-1} [1 - \exp(-x)].$$

The S/N per FID, therefore, decreases with decreasing T_2 . However, sensitivity should be evaluated relative to the achievable S/N in a given period of time. The optimum number of repetitive scans per unit time is $(T_{\text{acq}})^{-1} = (xT_2)^{-1}$. The achievable S/N is proportional to the square root of the number of scans and, therefore, on a time basis the S/N is given by:

$$(S/N)_t = (xT_2)^{-1/2} (S/N)_{\text{FID}} = (1/x) M_0 \bar{v}^{-1} [1 - \exp(-x)].$$

Under optimized T_{acq} conditions, therefore, $(S/N)_t$ is independent of T_2 and hence of the resonance width. Fig. 1 shows the spectra of acetone, dissolved to the same volume concentration in a viscous and a non-viscous solvent using optimized T_{acq} values. The S/N is similar in the two cases.

When a long fixed $T_{\text{acq}} \gg \pi T_2$ is used rather than a shorter optimized one, then, the above equation is reduced to:

$$(S/N)_t \propto M_0 T_2 \quad (5)$$

and line narrowing will result in increased peak intensity.

Effects of low-viscosity solvents—Use of supercritical solvents. Dilution of a high-viscosity liquid with a low viscosity solvent will cause a net reduction in S/N by the ratio of the concentration of the molecule in the solvent to that in the neat liquid. A compensating advantage is, however, that the linewidth of the solute resonance will be reduced because of the lower viscosity of the solution [**I.P. Gerothanassis**, *Org. Magn. Reson.* 21, 719-722 (1983)]. In most cases, a moderate dilution (~40-20% v/v) of the neat liquid by the solvent achieves an optimum balance of the S/N against resolution.

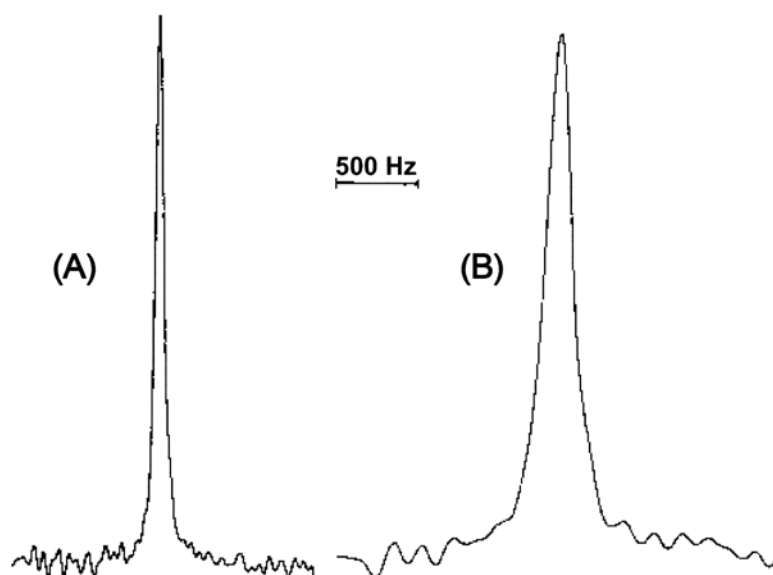


FIGURE 1. 27.12 MHz NMR spectra from ^{17}O in natural abundance of acetone in low- and high-viscosity solvents ((A) and (B) respectively). Temperature, 26°C; spectral width, 20 kHz; total experiment time 1h, with T_{acq} optimized in each case. (A) 0.5 ml acetone + 2 ml CHCl_3 (pre-acquisition delay, 40 μs); (B) 0.5 ml acetone + 2ml $(\text{CH}_2\text{OH})_2$ (pre-acquisition delay, 140 μs). [I.P. Gerotheranassis (*Org. Magn. Reson.* 21, 719-722 (1983) Wiley Heyden Ltd)].

When, the ^{17}O resonance of a large solute molecule exhibiting a short T_2 is measured simultaneously with that of a small-molecule solvent resonance with a long T_2 , then, the truncation of the solvent FID will cause oscillating side lobes in the frequency domain. Procedures involving mathematical manipulations of the FID in order to optimize the S/N for those resonances with T_2 close to a particular value, while diminishing the side lobes of sharper solvent resonances, have been described [J. Lauterwein*, I.P. Gerotheranassis, *J. Magn. Reson.* 51, 153-156 (1983)].

Effects of temperature. The integral of the NMR signal, for a given concentration of nuclei, is proportional to T^{-1} , where T is the absolute temperature. This results from the difference in population, Δn , between the upper and lower energy levels:

$$\Delta n \propto [1 - \exp(-h\nu/k_B T)] \approx h\nu/k_B T$$

where ν is the resonance frequency, k_B the Boltzmann constant and, in NMR, $h\nu \ll k_B T$.

Therefore, under conditions of optimized T_{acq} , raising the temperature of a solution will result in a decrease in S/N [I.P. Gerotheranassis, *Org. Magn. Reson.* 21, 719-722 (1983)]:

$$(S/N)_t \propto (x)^{-1} \frac{h\nu}{k_B T} [1 - \exp(-x)]$$

and in an improved resolution due to the reduced time for molecular tumbling at the higher temperature. Furthermore, in many cases the solubility or miscibility of a solute is increased with temperature resulting in a substantially improved S/N.

When a long fixed T_{acq} is used, then, a temperature-dependent line narrowing will also result in increased peak intensity. In S/N terms this may more than compensate for the inverse temperature dependence of the integrated resonance intensity:

$$(S/N)_t \propto \frac{h\nu}{k_B T} T_2 .$$

Referencing Techniques

For ^{17}O NMR, as is common with many heteronuclei, a variety of reference compounds and referencing procedures (both internal and external) have been suggested. Water and acetone, although readily available in ^{17}O enriched form, are not appropriate as internal standards because $\delta(^{17}\text{O})$ of both compounds are strongly dependent on the solvent. Nitromethane has been proposed as an internal standard for ^{17}O NMR of both diamagnetic and paramagnetic solutions [W.G. Klemperer*, *Angew. Chem. Int. Ed. Engl.* 17, 246-254 (1978); J.-P. Kintzinger, in: P. Diehl, E. Fluck, R. Kosfeld (Eds.), *NMR-Basic Principles and Progress*, Vol. 17, Springer, Berlin (1981) pp.1-64; E. Kupce*, R. Freeman, *J. Magn. Reson.* 98, 217-222 (1992)]. The conversion between the ^{17}O chemical shift of a 2M solution of nitromethane in water was reported to be:

$$\delta(\text{H}_2\text{O}) = \delta(\text{CH}_3\text{NO}_2) + 605 \text{ ppm} . \quad (9)$$

The ^{17}O resonance position of internal CH_3NO_2 , however, is strongly solvent dependent (-12 ppm on going from CCl_4 to H_2O) [I.P. Gerothanassis and J. Lauterwein*, *Magn. Reson. Chem.* 24, 1034-1038 (1986)].

For diamagnetic solutions an external standard in a combined use of two cylindrical cells has been recommended [I.P. Gerothanassis and J. Lauterwein*, *Magn. Reson. Chem.* 24, 1034-1038 (1986)]. The ppm scale is calibrated with the reference frequency at 0 ppm. Then, no reference is required in the subsequent sample spectra. Since the spectral reference is an absolute frequency, it depends only on the field strength as determined by the field potentiometer (when unlocked). Using this technique, doubly distilled water or 1,4-dioxane can be used as external reference. Both compounds have chemical shifts which are indistinguishable at 30-40°C and their magnetic susceptibility correction is small (<0.6 ppm) relative to common organic solvents. H_2O as an external standard, however, has the disadvantage that its chemical shift varies with temperature (-3 ppm between 27 and 90°C) due to breaking of intermolecular hydrogen bonds (the same implies for $^2\text{H}_2\text{O}$ in addition to an isotopic effect of -3 ppm. Eliel et al. [E.L. Eliel*, M.K. Pietrusiewicz, L.M. Jewell, W.R. Kenan Jr., *Tetrahedron Lett.* 38, 3649-3652 (1979)] reported a temperature variation of the ^{17}O chemical shifts (between 3 and 5 ppm when the temperature was increased from 24 to 90°C) of several dioxanes and dioxolanes, using water as external reference. Using 1,4-dioxane as external reference this temperature dependence was not confirmed. It was concluded [I.P. Gerothanassis and J. Lauterwein*, *Magn. Reson. Chem.* 24, 1034-

1038 (1986)] that the apparent temperature variation of the ^{17}O chemical shifts of the above compounds is due to the change in the shielding of the water reference. For the study of paramagnetic solutions the combined use of a cylindrical and a spherical cell was also proposed: the ^{17}O resonance of either the magnetically active solvent or a convenient compound added to the solution is recorded in both cells; the chemical shift difference between the two measurements is the bulk magnetic susceptibility shift.

Solvent (H_2O) Suppression

The increasing importance in ^{17}O NMR of biological systems has generated intense interest in the suppression of large solvent (H_2O) peaks. The most straightforward approach to solvent suppression is the use of ^{17}O depleted water (^{17}O content ca. $10^{-3}\%$) provided, of course, that rapid ^{17}O exchange does not occur between solvent and solute. Further suppression can be achieved by exploiting the special relaxation properties of the solvent, by post-experimental data processing and by selectively exciting the whole spectrum apart from the solvent [J. Lauterwein and **I.P. Gerothanassis**, *J. Magn. Reson.* 51, 153-156 (1983)]. By application of the steady-state pulse sequence comprising rapid pulsing with subsequent digital converter shift and zero-filling of the FID, a water suppression factor of 100 is readily achieved if the carrier frequency is positioned on the solvent (H_2O) signal. The short relaxation times of the ^{17}O nucleus allow the technique of rapid pulsing to be used, thus giving the most favourable signal-to-noise ratio since a large number of transients (and less noise per acquisition) can be accumulated per unit time.

Acoustic Ringing

Observation of very broad resonances in ^{17}O NMR is a serious problem due to baseline distortions. The most severe origin of baseline artifacts is the transient response of the NMR probe, often referred to as "acoustic ringing", caused by the generation of ultrasonic waves from the action of the rf pulse. Many efforts have been made to alleviate the distortions using new probe technology, computer, and multipulse methodology which are critically summarized in a relevant review article [I.P. Gerothanassis, *Progr. NMR Spectrosc.* 19, 267-329 (1987)]. The following aspects have been discussed in details:

- (1) The electromagnetic generation of acoustic waves, the r.f., B_{1m} and static, B_0 , field dependence of the distortion, the dependence of the amplitude of the acoustic distortion upon the probe wall material, on the separation of the r.f. coil from the probe wall, the resonance frequency, pulse duration and pulse carrier frequency and temperature dependence effects of the distortion.
- (2) Technical aspects of probe construction such as the choice of probe materials, shielding the probe walls from the r.f. field and damping the acoustic waves, probe geometrical and coil physical state and geometrical considerations.
- (3) Background subtractions of the distortion with the use of physical removal of the sample from the probe, off-resonance experiments, saturation of the NMR signal with the use of a 90° steady-state pulse sequences and a saturating comb sequence
- (4) Multi-pulse sequences such as the $(90^\circ-t-90^\circ\text{-FID}^{(-)}) - (90^\circ\text{-FID}^{(+)})$ pulse sequence and a reference – baseline –subtraction -90° pulse sequence.
- (5) Mathematical manipulations in the time domain such as time shifting (initial zero filling) Fourier transform, window-apodization functions, positive exponential function normalized to zero, inverted exponential and inverted Gaussian functions, a trapezoidal function, a sinebell function, a convolution difference, Gaussian-exponential transformation and retrieval of spectral parameters from time domain data using a linear least-squares procedure.
- (6) Mathematical manipulations of the frequency domain spectrum including, time delay Fourier transform, the case of a single resonance or a two resonance spectrum, the case of multi line spectrum: linear phase correction procedures, the case of a non Lorentzian lineshape, absolute and absolute square value presentation of FTNMR spectra, deconvolution in the frequency domain spectrum, baseline-recognition and baseline-flattering algorithms.
- (7) Mathematical manipulations applied to both time domain and frequency domain spectra such as a reconstruction procedure of the FID dead-time segment and maximum entropy methods (MEM).
- (8) Multipulse sequences including echo techniques, spin-echo Fourier transform techniques and their variants, the quadrupolar or solid echo and its variants, pulse sequences based on the linear properties of the distortions, alternating or cyclically ordered pulse sequences, the $(90^\circ-$

$\text{FID}^{(+)}_3$ - (270° - $\text{FID}^{(-)}$) pulse sequence and its variants, reversal of the spin temperature in cross-polarization NMR, a spin locking pulse sequence, a three pulse sequence and its variants, hybrid sequences, phase alternation in the quadrupolar echo, and various versions of an extended spin-echo sequence

(9) Comparison of the various multipulse sequences.

(10) Instrumental requirements.

From the examples presented in this review it is clear that optimization of probe construction and/or multipulse sequences are the best approaches to overcoming acoustic ringing effects. Multipulse sequences have the additional advantage that they are readily applicable in a routine way and they do not require knowledge of probe design. The aesthetic appearance of the spectra can be improved further by the supplementary application of the data manipulation techniques. It is clear that in many cases, broad resonances can now be detected with confidence. Although any hypothesis on the maximum linewidth detectable inevitably contains several quantifying conditions, such as spectrometer specifications, nucleus and sample properties (as well as the investigator's intuition), a conservative estimate of 5-20 kHz seems to be assured for several nuclei. These linewidth limits certainly cover a very useful range of chemical applications, but several biochemical, biological and solid state applications give rise to even broader lines. Therefore, four areas where further research could be profitable were discussed.

(1) Investigation of the coil effects; of the differences between theory and experiment concerning the intensity and frequency distribution properties of the acoustic ringing, pulse carrier frequency and pulse duration effects; of the causes of deviation of the acoustic waves from ideal linearity and whether there exist other types of wave emission.

(2) Improvement of the data manipulation techniques.

(3) Development of commercially available probe systems which handle very efficiently a given pulse power, thereby offering sufficiently short pulse lengths.

(4) Development of other methods of spin excitation especially those of conventional CW, non adiabatic superfast passage (NASP) CW, and correlation spectroscopy techniques.

As previously emphasized multipulse sequences have the advantage that they can be applied in a routine way and they do not require modification of probe design (Figs. 2 and 3). For experiments in solution, the three-pulse sequence:

$$90^\circ - \Delta t - \text{FID}^{(+)} - 180^\circ - \tau - 90^\circ - \Delta t - \text{FID}^{(-)} \quad [1]$$

where (\pm) denotes addition or subtraction of the data, and its variant:

$$90^\circ_x - \Delta t - \text{FID}^{(+)} - 180^\circ_{\pm x} - \tau - 90^\circ_x - \Delta t - \text{FID}^{(-)} \quad [2]$$

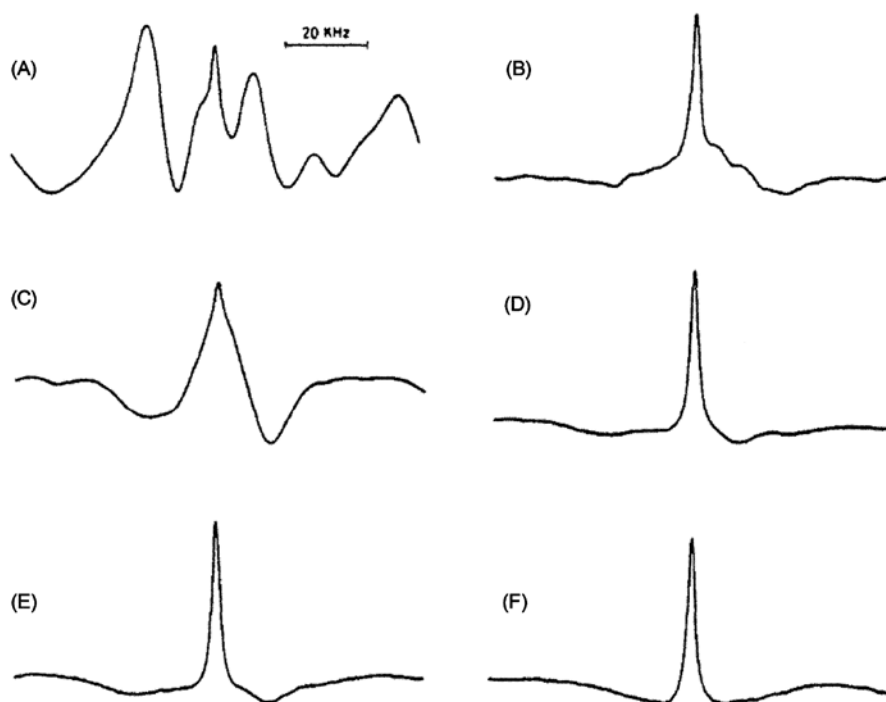


FIGURE 2. 48.82 MHz ^{17}O NMR spectra of 0.05M solution of t-Boc-Gly ^{17}OH (10 at. % enrichment in ^{17}O) in CHCl_3 at 24°C. Acquisition parameters: SW=100 kHz; $T_{\text{acq}}=1.3$ ms (256 points); NS=120,000. Carrier frequency near on-resonance. Processing parameters: exponential multiplication of the FID by a line broadening (LB) factor of 1 kHz. (A) Simple 90° pulse train sequence, preacquisition delay time $\Delta t=3$ μs , pulse repetition time $T_p=5$ ms. (B) The same conditions as in (A) but $\Delta t=100$ μs . (C)-(E) Three pulse sequence, $\tau=2$ μs , $\Delta t=3$ μs ; (C) without phase cycling [1]; (D) and (E) with phase cycling according to pulse sequences [2] and [3], respectively. (F) Extended spin-echo sequence [4]: $\tau=3$ μs , $\tau_2 < 2\mu\text{s}$. In (C)-(F) T_d was chosen as its minimum value (conditioned by the Bruker pulse programmer/software structure): $T_d=20$ ms. [I.P. Gerothanassis, J. Lauterwein, *J. Magn. Reson.* 66, 32 (1986); I.P. Gerothanassis, *Progr. NMR Spectrosc.* 19, 267-329 (1987)].

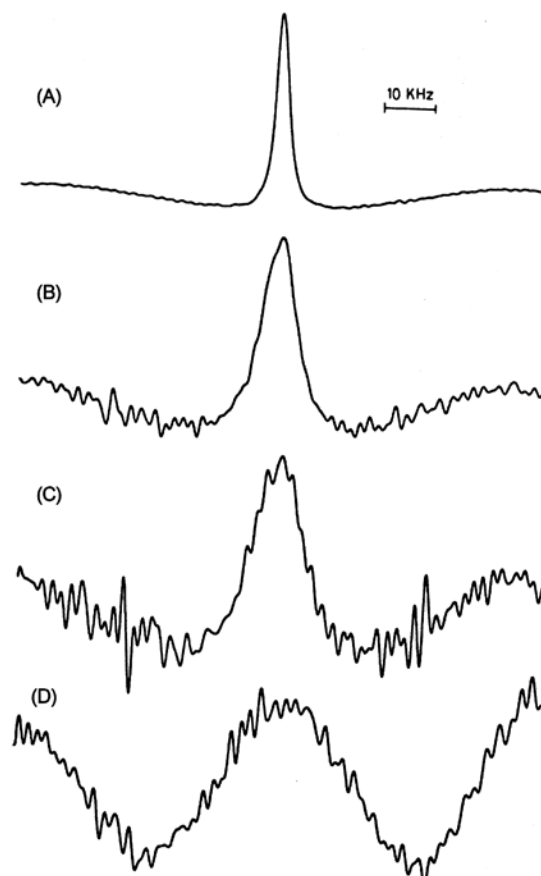


FIGURE 3. 48.82 MHz ^{17}O NMR spectra of glycerol, at natural abundance, and applying the extended spin-echo pulse sequence [4]. Experimental conditions and data acquisition parameters: carrier frequency on the absorption resonance (quadrature phase detection), 10 mm o.d. sample tube, SW=10 kHz, $T_{\text{acq}}=600 \mu\text{s}$, $\tau=3 \mu\text{s}$, $\tau_1 < 2 \mu\text{s}$, $T_d=20 \text{ ms}$, $\text{NS}=2 \times 10^6$, zero-filling to 16k. (A) $T=59^\circ\text{C}$; (B) $T=41^\circ\text{C}$; (C) $T=33^\circ\text{C}$, (D) $T=24^\circ\text{C}$. [I.P. Gerothanassis, J. Lauterwein, *J. Magn. Reson.* 66, 32 (1986); I.P. Gerothanassis, *Progr. NMR Spectrosc.* 19, 267-329 (1987)]

A reference baseline subtraction pulse sequence, which makes use only of 90° pulses with the same phase and does not suffer from the above disadvantages, has been suggested [I.P. Gerothanassis, *Magn. Reson. Chem.* 24, 428-433 (1986)]. The efficiency of the pulse sequence:

$$90_x^\circ - \Delta t_1 - \text{FID}^{(+)} - T_d \quad 90_x^\circ - (\tau + \tau_p + \Delta t_1) - \text{FID}^{(+)} - T_d \quad [3]$$

$$90_x^\circ - \tau - 90_x^\circ - \Delta t_1 - \text{FID}^{(-)} - T_d$$

for recording resonances of low-frequency nuclei having extremely fast relaxation rates, the achievable sensitivity and the off-resonance were discussed in detail. The ^{17}O NMR spectrum of glycerol at 30°C was successfully recorded with a line width at half-height of $14.8 \pm 0.8 \text{ kHz}$ ($T_2 \approx 21 \mu\text{s}$) (Figure 4). It should also be emphasized that previous attempts to record the ^{17}O NMR spectra of glycerol in the

temperature range 35-24°C using the extended spin-echo pulse sequence, and under identical instrumental conditions, have failed or have given inconsistent results.

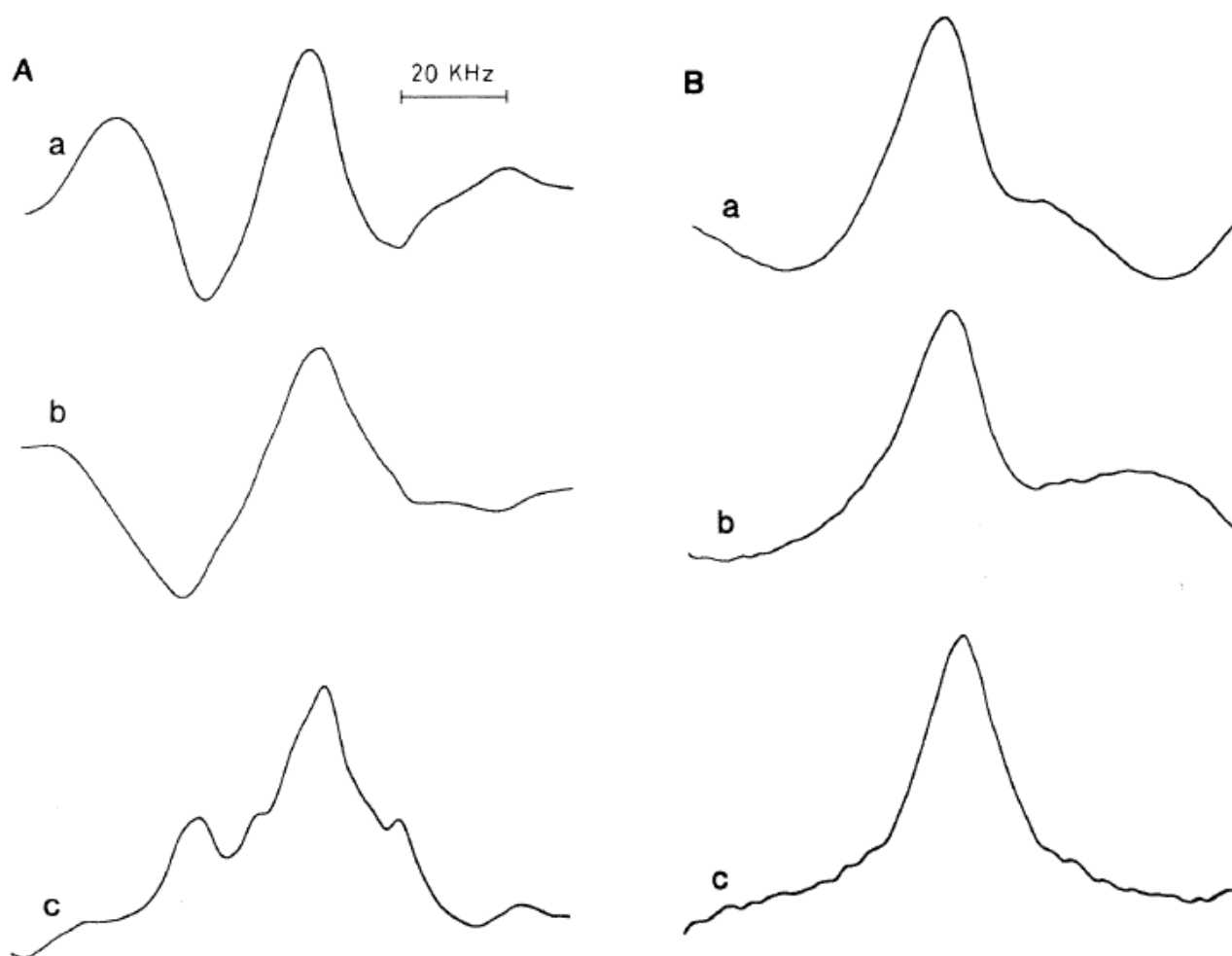


FIGURE 4. ^{17}O NMR spectra of pure glycerol at natural abundance using a Brüker WH-360 MHz spectrometer $T=30^\circ\text{C}$ and $\text{NS}=2 \times 10^6$. (A) Normal 90°C pulse train sequence: (a) preacquisition delay $\Delta t=0.3 \mu\text{s}$; (b) and (c) the same time domain data block as in (a) but shifted to the left by one complex pair of points ($\Delta t=5 \mu\text{s}$) and two complex pairs of points ($\Delta t=10 \mu\text{s}$), respectively. (B) Reference baseline subtraction- 90° pulse sequence [3]: (a) $\tau = \Delta t_1 = 0.3 \mu\text{s}$, $\tau_p = 30 \mu\text{s}$; (b) and (c) the same time domain data block as in (a) but shifted to the left by one complex pair of points ($\Delta t = 5 \mu\text{s}$) and two complex pairs of points ($\Delta t = 10 \mu\text{s}$), respectively. **I.P. Gerothanassis***, *Magn. Reson. Chem.* 24, 428-493 (1986).

Goc and Fiat [*J. Magn. Reson.* 70, 295 (1986)] published experimental results on a simple pulse sequence

$$270^\circ - T_{\text{acq}}^{(-)} - T_d - 90^\circ - T_{\text{acq}}^{(+)} - T_d \quad [4]$$

which does not involve phase cycling (T_d is the relaxation delay and (\pm) denotes computer treatment of the data). They concluded that this pulse sequence results in a significant alleviation of baseline distortions similar to that achieved by the use of the variants of the three pulse sequence and the extended spin-echo pulse sequence. **Gerothanassis** [*J. Magn. Reson.* 75, 361-363 (1987)] criticized the

above conclusion and suggested that the pulse sequence [4] does not effectively eliminate acoustic ringing since the distortion resulting from the 90° pulse is not identical to that resulting for the 270° pulse. A radio frequency pulse of carrier frequency ν_0 and finite duration t_p has frequency components whose power spectrum $P(\nu)$ is given by:

$$P(\nu) \propto \left\{ \frac{\sin [\pi t_p (\nu_0 - \nu)]}{(\nu_0 - \nu)} \right\}^2 \quad [1]$$

where $P(\nu_0)$ is the central maximum, $\nu = \nu_0 \pm \kappa'/2t_p$ ($\kappa' = 3, 5, 7, \dots$) are the subsidiary maxima, with amplitude proportional to $(\nu_0 - \nu)^{-2}$, and $\nu = \nu_0 \pm \kappa''/t_p$ ($\kappa'' = 1, 2, 3, \dots$) are the subsidiary minima (zeros). It is evident that a given acoustic distortion of central frequency $\nu_\kappa \neq \nu_0$ will be convoluted by the profile of Eq. [1]. The acoustic components, therefore, will exhibit a strong dependence on the pulse length. It was similarly concluded that the analogous pulse sequence [C. Brevard, in "The Multinuclear Approach to NMR Spectroscopy", J. B. Lambert and F.G. Riddell, Eds., Ch.1, Reidel, Dordrecht, 1983]

$$270^\circ - T_{\text{acq}}^{(-)} - T_d - [90^\circ - T_{\text{acq}}^{(+)}]_3 - T_d \quad [5]$$

also has limited success in eliminating acoustic distortions due, in part, to the nonlinear character of Eq. [1].

Temperature Dependence of ^{17}O Shieldings

^{17}O shieldings of several oxygen functional groups which are very sensitive to both intra- and intermolecular hydrogen bonding interactions. Thus, temperature dependence coefficients (in ppb/K) of ^{17}O NMR chemical shifts of amides and peptides [N. Birlirakis, **I.P. Gerotheranassis**, C. Sakarellos, M. Marraud, Unpublished results; **I.P. Gerotheranassis**, *Progr. NMR Spectrosc.* 56, 95-197 (2010)] were found to be an order of magnitude larger than those observed for other nuclei, such as the amide protons (Fig. 5). It remains to be investigated whether or not the large $\Delta\delta(^{17}\text{O})/\Delta T$ temperature coefficient will be used widely in conformational studies of peptides and particularly in the identification of intramolecular hydrogen bonds as $\Delta\delta(\text{N}^1\text{H})/\Delta T$.

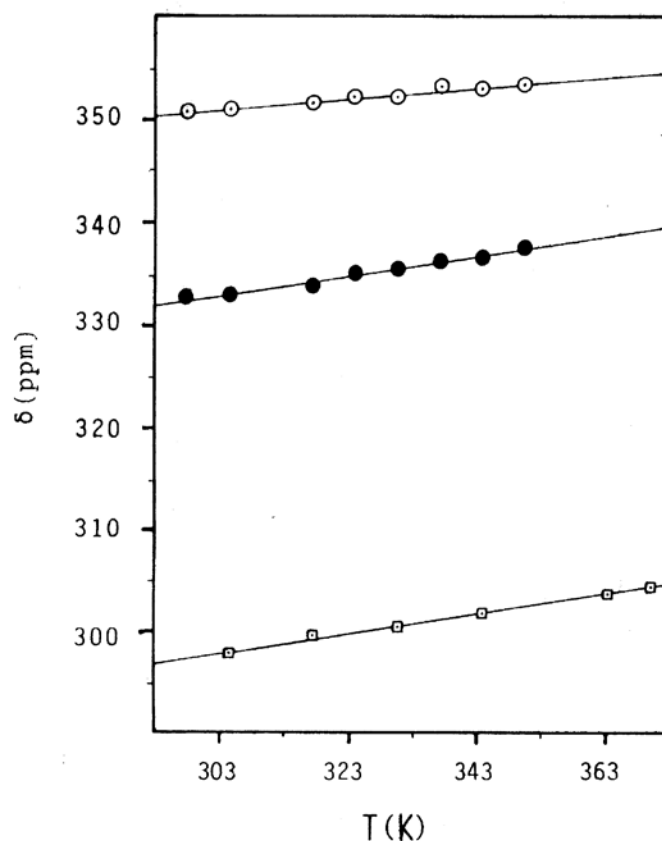


FIGURE 5. Temperature dependence of the amide ^{17}O chemical shifts of $[^{17}\text{O}]\text{Ac-L-Pro-D-Ala-NHMe}$ in CH_3CN solution: cis(○) and trans(●); in aqueous solution (□) [N. Birlirakis, **I.P. Gerothanassis**, C. Sakarellos, M. Marraud, unpublished results; **I.P. Gerothanassis**, *Progr. NMR Spectrosc.* 56, 95-197 (2010)].

^{17}O Shieldings in Chemical Education

NMR shieldings depend upon the structure of the compound investigated, therefore, shielding values are used as the starting point to discuss NMR spectra in the classroom. In most cases, however, these data are interpreted by applying the rule "the higher the electron density around an atom, the more it is shielded". This rule, which is based on the diamagnetic shielding term σ^d , has been particularly valuable in ^1H NMR and for restricted classes of compounds. But very often it turns out to be inadequate for heteronuclei, such as ^{17}O .

Gerothanassis* and Kalodimos [*J. Chem. Educ.* 73, 801-804 (1996)] investigated periodic, structurally significant properties that can be correlated to the nuclear shieldings or alternatively to investigate whether the chemical shift can be used to identify the periodic disposition of valence electrons. ^1H shieldings have a much smaller range (ca.20 ppm with a few exceptions) than other nuclei (eg. ≥ 2500 ppm for ^{17}O). This is because the total number of electrons in the vicinity of ^1H is smaller than for other nuclei, e.g. ^{17}O , so the magnitude of σ is smaller and consequently changes in σ from one molecule to another are also small. Further, the lowest excitation energy involved in σ^p for ^1H is of the

type $1s \rightarrow 2p$ (which implies a large value of ΔE and a small lower-state LCAO p-orbital coefficient), whereas for ^{17}O there are lower-lying orbitals and the ground-state bonding orbital involves p-electrons. Thus, $^{14,15}\text{N}$, ^{17}O and ^{19}F nuclei have larger ranges than ^{11}B and ^{13}C and that a parallel situation occurs amongst the third row elements. These shielding ranges reflect the presence of non-bonding electrons on N, O and F. In general, these electrons give rise to low energy $n \rightarrow \pi^*$ transitions and thus to large values of $\sigma^p(\text{local})$ which cause nuclear deshielding. If the lone pairs are involved in bonding, then, this contribution to $\sigma^p(\text{local})$ is removed and the nuclear shielding increases. This effect is well demonstrated in ^{17}O shielding variations.

Oxygen-17 NMR studies of molecules of biological interest

(in bold is indicated the principal author)

1. Dynamic and Molecular Reorientation Studies

The ^{17}O [J. Lauterwein*, I.P. Gerothanassis, R.N. Hunston, M. Schumacher, *J. Phys. Chem.* 95, 3804-3811 (1991); A.N. Troganis*, C. Tsanaktsidis, I.P. Gerothanassis, *J. Magn. Reson.* 164, 294-303 (2003)] and ^{14}N [A.N. Troganis*, C. Tsanaktsidis, I.P. Gerothanassis, *J. Magn. Reson.* 164, 294-303 (2003)] NMR line widths of several protein amino acids were measured in aqueous solution to investigate the effect of molecular weight on the line widths. The ^{14}N and ^{17}O line widths, under composite proton decoupling, increase with the bulk of the amino acid, and increase at low pH. The experimental ^{14}N and ^{17}O NMR data were statistically treated by the use of two models: (i) an isotropic molecular reorientation of a rigid sphere, and (ii) a stochastic diffusion of the amino and carboxyl groups comprising contributions from internal (τ_{int}) and overall (τ_{mol}) motions.

Assuming a single correlation time from overall molecular reorientation (τ_{mol}), then:

$$\Delta\nu_{1/2} = \alpha_0 + \alpha_1 \text{ MW},$$

where MW is the molecular weight, α_1 is the contribution to the linewidth of the quadrupolar coupling constant, density and temperature, and α_0 is the solvent viscosity independent contributions to the linewidth due to the primary hydration sphere of the amino acids. The linear correlation between $\Delta\nu_{1/2}$ and MW at pH 6 for both ^{14}N and ^{17}O nuclei (Fig. 1) is in agreement with the hydrodynamic model. The values, therefore, of χ for the nitrogen and oxygen nuclei in the amino acids change little from one compound to another. Furthermore, the $\chi(^{17}\text{O})$ of the amino acid is independent of both the ionization and the degree of hydration of the carboxyl group. The increase in the ^{17}O linewidths at acidic pH ($\sim 100 \pm 31$ Hz), relative to those at neutral pH, was interpreted by a change in the rotational correlation time of the amino acids, which implies that the cationic form of the amino acids is more hydrated by an average of 1.3-2.5 molecules of water than the zwitterionic form.

In the case of internal rotation, the effective correlation time, τ_c , is a superposition of contributions from the internal rotation and the overall molecular motion. Assuming stochastic diffusion of the amino and carboxyl groups, τ_c for ^{14}N or ^{17}O is given by [D.E. Woessner, *J. Chem. Phys.* 42, 1855-1859 (1965)]:

$$\Delta\nu_{1/2} = \alpha_0 + \alpha_1 \text{ MW} + \frac{\alpha_2}{\text{MW} + \alpha_3},$$

where α_0 - α_3 are constants.

The minimization of the above equation on the basis of the ^{17}O experimental data, gave the mean difference of 35.8 ± 17.3 in MW between pH 0.5 and 6.0 for three different $\Delta\nu_{1/2}$ values: 250, 350 (Fig. 1(B)) and 500 Hz. This was interpreted by an excess of 1-3 water molecules at pH = 0.5.

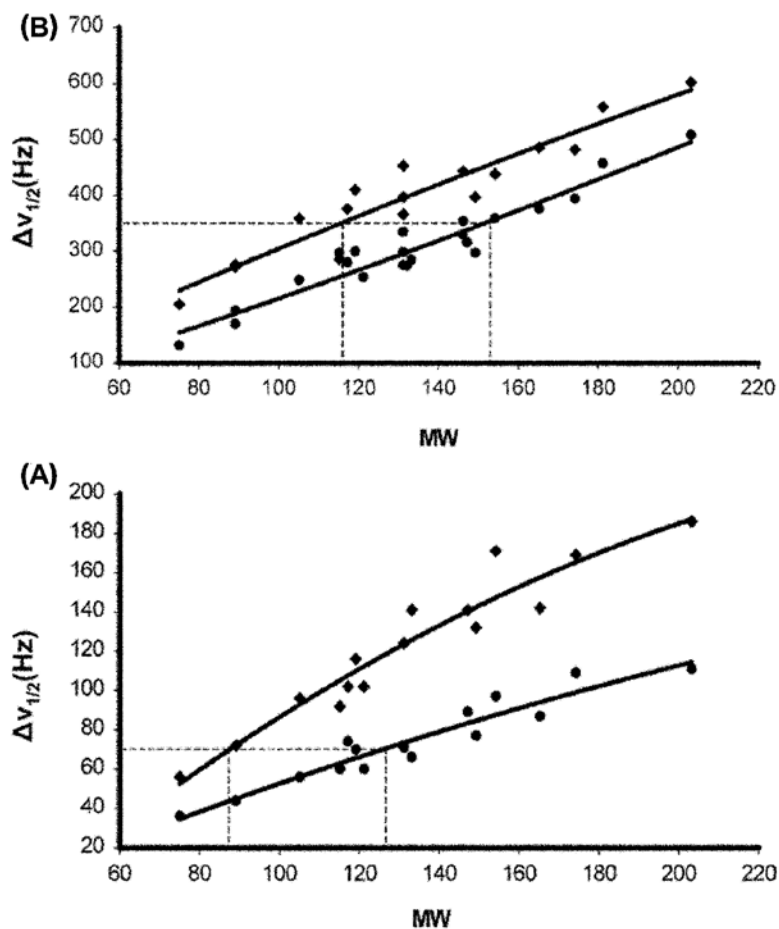


FIGURE 1. Plot of the ^{14}N (28.9 MHz) (A) and ^{17}O (48.8 MHz) (B) linewidths, $\Delta v_{1/2}$, of the protein amino acids versus their molecular weights, MW: (\blacklozenge) pH 0.5; (\bullet) pH 6.0. All lines correspond to a nonlinear least squares fit of the experimental points according to Eqn. (134). Dotted lines indicate the difference in MW for the same $\Delta v_{1/2}$ values. [A.N. Troganis*, C. Tsanaktsidis, I.P. Gerotheranassis, *J. Magn. Reson.* 164, 294-303 (2003), Elsevier Inc.]

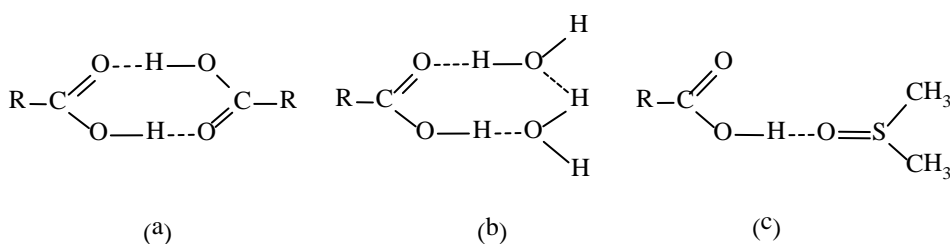
The difference in the ^{14}N linewidths at the two ionization states is dependent upon the MW and the intercept of the plot of the linewidths versus MW is, statistically, equal to zero. Differences, therefore, in $\Delta v_{1/2}$ should be attributed to differences in the correlation times and to a decrease in the $\chi(^{14}\text{N})$ on deprotonation of the carboxyl group. In the case of the linear model, the influence of variations of values of the $\chi(^{14}\text{N})$ to the linewidth, $\Delta v_{1/2}$, is less for small molecular weights. Therefore, for $\Delta v_{1/2} = 70$ Hz (Fig. 1(A)), the difference in MW will be a good approximation of the difference in hydration in the two states. The calculated value was found to be 45.2 ± 7.4 , which corresponds to an excess of 2-3 water molecules in the cationic form compared to that in the zwitterionic form, in reasonable agreement with the ^{17}O NMR data.

Activation energies, E_a , for rotational processes were determined [C. Sakarellos, **I.P. Gerotheranassis**, N. Birlirakis, T. Karayannis, M. Sakarellos-Daitsiotis, M. Marraud, *Biopolymers* 28, 15-26 (1989)] from typical plots of $\ln(1/T_1)$ vs $1/T$. The E_a values for [^{17}O -Gly², Leu⁵]- and [^{17}O -Gly³,

Leu⁵]-enkephalins were found to be very similar at both pH~1.9 and 5.6. This was interpreted with the hypothesis that both Gly² and Gly³ sites are motionally equivalent and that specific 2 ← 5 intramolecular β-turn structure should be excluded, in agreement with the chemical shift data. E_a values were found to be highly dependent on concentration due to significant aggregation which persists at C=10 mM presumably due to strong intermolecular head-to-tail interactions.

2. Proton and Oxygen Exchange

Tsikaris et al. [V. Tsikaris*, V. Moussis, M. Sakarellos-Daitsiotis, C. Sakarellos, *Tetrahedron Lett.* 41, 8651-8654 (2000)] observed two resonances at 340.3 and 175 ppm for the carboxylic oxygens of the labelled amino acid Boc-[¹⁷O]Tyr(2,6-diClBzl)-OH (Boc=tert-butyloxycarbonyl; 2,6-diClBzl=2,6-dichlorobenzoyl in DMSO-d₆ solution. This was attributed to a strong intramolecular hydrogen bond interaction between the carboxy group (COOH) and the carbonyl part (C=O) of the Boc group, stabilizing a γ-turn structure, and to the effect of DMSO viscosity, which reduce the intramolecular conformational exchange rate. Gerothanassis et al. [V. Theodorou, A.N. Troganis and **I.P. Gerothanassis***, *Tetrahedron Lett.* 45, 2243-2245 (2004)] strongly criticized the conclusions of Tsikaris et al and provided a coherent comment on the observation of both carbonyl and hydroxyl oxygens in amino acid derivatives which was attributed to the effects of proton transfer. In order to further support their hypothesis, Gerothanassis et al. performed further experiments with Ac-[¹⁷O]Pro-OH, which is a model of γ-turn structures, Ac-[¹⁷O]Pro-OMe, Boc-[¹⁷O]Tyr(2,6-diClBzl)-OMe and [¹⁷O]PhCOOH. Two resonances at 320 and 180 ppm were observed for the two oxygens (C=O, OH) of Ac-[¹⁷O]Pro-OH in DMSO-d₆ (Fig. 2(A)). It was suggested that DMSO behaves as a strong hydrogen bond acceptor with the COOH group of Ac-[¹⁷O]Pro-OH. As the concentration of the DMSO is increased, the cyclic dimer of the carboxylic acid is suppressed effectively, in favour of the complex with solvent molecules which reduces the intermolecular proton transfer, resulting in a clear differentiation of the two oxygens.



The chemical shifts of the two resonances are in good agreement with those observed for the two oxygens (C=O, -OCH₃) of the two methyl esters Ac-[¹⁷O]Pro-OMe (335 and 130 ppm) and Boc-[¹⁷O]Tyr-(2,6-diClBzl)-OMe (342 and 135 ppm) in CDCl₃ (40 °C). In contrast, the ¹⁷O NMR of Ac-[¹⁷O]Pro-OH in CDCl₃ indicates only one resonance at 255 ppm due to the formation of cyclic dimers or linear polymeric forms, despite the presence of a major amount of γ-turn structure.

The ^{17}O NMR spectrum of [^{17}O] benzoic acid, has two broad resonances for the two oxygens of the carboxyl in DMSO- d_6 at 40°C (Fig. 2(B)). Since this carboxylic acid cannot form a γ -turn structure, the presence of two resonances must be attributed to the formation of the PhCOOH·DMSO complex, with disruption of the cyclic dimers. Meschede et al. [L. Me Schede and H. H. Limbach, *J. Phys. Chem.* 95, 10267 (1991)] demonstrated that the pseudo-first order proton exchange rate constant k_{obs} observed by NMR (in the slow exchange regime) is given by $k_{\text{obs}} = K_2 k C$, where K_2 is the dimerization constant, C the concentration of the acid, and k the true exchange rate in the dimer. Indeed, increasing the concentration from 30 mM (Fig. 2(B)) to 100 mM (Fig. 2(C)) results in an increased k_{obs} and an averaged single resonance absorption at 250 ppm.

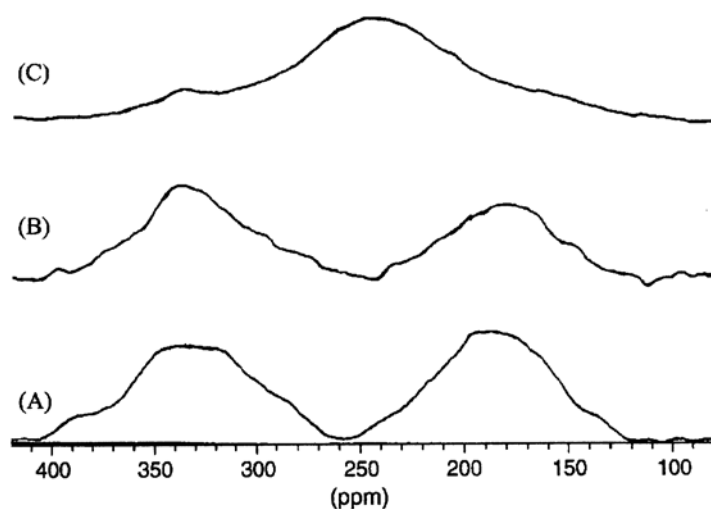


FIGURE 2. ^{17}O NMR spectra at 54.4 MHz of Ac- ^{17}O ProOH ($C=40$ mM) (A), ^{17}O PhCOOH ($C=30$ mM) (B), and ^{17}O PhCOOH ($C=100$ mM) (C) in DMSO- d_6 , containing 0.4M of water, at 40°C. 800000 scans were accumulated with a repetition rate of 20 s^{-1} and an exponential line broadening of 200 Hz. [V. Theodorou, A.N. Troganis, **I.P. Gerotheranassis***, *Tetrahedron Lett.* 45, 2243-2245 (2004)].

The detection, therefore, of both carbonyl and hydroxyl oxygens in ^{17}O NMR of amino acid derivatives in DMSO solution, contrary to the case in CDCl_3 solution, should not be attributed to a reduction of the intramolecular conformational exchange rate, but, to the strong hydrogen bond interaction of DMSO- d_6 with the COOH group which reduces effectively the exchange rate for proton transfer [V. Theodorou, A.N. Troganis and **I.P. Gerotheranassis***, *Tetrahedron Lett.* 45, 2243-2245 (2004)].

3. ^{17}O NMR and Steric Perturbation Effects

^{17}O NMR spectroscopy is a powerful method for detection of steric effects in molecules in which steric interactions are characterised by rotation of functional groups around single bonds to relieve van der Waals interactions or on rigid systems in which steric interactions result in bond angle and/or bond length distortions. ^{17}O NMR studies, at natural abundance, of substituted quinoxaline-2(1H), 3(4H)-

dione [(a) **I.P. Gerothanassis***, J. Cobb, A. Kimbaris, J.A.S. Smith, G. Varvounis, *Tetrahedron Lett.* 37, 3191-3194 (1996); (b) **I.P. Gerothanassis**, G. Varvounis, *J. Heterocyclic Chem.* 33, 643-646 (1996)] demonstrated that $\delta(^{17}\text{O})$ data can provide new insights into steric and electronic interactions due to long range through six bond substituent effects on the aromatic ring. The role of considerable “keto” character and torsion angle deformation of the diamide group in solution was emphasized.

4. Inter-molecular hydrogen bonding effects

^{17}O NMR appears to be especially promising for studying hydrogen bonding interactions because of the large chemical shift range of the oxygen nucleus. The dominance of inter- and intra-molecular hydrogen bonding effects over substituent effects has been clearly demonstrated in several molecular systems.

Solvent effects on $\delta(^{17}\text{O})$ of acetone have been investigated in detail and the differential shift between n-hexane and water is 67.8 ppm and between CH_3CN and H_2O is 45.2 ppm [**I.P. Gerothanassis***, C. Vakka, A. Troganis, *J. Magn. Reson. B.* 111, 220-229 (1996)]. Comparison with SOS and FPT molecular orbital calculations and correlation with the $n \rightarrow \pi^*$ transition was also investigated.

Gerothanassis* and Vakka [*J. Org. Chem.* 59, 2341-2348 (1994)] investigated in detail: (i) substituent effects; (ii) the cooperativity contribution of solvation of the NH group on the amide oxygen-17 shielding; (iii) effects of long-range dipole-dipole interactions, of the bulk dielectric constant of the medium and effects of proton donor solvents; and (iv) cooperativity and nonadditive contributions of hydration phenomena on the amide oxygen. A synopsis of this work will be given below. On decreasing the concentration in the apolar and low dielectric constant solvents n-hexane, CCl_4 and toluene, the amide ^{17}O absorption indicates a strong deshielding for NMF and NMA due to a decrease of the intermolecular interactions between the amide NH group of one with the CO group of another molecule (Fig. 3). As expected, $\delta(^{17}\text{O})$ of DMF and DMA indicate significantly smaller concentration dependence due to absence of NH---OC hydrogen bonds. The difference in the chemical shift of NMF and DMF at infinite dilution in CCl_4 and toluene is rather small (4-6 ppm), practically independent of the solvent, and should be attributed to the substituent effect of the methyl group of the amide nitrogen. For DMA and NMA the difference in the chemical shift in CH_2Cl_2 and CHCl_3 is ~-5 to -6 ppm and ~-8 ppm in H_2O . It was concluded that the substituent effect of the methyl group of the amide nitrogen on the ^{17}O shielding is -6 ppm. Methyl substitution on the amide carbon induces a shift of <-4 ppm for NMF and DMF and ~-11 to -16 ppm for NMA and DMA. Both effects are in the opposite direction and much smaller in magnitude than that observed on methyl substitution at the carbonyl carbon of aldehydes (24 ppm) presumably due to the reduced π -bond order in $\text{C}=\text{O}$ bonds in amides.

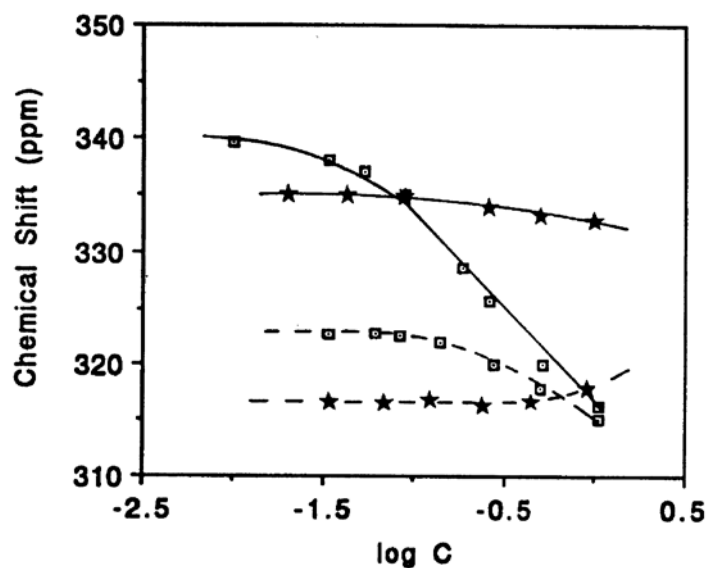


FIGURE 3. ^{17}O NMR chemical shifts of NMF (\square) and DMF ($*$) as a function of the logarithm of concentration, in toluene (—; in CH_2Cl_2 (---). [I.P. Gerothanassis & C. Vakka, *J. Org. Chem.* 59, 2341-2348 (1994)].

$\delta(^{17}\text{O})$ of NMF, DMF, NMA, and DMA in acetone, CH_3CN , and DMSO, which form a hydrogen bond with the amide hydrogen but not with the amide oxygen, was used to verify the significance of this hydrogen bond interaction on the amide ^{17}O shielding. It is evident that solvation of the amide hydrogen induces a shift of 2-3 ppm for NMF and NMA, respectively, and, thus, can be neglected. The extrapolated shielding constants of DMF, NMF, DMA, and NMA in n-hexane, CCl_4 , and toluene, at “infinite” dilution, were found to be significantly different compared with the values of 323 ppm and 340 ppm suggested for formamides and acetamides in the absence of hydrogen bonding interactions. These differences can be attributed to non specific dipole-dipole solute-solvent interactions which are a function $(\epsilon-1)/2\epsilon$ of the dielectric constant, ϵ , of the medium. Proton donor solvents like MeOH (with dielectric constant $\epsilon=32.7$) and EtOH ($\epsilon=24.5$) induce a significant shielding, due to formation of monosolvates and disolvates of the type $\text{C}=\text{O}\cdots\text{HOR}$ and $\text{C}=\text{O}\cdots(\text{HOR})_2$, respectively. In aqueous solution $\delta(^{17}\text{O})$ is significantly more shielded and this reflects the solvation of the amide oxygen by two molecules of water.

Diez et al. [E. Diez*, J. San Fabian, I.P. Gerothanassis, A.L. Esteban, J-L.M. Abboud, R.H. Contreras, D.G.De Kowalewski, *J. Magn. Reson.* 124, 8-19 (1997)] performed a detailed multiple-linear-regression analysis (MLRA) using the Kamplet-Abboud-Taft (KAT) solvatochromic parameters π^* , α , and β in order to quantify solvent effects on $\delta(^{17}\text{O})$ of NMF, DMF, NMA and DMA. The π^* scale is an index of solvent dipolarity/polarizability, which measures the ability of the solvent to stabilize a charge or a dipole due to its dielectric effect. The α scale describes the ability of the solvent to donate a proton in a solvent-to-solute hydrogen bond. The β scale measures the ability of the solvent to accept a proton (i.e. to donate an electron pair) in a solute-to-solvent hydrogen bond. The chemical shifts of the

four molecules show the same dependence (in ppm) on the solvent dipolarity-polarizability, i.e., $-22\pi^*$. The effect of the solvent hydrogen bond donor acidities is slightly larger for NMA and DMA, i.e., -48α , than for NMF and DMF, i.e., -42α . The effect of the solvent hydrogen bond acceptor basicities is negligible for the non-protic molecules DMF and DMA but significant for the protic molecules NMF and NMA, i.e., -9β . The effect of substitution of the N–H hydrogen by a methyl group is -5.9 ppm in NMF and 5.4 ppm in NMA. The effect of substitution of the O=C–H hydrogen by a methyl group is 5.5 ppm in NMF and 16.8 ppm in DMF. Furthermore, ^{17}O hydration shifts have been calculated for formamide by the ab initio LORG method at the $6\text{-}31\text{ G}^*$ level.

^{17}O shieldings have been utilized [**I.P. Gerothanassis***, C. Vakka, A. Troganis, *J. Magn. Reson. B.* 111, 220-229 (1996); **I.P. Gerothanassis***, I.N. Demetropoulos, C. Vakka, *Biopolymers* 36, 415-418 (1995)] to investigate solvation differences of the cis/trans isomers of NMF, N-ethylformamide (NEF), and tert-butylformamide (TBF) in a variety of solvents with particular emphasis on aqueous solution. Hydration at the amide oxygen induces large and specific modifications of $\delta(^{17}\text{O})$ which are practically the same for the cis and trans isomers for NMF and NEF. It was concluded that both cis and trans amide oxygens are solvated by into molecules of water which are rather exposed to the aqueous environment. For TBF, the strong deshielding of the trans isomer compared with that of the cis isomer (Fig. 4) may be attributed to an out-of-plane (torsion-angle) deformation of the amide bond and/or a significant reduction on the hydration of the trans isomer due to steric inhibition of the bulky tert-butyl group [**I.P. Gerothanassis***, C. Vakka, A. Troganis, *J. Magn. Reson. B.* 111, 220-229 (1996)]. Good linear correlation between $\delta(^{17}\text{O})$ of amides and $\delta(^{17}\text{O})$ of acetone was found for different solvents which have varying dielectric constants and solvation abilities. Amides and carbonyl compounds, therefore, appear to be reflecting a similar type of electronic perturbation. Sum-over-states calculations, within the solvation model, underestimate the effect on $\delta(^{17}\text{O})$ of changes in the dielectric constant of the medium, while finite perturbation theory calculations give good agreement with experiment.

Further combined studies of ^{17}O NMR and ^1H - ^{15}N Heteronuclear Multiple Quantum Coherence (^1H - ^{15}N HMQC) NMR of amides demonstrated [**I.P. Gerothanassis**, A. Troganis and C. Vakka, *Tetrahedron*, 51, 9493-9500 (1995)] that ^{17}O and ^{15}N shielding differences between the cis and trans isomers are a useful tool for investigating out of plane deformation of the amide bond and pyramidity at the amide nitrogen. Solvent accessibility, steric hindrance and, thus, torsion angle deformation was shown to be strongly solvent dependent.

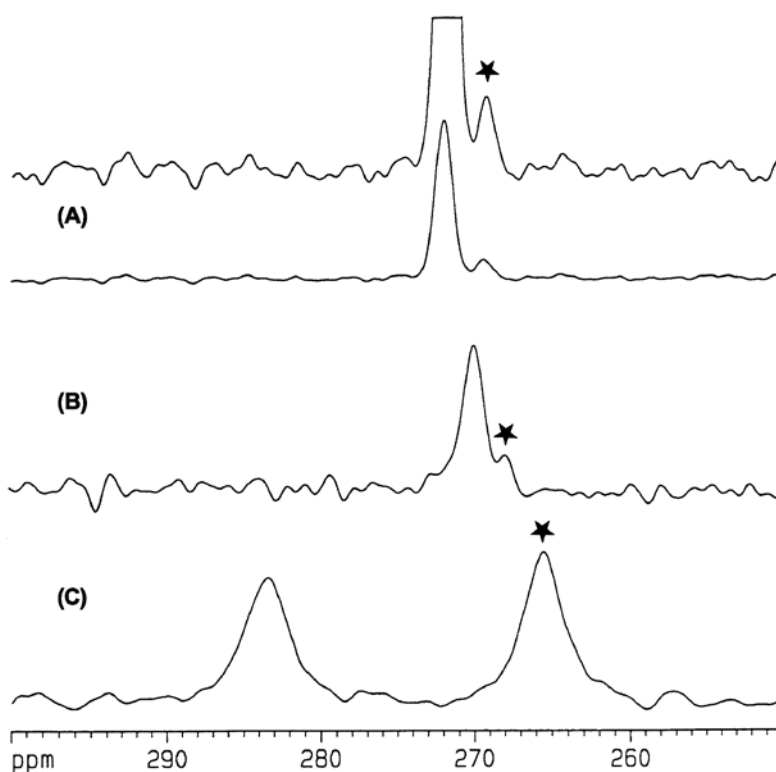


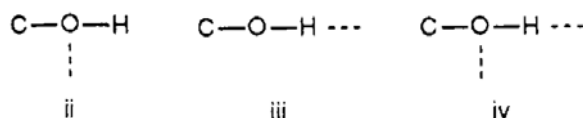
FIGURE 4. NMR spectra (54.4MHz) of ^{17}O , in natural abundance of N-alkylformamides, concentration 0.1M in H_2O , at 30°C . (A) N-methylformamide, $T_{\text{acq}} \sim 18$ ms; number of scans, 1,740,000; after resolution enhancement by a Gaussian-exponential function. (Upper trace) after vertical expansion (4x). (B) N-ethylformamide, $T_{\text{acq}} \sim 18$ ms; number of scans, 2,000,000; after resolution enhancement by a Gaussian-exponential function. (C) N-tert-butylformamide, $T_{\text{acq}} \sim 18$ ms; number of scans, 1,600,000; after multiplication of the FID with a line-broadening exponential function (LB=70 Hz). The asterisks denote the resonance positions of the cis isomers. (I.P. Gerothanassis, I.N. Demetropoulos, C. Vakka, *J. Magn. Reson. B.* 111, 220-229 (1996), Academic Press, Inc.).

From the above studies it can be concluded that in amides both long range dipole-dipole interactions and specific hydrogen bonds at the amide oxygen induce significant and specific shielding of the ^{17}O nucleus. Thus the overall chemical shift change between an amide oxygen in the absence of hydrogen bonding interactions in vacuum and that which is fully hydrated in aqueous solution is, very probably, over 95 ppm. Linear correlation between $\delta(^{17}\text{O})$ and $\nu(\text{CO})$, the IR amide I stretching vibration, exists for different solvents which have varying dielectric constants and solvation abilities [I.P. Gerothanassis* and C. Vakka, *J. Org. Chem.* 59, 2341-2348 (1994)]. This demonstrates that both IR and ^{17}O NMR spectroscopy appear to be reflecting a similar type of electronic perturbation i.e. hydrogen bonding and dipole-dipole solute-solvent interactions, although, the slope of the plots show that $\delta(^{17}\text{O})$ is more sensitive than the corresponding $\nu(\text{CO})$.

$\delta(^{17}\text{O})$ of methanol is deshielded by ~ 9.4 ppm upon “infinite” dilution in H_2O [J. Reuben, *J. Am. Chem. Soc.* 91, 5725-5729 (1968)] due to increase in the number of hydrogen bonds. In contrast, the effect of solvent induced hydrogen bonding interactions on the $-\text{OH}$ group of *p*-cresol is surprisingly

small and does not appear to correlate with the hydrogen-bonding strength of the solvents [I.P. Gerothanassis*, N. Birlirakis, C. Sakarellos*, M. Marraud, *J. Am. Chem. Soc.* 114, 9043-9047 (1992)]. This behaviour of *p*-cresol is at variance with that of alcohols. Thus, on transfer of *p*-cresol from CCl₄ to H₂O a chemical shift of only 1.9 ppm is observed. Since the COH group can act both as a proton donor and acceptor, it may be concluded that the two modes of hydrogen bonding induce chemical shifts of opposite directions, thus resulting in a significant reduction in the overall chemical shift. However, this hypothesis can be ruled out since the chemical shift of (¹⁷O)*p*-cresol in acetone, which can act only as a proton acceptor, is very similar to that in the absence of hydrogen bonding in dilute CCl₄. Similar results were obtained from ¹⁷O NMR studies of N^α-Ac-(¹⁷O)Tyr-OMe. On the contrary, the ν_{C-O-H} bending vibration was shown to be an excellent method for investigating discrete hydrogen bonding and solvation species of the phenol type C-O-H moiety. The COH deformation modes in the region of 1245-1210 cm⁻¹ are shifted to higher frequencies on increasing the strength of hydrogen bonding. The formation of hydrogen bonds constrains the deformation vibrations and therefore increases the force constants of these modes. Although these shifts are appreciably smaller than those found for the ν_{OH} stretching vibrations, the COH bending vibrations have three distinct advantages:

- (i) They do not exhibit any substantial band broadening when H-bonding occurs; therefore, discrete hydrogen-bonded species:



could be resolved and identified. On the contrary, the ν_{OH} stretching vibrations due to H-bonded species exhibit extremely broad absorption bands.

- (ii) The COH deformation absorption modes do not exhibit substantial changes in their intensity when H-bonding occurs.
- (iii) Discrete hydrogen bonding species can be identified even in aqueous solutions where the IR region of 3700-3100 cm⁻¹ cannot be studied. It is therefore clear that the region of bending vibrations has significant advantages over the classical region of the ν_{OH} stretching vibrations for phenol type groupings such as Tyr in peptide hormones.

δ(¹⁷O) of aliphatic nitro compounds are solvent dependent. Thus, CH₃NO₂ exhibits a shielding of -12 ppm on going from CCl₄ to H₂O [I.P. Gerothanassis and J. Lauterwein*, *Magn. Reson. Chem.* 24, 1034-1038 (1986)].

5. Heme Proteins and Model Compounds

Maricic and co-workers reported [S. Maricic*, J.S. Leigh Jr., D.E. Sunko, *Nature* 214, 462-466 (1967)] that they had observed single resonance absorption of ¹⁷O₂ bound to hemoglobin at ~0 ppm. They concluded that both oxygen nuclei are magnetically equivalent in support of the Griffith's

proposal that the heme-iron oxygen bond is a three-center bond. It was subsequently shown [C.S. Irving, A. Lapidot, *Nature* 230, 224 (1971)] that the observed signal is due to H_2^{17}O since bacteria had metabolised $^{17}\text{O}_2$ into H_2^{17}O and deoxyhemoglobin had oxidised to methemoglobin. It was suggested that the observation of ^{17}O NMR spectra of oxymyoglobin and oxyhemoglobin in solution may be quite difficult since, although the ^{13}C NMR resonances of the hemes in carbonmonoxymyoglobin and carbonmonoxyhemoglobin in solution could readily be detected, the corresponding ^{13}C NMR spectra of MbO_2 and HbO_2 have never been observed even after laborious manipulations of buffer type, pH, pO_2 , and temperature.

In contrast to the results from heme proteins, the ^{17}O NMR spectra of several heme model compounds (Fig. 5, Table 1) in solution have been successfully carried out by Gerotheranassis et al. [**I.P. Gerotheranassis**, *Progr. NMR Spectrosc.* 26, 239-292 (1994); **I.P. Gerotheranassis*** and M. Momenteau, *J. Am. Chem. Soc.* 109, 6944-6947 (1987); **I.P. Gerotheranassis***, M. Momenteau and B. Loock, *J. Am. Chem. Soc.* 111, 7006-7012 (1989); **I.P. Gerotheranassis***, B. Loock and M. Momenteau, *J. Chem. Soc., Chem. Commun.* 598-600 (1992); **I.P. Gerotheranassis**, M. Momenteau, in: J. Anastassopoulou, P. Collery, J. C. Etienne, T. Theophanides (Eds.), *Metal Ions in Biology and Medicine*, Vol. 2, John Libbey (1992) pp.14-19]. Two signals at ~ 1750 and ~ 2500 ppm were observed for the FeO_2 linkage (Fig. 6). The data were interpreted to rule out sideways triangular bonding in favour of an end-on angular bonding arrangement (Fig. 7). The data were explained in terms of bonding models in which the electrons of the FeO_2 moiety are totally paired. This area of applications of ^{17}O NMR, experimental details and the biochemical significance of the results were analyzed in details in a relevant review article [**I.P. Gerotheranassis**, *Progr. NMR Spectrosc.* 26, 239-292 (1994)].

Examination of the linewidth data in Table 1 reveals that in the picket fence porphyrin **1**, the linewidth of the bridge oxygen O(b) exhibits a minimum at ~ 273 K and then increases drastically on increasing the temperature. The linewidth of the terminal oxygen O(t) resonance exhibits a minimum around 283K and increases at higher temperatures. Several interpretations can be proposed for this behavior (i) exchange broadening due to O_2 exchange; (ii) broadening due to unresolved $^1J_{^{17}\text{Fe}-^{17}\text{O}}$ coupling constant; and (iii) two possible conformational states of the Fe-O_2 moiety as suggested by Spatalian et al. [K. Spatalian, G. Lang, J.P. Collman, R.R. Gagne and C.A. Reed, *J. Chem. Phys.* 63, 5375 (1975)] on the basis of zero field, variable temperature, Mossbauer experiments in the solid state. The ^{17}O NMR linewidth data may be interpreted two different types of FeO_2 conformation (Figure 8) with significantly different electric field gradient tensors at both oxygen sites, especially that of O(t). Three interpretations can be proposed for this linewidth behaviour. (i) Dipole-dipole interactions at distances longer than conventional hydrogen bonds. Detailed ^{17}O NQR and NMR studies showed that nuclear quadrupole coupling constants are dependent on the individual H-bond geometry and strength but the changes are usually below $\sim 13\%$ even for molecules with intramolecular hydrogen bonds with very short O---O distances and strong deviations from linearity. It was suggested that the large changes

of the electric field gradient tensors around each oxygen nucleus cannot be primarily due to long-range dipole-dipole interactions which would mainly affect the terminal oxygen of the Fe–O bond, contrary to the experimental data. (ii) A second interpretation would be and elongation of the Fe–O bond due to anharmonic vibrations of the oxygen molecule in the iron binding potential the experimental results (Table 1); however, it is not expected to affect drastically the symmetry and, therefore, the electric field gradient tensor at the oxygen bound to iron. (iii) A change of the electric field gradient tensor at O(b) might result from a difference in the local symmetry due to differences in the M–O–O bond angle. Jameson and Drago [*J. Am. Chem. Soc.* 107, 3017 (1985)] noted that in the maximization of the electrostatic attractions between the oxygen molecule and the NH moieties, substantial distortions up to 25 of the M–O–O bond angles may occur. Furthermore, the F–O–O angle in Hb, Mb, and model complexes varies over a wide range depending on the shape and chemical constitution of the heme pocket.

¹³C, ¹⁷O and ⁵⁷Fe NMR spectra of several carbonmonoxy hemoprotein models with varying polar and steric effects of the distal organic superstructure, constraints of the proximal side, and porphyrin ruffling were reported [C.G. Kalodimos, **I.P. Gerotheranassis***, R. Pierattelli and B. Ancian, *Inorg. Chem.* 38, 4283-4293 (1999); C.G. Kalodimos, **I.P. Gerotheranassis***, R. Pierattelli and A. Troganis, *J. Inorg. Biochem.* 79, 371-380 (2000)]. It was suggested [C.G. Kalodimos, **I.P. Gerotheranassis***, R. Pierattelli and B. Ancian, *Inorg. Chem.* 38, 4283-4293 (1999)] that polarisable carbon monoxide [J. D. Augspurger, C. E. Dykstra*, E. Oldfield, *J. Am. Chem. Soc.* 113, 2447-2451 (1991)] is not an adequate model for distal ligand effects in carbonmonoxy heme proteins and synthetic model compounds. The lack of correlation between $\delta(^{13}\text{C})$ and $\delta(^{17}\text{O})$, contrary to the case of a moderately good correlation for His-coordinated hemoproteins [K. D. Park, K. Guo, F. Adebodun, M. L. Chiu, S. G. Sligar, E. Oldfield*, *Biochemistry* 30, 2333-2347 (1991)], suggests that the two probes do not reflect a similar type of electronic and structural perturbation. The $\delta(^{17}\text{O})$ value is not primarily influenced by the local distal field interactions and does not correlate with a single structural property of the Fe–C–O moiety derived from X-ray diffraction studies. Atropisomerism and deformation (ruffling) of the porphyrin geometry, however, appear to play an important role [C. G. Kalodimos, **I. P. Gerotheranassis***, R. Pierattelli and A. Troganis, *J. Inorg. Biochem.* 79, 371-380 (2000)].

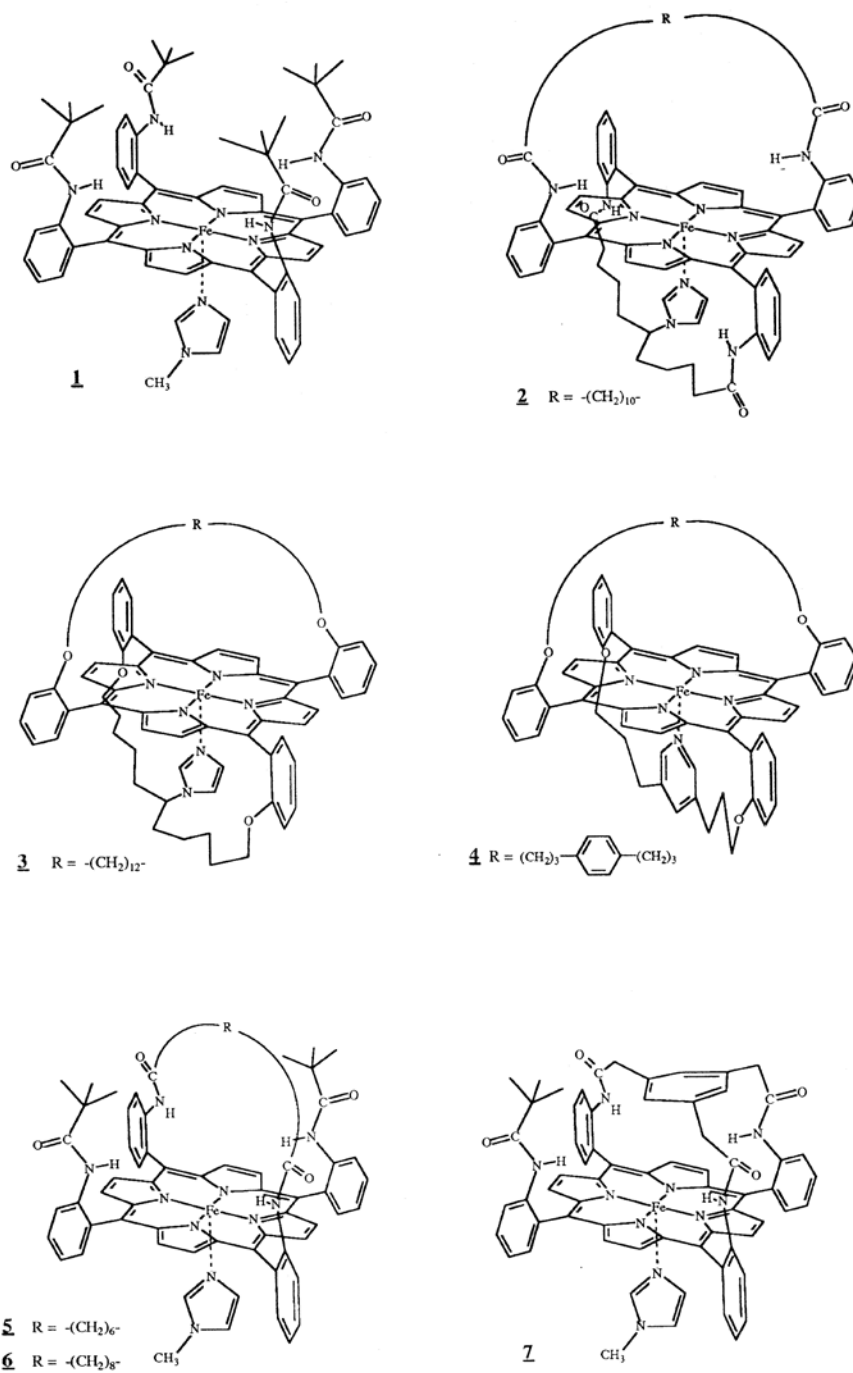


FIGURE 5. Synthetic model compounds of the active site of oxygen carrier hemoproteins: **1**, picket fence porphyrin; **2**, basket handle porphyrin in amide series; **3**, **4**, basket handle porphyrins in ether series; **5**, **6**, hybrid porphyrins; **7**, picket pocket porphyrin. [I.P. Gerohanassis, *Progr. NMR Spectrosc.* 26, 239-292 (1994), Pergamon].

TABLE 1. ^{17}O chemical shifts^a of the terminal oxygen, δ_t , and the bridging oxygen coordinated to iron, δ_b , linewidths^b of the terminal oxygen, $(\Delta\nu_{1/2})_t$, and the bridging oxygen coordinated to iron, $(\Delta\nu_{1/2})_b$, chemical shift differences $\Delta\delta = \delta_t - \delta_b$, ratios of the linewidths, and the expressions $\chi^2(1+\eta^2/3)$ where χ and η are the quadrupole coupling constant and asymmetry parameter, respectively, of the oxygens of the Fe-O₂ moiety of the hemoprotein models of Fig. 5 at 54.2 MHz

Compound	Solvent	Concentration ^c (x 10 ² M)	Temperature (K)	δ_b^d (ppm)	$(\Delta\nu_{1/2})_b^d$ (Hz)	δ_t^e (ppm)	$(\Delta\nu_{1/2})_t^e$ (Hz)	$\Delta\delta$ (ppm)	$(\Delta\nu_{1/2})_t/(\Delta\nu_{1/2})_b$	$\chi^2(1+\eta^2/3)_t/\chi^2(1+\eta^2/3)_b$
<u>1</u>	CH ₂ Cl ₂	2.5	253	1750.0	410	2524.0	3340	774.0	8.15	2.85
<u>1</u>	CH ₂ Cl ₂	2.5	263	1749.0	380	2521.8	2910	772.8	7.66	2.77
<u>1</u>	CH ₂ Cl ₂	2.5	273	1747.9	370	2518.7	2480	770.8	6.70	2.59
<u>1</u>	CH ₂ Cl ₂	2.5	283	1747.3	450	2518.2	1960	770.9	4.36	2.09
<u>1</u>	CH ₂ Cl ₂	2.5	298	1744.9	1090	2512.6	2070	767.7	1.90	1.37
<u>1</u>	CH ₂ Cl ₂	2.5	303	1747.0	1680	2512.2	2770	765.2	1.65	1.28
<u>2</u>	CH ₂ Cl ₂	1.5	273	1764.8	2640	f	f			
<u>2</u>	CH ₂ Cl ₂	1.5	283	1762.5	2280	2486.9	6450	724.4	2.83	1.68
<u>3</u>	CH ₂ Cl ₂	1.8	273	1754.5	990	2514.6	3750	760.1	3.79	1.95 ^g
<u>4</u>	toluene	1.0	263	h	h	h	h			
<u>5</u>	toluene	1.4	253	1737.8	1770	f	f			
<u>5</u>	toluene	1.4	273	1738.0	910	2480.5	3390	743.7	3.73	1.93
<u>5</u>	toluene	1.4	283	1739.4	710	2479.9	3170	740.5	4.46	2.11
<u>5</u>	toluene	1.4	288	1739.5	660	2480.12	3100	740.6	4.70	2.17
<u>5</u>	toluene	1.4	297	1739.5	600	2484.2	2480	744.7	4.13	2.03
<u>5</u>	toluene	1.4	307	1740.2	560	2485.7	2040	745.5	3.64	1.91
<u>6</u>	toluene	2.5	273	1760.5	2017	f	f			
<u>6</u>	toluene	2.5	283	1757.9	1399	2484.7	4319	726.8	3.08	1.75
<u>6</u>	toluene	2.5	297	1756.3	890	2487.7	3220	731.4	3.61	1.90
<u>6</u>	toluene	2.5	307	1755.0	811	2488.3	2584	733.3	3.18	1.78

* The values given are adapted from *J. Am. Chem. Soc.* **I.P. Gerothanassis*** and M. Momenteau, *J. Am. Chem. Soc.* 109, 6944-6947 (1987); **I.P. Gerothanassis***, M. Momenteau and B. Look, 111, 7006-7012 (1989).

- ^a Chemical shifts are reported relative to external 1,4-dioxane by using the sample replacement technique. Estimated errors from ± 0.6 to 2.5 ppm, depending on the linewidth of the resonance. Positive values indicate deshielding.
- ^b Linewidths of the resonances at half-height corrected for the line-broadening factors. Estimated error $< 5\%$ for linewidths up to 2 kHz, $\sim 10\%$ for linewidths larger than 2 kHz.
- ^c Upper values since some precipitation of the compounds was observed during experimentation.
- ^d Oxygen coordinated to iron (bridge oxygen).
- ^e Terminal oxygen.
- ^f The breadth of the resonance prohibits accurate estimation of spectral parameters.
- ^g Ether-BHP exhibit higher dissociation rates relative to that of amide-BHP. Therefore caution is necessary in interpreting ratios of linewidths exclusively in terms of ratios of the parameter $\chi^2(1+\eta^2/3)$.
- ^h No signal

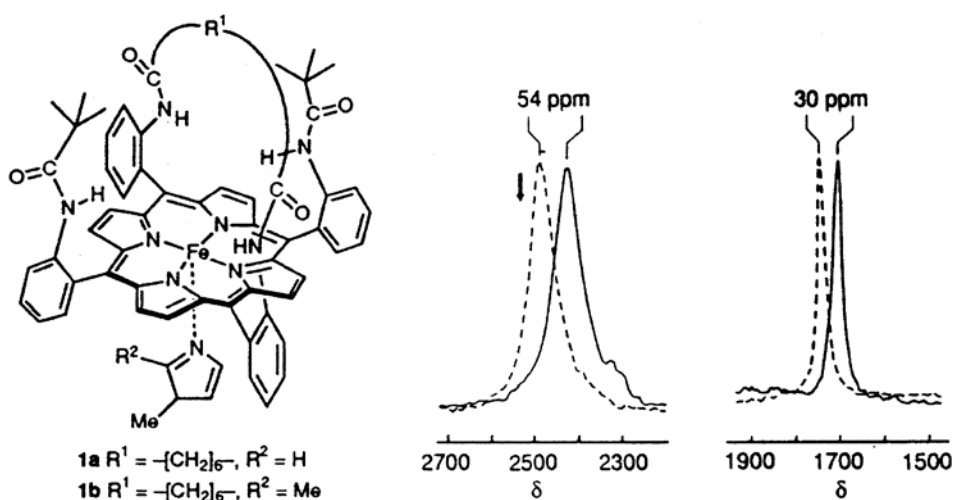


FIGURE 6. ^{17}O NMR spectra (54.2 MHz) of the oxygenated compounds **1b**(—) and **1a**(---) with a preacquisition delay time $\Delta t=50 \mu s$ and recorded in two steps with the carrier frequency on the absorption resonances. Maximum concentration $\sim 10^{-2}$ M in toluene solution. Concentration of 1,2-Me₂Im $\sim 5 \cdot 10^{-1}$ M, $T=297$ K, NS=1080000 (LB=1 kHz) and 350000 (LB=500 Hz) for the high- and low-frequency resonances, respectively. The arrow \downarrow denotes the region of the resonance position of the terminal oxygen of the picket-fence porphyrin model, with excess of 1-MeIm, and ether-models in which no hydrogen bonding interactions are expected. [I.P. Gerotheranassis*, B. Looock and M. Momenteau, *J. Chem. Soc., Chem. Commun.* 598-600 (1992), the Royal Society of Chemistry).



FIGURE 7. Pauling (a) and Griffith (b) models of the Fe-O₂ moiety [I.P. Gerotheranassis, *Progr. NMR Spectrosc.* 26, 239-292 (1994)].

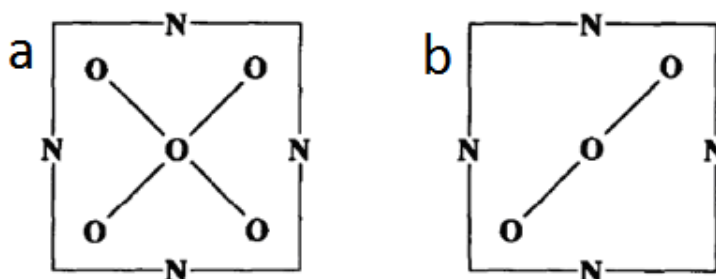


FIGURE 8. Schematic presentation of the Fe-O-O plane in (a) 1-Melm picket fence porphyrin, and (b) amide-BHP. Reprinted, from I.P. Gerotheranassis*, M. Momenteau* and B. Looock, *J. Am. Chem. Soc.* 111, 7006-7012 (1989) American Chemical Society.

bonding can occur. The ^{17}O NMR spectra in organic solvents exhibit two resonances (Fig. 10), which can be attributed to the cis-trans isomerization of the Ac-Pro amide bond. The smaller deshielded resonance absorption can be attributed to the cis conformer, and its intensity corresponds to a population of ca. 6%. The ^{17}O resonance of the trans isomer of (^{17}O)Ac-L-Pro-D-Ala-NHMe is shifted to low frequency relative to the cis isomer by -21.3 ppm. This large chemical shift can be correlated with the existence of a folded β -turn structure, stabilized by an intramolecular $i+3\rightarrow i$ hydrogen bond interaction involving the acetyl oxygen of residue i and the NH of the aminoacid residue $i+3$, particularly in cases involving heterochiral sequences.

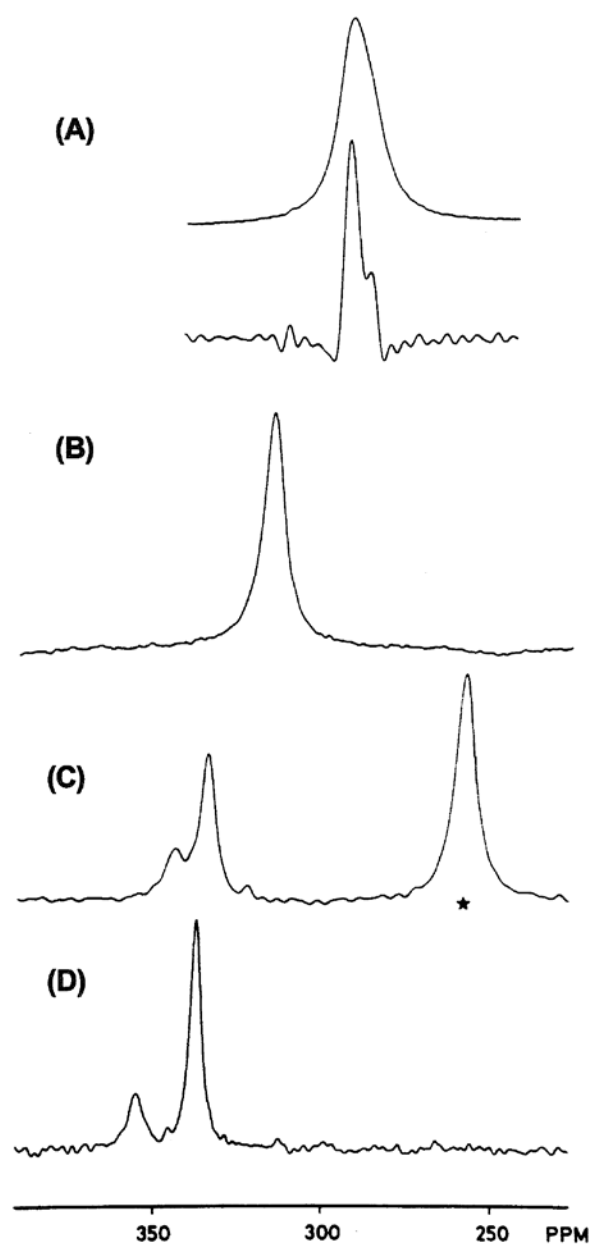


FIGURE 9. ^{17}O NMR spectra (48.8 MHz) of N- ^{17}O acetyl-L-proline (A) 10% enrichment in ^{17}O , 0.1M in aqueous solution containing 1M NaCl and 5.10^{-5} M EDTA; $T_{\text{acq}}=12$ ms; NS=300000; total experimental time=1 h. Upper trace: normal spectrum. Lower trace: after a Gaussian-exponential resolution enhancement. (B) 1% enrichment in ^{17}O , 0.1M in methanol, $T_{\text{acq}}=10$ ms, NS=200000, total experimental time=32 min, LB=50 Hz. (C) 0.4M natural abundance in acetone (an asterisk marks the carboxyl oxygen resonance, $T_{\text{acq}}=5$ ms, NS=1900000, total experimental time ca. 10 h, LB=50 Hz); (D) 1% enrichment in ^{17}O , 0.1M in acetone, $T_{\text{acq}}=10$ ms, NS=1350000, total experimental time ca. 8 h, LB=50 Hz. All spectra were recorded at 40°C. [R.N. Hunston, I.P. Gerotheranassis and J. Lauterwein* *J. Am. Chem. Soc.* 107, 2654-2661 (1985) The American Chemical Society).

TABLE 2. Observed chemical shifts $\delta(\text{COOH})$ and $\delta(\text{CH}_3\text{CO})$ and chemical shifts differences, Δ , of $\delta(\text{CH}_3\text{CO})$ of the cis and trans isomers of ^{17}O in N-acetyl-L-proline, N-acetylsarcosine, N-acetyl-L-proline-NHMe and N-acetyl-sarcosine-NHMe in aqueous and organic solutions [L.P. Gerothanassis, *Progr. NMR Spectrosc.* 26, 171-237 (1994)]

compd	solvent	Concn,M	$\delta(\text{COOH})$		$\delta(\text{CH}_3\text{CO})$		Δ
			cis	trans	cis	trans	
Ac-L-ProOH ^a	H ₂ O ^c	0.1 ^d	251.1 ^e	246.1 ^e	297.2 ^e	298.4 ^e	-1.2
	CH ₃ OH	0.1 ^d	255.6	248.6	316.4 ^f		d
	CH ₃ CH ₂ OH	0.1 ^d	257.1	250.2	g		e
	CH ₃ OCH ₃	0.6 ^{h,i}		258.0 ^f	341.2	332.8	8.4
		0.1		258.7 ^f	352.0	336.9	15.1
		0.02		258.8 ^f	354.7	337.2	17.5
		0.01		258.5 ^f	354.7	337.2	17.5
	CHCl ₃	0.6 ^h		255.6 ^f		315.6 ^f	d
		0.35 ^h		257.2 ^f		315.5 ^f	d
		0.1		259.1 ^f	332.7	316.0	16.7
		0.04		261.4 ^f	335.2	313.8	21.4
		0.02		262.9 ^f	335.5	313.9	21.6
		0.01		264.6 ^f	j	313.7	
AcSarOH ^a	H ₂ O ^c	0.1 ^d	252.0 ^e	249.5 ^e		300.2 ^{e,f}	
	CH ₃ OH	0.1 ^d	255.2	252.1		317.7 ^f	
	CH ₃ COCH ₃	0.14 ^{h,i}		258.0 ^f	350.8	344.9	5.8
		0.04	261.6	258.8	354.4	348.1	6.3
		0.005		258.6	354.9	348.6	6.3
Ac-L-Pro-NHMe ^b	H ₂ O	0.1 ^d				303.1 ^f	
	MeOH	0.1 ^d				319.8 ^f	
	CH ₃ CN	0.1 ^d			352.4	345.4	7.0
	CH ₃ COCH ₃	0.1			356.6	347.6	9.0
		0.05			356.5	347.2	9.3
		0.025			356.6	347.2	9.4
		0.008			356.7	347.3	9.4
	CHCl ₃	0.1			346.2	329.7	16.5
		0.05			346.9	328.8	18.1
		0.025			347.9	328.9	19.0
		0.008			348.2	329.1	19.1
Ac-Sar-NHMe ^b	H ₂ O	0.1 ^d			301.9	304.9	-2.9
	CH ₃ OH	0.1 ^d			318.0	320.8	-2.8
	CH ₃ COCH ₃	0.1			353.5	346.6	6.9
		0.05			353.7	346.7	7.0
		0.025			353.9	346.8	7.1
		0.008			354.2	347.0	7.2
	CHCl ₃	0.1			344.9	333.0	11.9
		0.05			346.4	333.0	13.4
		0.025			347.2	333.0	14.2
		0.008			347.5	333.0	14.5

^aAt 40°C., ^bAt 30°C., ^cSolutions contained 1M NaCl and 0.0005 M EDTA (ethylenediamine-*N,N,N',N'*-tetraacetate), ^dChemical shifts were independent of concentration, ^eExtrapolated values for the fully protonated carboxyl group, ^fThe cis and trans isomers appear as a composite resonance. ^gNot measured, ^hMeasured at natural abundance in ^{17}O , ⁱSaturated solution, ^jPercent cis isomer <2%.

The observed chemical shift, δ_{obs} , is linearly related to the two contributions δ_{turn} for the β II-turn and δ_{open} for the “open” conformers, which are in rapid exchange, by:

$$\delta_{\text{obs}} = f \delta_{\text{turn}} + (1-f)\delta_{\text{open}}$$

where f is the fraction of β II-folded trans isomer. An estimation of δ_{turn} can be obtained providing that the fraction f is known. Boussard and Marraud [G. Boussard, M. Marraud*, *J. Am. Chem. Soc.* 107 1825-1828 (1985)] have shown by the use of IR spectroscopy that for dilute solutions of $\text{Bu}^t\text{CO-L-Pro-D-Ala-NHMe}$ in CH_2Cl_2 , ca. 90% of the molecules exist in the intra-molecular β -turn hydrogen bonded form. If we assume a similar β -turn probability for $\text{Ac-L-Pro-D-Ala-NHMe}$, then, a shift of -20.3 ppm can be estimated for a β -turn hydrogen bond; this is comparable to a shift of -22 ppm for a γ -turn intramolecular hydrogen bond of AcProOH .

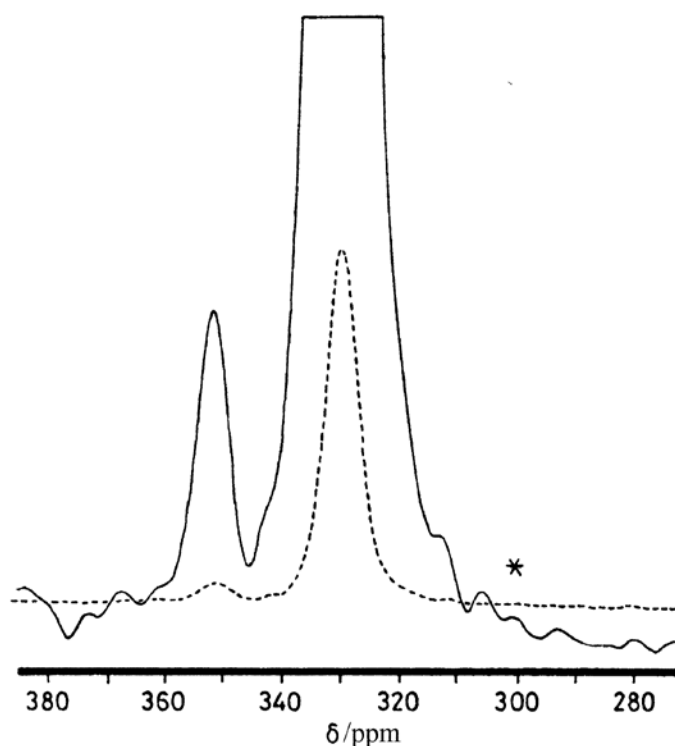


FIGURE 10. 54.48 MHz ^{17}O NMR spectra of $[^{17}\text{O}]\text{Ac-L-Pro-D-Ala-NHMe}$ (10 mm sample tubes, quadrature detection) at 30°C in CH_2Cl_2 solution. Data acquisition time 7.2 ms, number of scans 450000. Prior to transformation the free induction decay was multiplied with a Gaussian-exponential function (line broadening = -200 Hz; Gaussian broadening 0.18). The asterisk marks the position of the composite resonance in aqueous solution. [N. Birlirakis, I.P. Gerothanassis, C. Sakarellos* and M. Marraud, *J. Chem. Soc., Chem. Commun.* 1122-1123 (1989), The Royal Society of Chemistry).

The ^{17}O NMR shielding range and shielding time scale resulting from hydrogen-bonding interactions in peptides have been critically evaluated by **Gerothanassis** [*Biopolymers* 59, 125-130 (2001)] relative to those of ^1H NMR. Furthermore, the hypothesis and conclusions in

previous ^{17}O NMR studies by Tsikaris et al. [V. Tsikaris*, A. Troganis, V. Moussis, E. Panou-Pomonis, M. Sakarellos-Daitsiotis, C. Sakarellos, *Biopolymers* 53, 135 (2000)] on the detection of discrete conformational states in the peptides Ac-Arg-Ala- $(^{17}\text{O})\text{Pro-NH}_2$, selectively ^{17}O enriched at the Pro- $(^{17}\text{O})\text{CONH}_2$ group, and Piv-Arg- $(^{17}\text{O})\text{GlyNH}_2$ (the C-terminal segment of LH-RH), were reconsidered. It was demonstrated that although ^{17}O shieldings of peptide oxygens are very sensitive to hydrogen bonding interactions, the ^{17}O NMR shielding time scale is not advantageous compared to that of ^1H NMR, and thus it is not suitable for the detection of discrete hydrogen-bonded conformational states in peptides. ^{17}O NMR spectroscopy is also prone to interpretation errors due to the formation of ^{17}O -labelled impurities during the synthetic procedures.

Gerothanassis et al. [**I.P. Gerothanassis***, N. Birlirakis, T. Karayannis, M. Sakarellos-Daitsiotis, C. Sakarellos*, B. Vitoux, M. Marraud, *Eur. J. Biochem.* 210, 693-698 (1992); C. Sakarellos, **I.P. Gerothanassis**, N. Birlirakis, T. Karayannis, M. Sakarellos-Daitsiotis, M. Marraud, *Biopolymers* 28, 15-26 (1989)] investigated in detail Leu-enkephalin (Tyr-Gly-Gly-Phe-Leu) which is a brain neurotransmitter peptide that has been extensively investigated during the past 30 years with a variety of spectroscopic methods. Both (^{17}O -Gly2, Leu5)-enkephalin and (^{17}O -Gly3, Leu5)-enkephalin have similar ^{17}O chemical shifts in CH_3CN -DMSO (4:1; vol.) at pH values of 1.9 and 5.6. This suggests that both Gly2 and Gly3 sites have similar environments in this organic medium. In aqueous solution, the ^{17}O NMR shielding of (^{17}O -Gly2, Leu5)-enkephalin and (^{17}O -Gly-3, Leu-5)-enkephalin are both shifted to low frequency by approximately -27 to -29 ppm. These results indicate that the solvent-induced spectral modifications of the ^{17}O shieldings of both Gly2 and Gly3 peptide oxygens of (Leu)-enkephalin are significantly smaller as compared with those observed in model amides. One possibility is that both Gly2 and Gly3 peptide oxygens form largely monohydrates, contrary to model amide oxygens which are solvated by two molecules of H_2O in aqueous solution. An alternative interpretation is that a water molecule competes with an intramolecular interaction existing in the organic medium. This probably does not apply to (Leu)-enkephalin since it has been reported by the use of ROE experiments that this molecule is most probably devoid of intramolecular hydrogen bonds in the CH_3CN - Me_2SO (4:1) mixture and in several organic solvents.

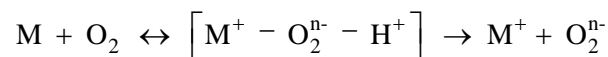
The ^{17}O chemical shifts of the fully protected ($(^{17}\text{O})\text{Gly-2,Leu-5}$)- and ($(^{17}\text{O})\text{Gly-3,Leu-5}$)-enkephalin were found to be identical in acetone solution [E. Moret, I. P. Gerothanassis, R. N. Hunston, J. Lauterwein*, *FEBS Letters* 262, 173-175 (1990)]. This allowed the conclusion that neither of these peptide oxygens is hydrogen bonded and that no specific 2 \leftarrow 5 β -turn structure which has been suggested in the literature, exists to an appreciable extent.

Detailed investigations of the selectively enriched in ^{17}O in the C-terminal carboxyl group of Leu-enkephalin and enkephalin-related fragments Phe-Leu, Gly-Phe-Leu and Gly-Gly-Phe-Leu were reported in aqueous solution over the entire pH range [T. Karayannis, **I. P. Gerotheranassis***, M. Sakarellos-Daitsiotis, C. Sakarellos, M. Marraud, *Biopolymers* 29, 423-439 (1990)]. Deprotonation of the carboxyl group results in a chemical shift to high frequency by 18.8 to 19.8 ppm for the peptides studied. This is in close agreement with the values found for AcProOH and AcProOH which were shown to be devoid of intramolecular hydrogen bonding and fully exposed to the aqueous environment.

The ionization state of Leu-enkephalin in DMSO and $\text{CH}_3\text{CN}/\text{DMSO}$ (4:1) solutions has been studied by the combined use of ^{17}O NMR and FT-IR spectroscopy [**I. P. Gerotheranassis***, N. Birlirakis, T. Karayannis, V. Tsikaris, M. Sakarellos-Daitsiotis, C. Sakarellos*, B. Vitoux, M. Marraud, *FEBS Letters* 298, 188-190 (1992)]. The results indicate that Leu-enkephalin at neutral pH essentially exists in the neutral form instead of the zwitterionic one in $\text{CH}_3\text{CN}/\text{DMSO}$ (4:1) solution and that only ~40% of the molecules are in the zwitterionic state in pure DMSO at the same pH value. This conclusion is of particular importance since numerous NMR studies of peptide hormones in the literature were interpreted with the hypothesis that they exist essentially in the dipolar form in organic solvents.

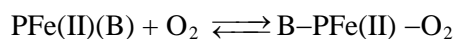
7. ^{17}O NMR as a Mechanistic Probe

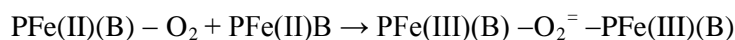
Gerotheranassis et al. [**I. P. Gerotheranassis***, M. Momenteau*, B. Looock, *J. Am. Chem. Soc.* 111, 7006-7012 (1989)] have investigated the oxidation mechanism in hemoprotein models. Oxygenated species can dissociate via two competing processes: either by the release of the dioxygen molecule from the carrier (transport process) or by oxidative dissociation leading to an oxidized metal center and reduced oxygen species (oxidation process):



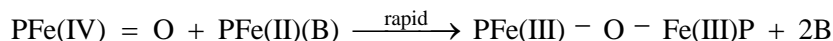
Transport	Oxidation
process	process

Flat open iron (II) porphyrins (PFe) at room temperature and in the absence of large excess of nitrogenous ligand, B, form dioxygen complexes which are quickly and irreversibly converted to the μ -oxo dimer via a μ -peroxo dimer and an iron (IV)-oxo species following a bimolecular reaction:



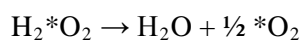
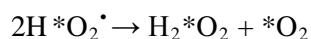
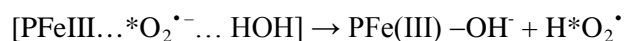


μ -peroxo dimer



μ -oxo dimer

In the protected hemoglobin models this bimolecular process is prevented due to the steric hindrance of both faces. These synthetic model compounds, therefore, appear as appropriate models to study the oxidation process of iron (II) hemoproteins. During the oxidation process of the basket handle porphyrin model compound **3** some characteristic resonances of oxygen-17 enriched species were detected in the region of 0-200 ppm. The resonance at $\delta=11.1$ ppm was assigned to H_2^{17}O which is deshielded due to the presence of paramagnetic iron species. The two resonances at $\delta=168.5$ and 173.3 ppm can be assigned to $\text{H}_2^{17}\text{O}_2$ (the former absorption is probably due to $\text{H}_2^{17}\text{O}_2$ in microscopic water droplets, which are present in organic solutions and/or on the wall of the sample tube). From the presence of the above-enriched species, the following reaction scheme was proposed (^{17}O is denoted as O^*) [**I.P. Gerotheranassis**, *Progr. NMR Spectrosc.* 26, 239-292 (1994); **I.P. Gerotheranassis***, **M. Momenteau*** and **B. Looek**, *J. Am. Chem. Soc.* 111, 7006-7012 (1989)]:



8. Photochemical and Ozonation Reactions

Braun et al. [A.M. Braun*, H. Dahn, E. Gassmann, I. Gerotheranassis, L. Jakob, J. Kateva, C.G. Martinez, E. Oliveros, *Photochem. Photobiol.* 70, 868-874 (1999)] investigated in detail the reactivity of the endoperoxide (**II**) produced by the (2+4)-cycloaddition of $^{17}\text{O}_2$ ($^1\Delta_g$) to furfuryl alcohol (**I**) in water and methanol (^{17}O is denoted as O^*) (Figure 11). In methanol, 5-methoxy-5-hydroxy-methyl-2-furanone (**VII**) is found with the highest yield (59%) and a $\text{S}_{\text{N}}1$ reaction at position 2 of (**II**) was suggested as the main reaction mechanism. However, the $\text{S}_{\text{N}}2$ reaction of (**II**) with methanol leading to 5-methoxy-2(5H)-furanone (**VI**) (30%) is of

almost equal importance. The experiments in methanol give strong indication that the endoperoxide (II) reacts via a nucleophilic substitution reaction. 5-Hydroxy-2(5H)-furanone (III) labelled at the two oxygen atoms of the carbonyl (lactone) function was found to be the major product in aqueous solution; however, product analysis and $^{17}\text{O}_2$ -labeling are not sufficient to differentiate between an $\text{S}_{\text{N}}1$ reaction, rearrangement or fragmentation of the ozonide as possible reaction paths. The formation of product (III) in methanol solution is minor and only due to the water contained in the solvent. This indicates that (III) is formed via a reaction path involving H_2O , i.e. $\text{S}_{\text{N}}2$ reaction. The products (IV) and (V) and the corresponding reaction paths are of minor importance (Figure 10).

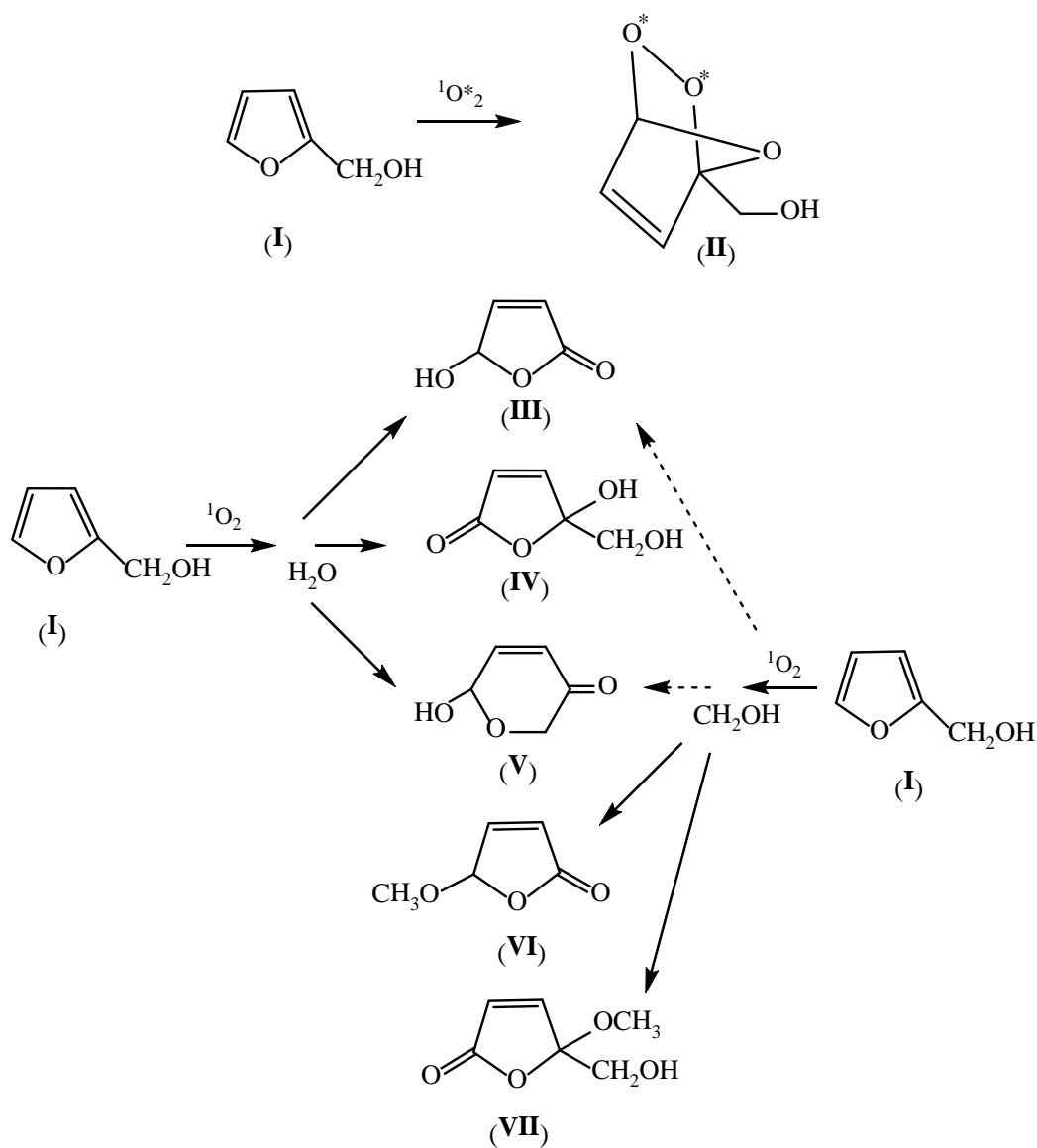


FIGURE 11. Products of the photooxidation of (I) to (II) in water and methanol, respectively. [A.M. Braun*, H. Dahn, I.P. Gerathanassis, L. Jakob, J. Kateva, C.G. Martinez, E. Oliveros, *Photochem. Photobiol.* 70, 868-874 (1999), American Society for Photobiology].

9. *Comprehensive Review Articles*

Compared to ^1H , ^{13}C , ^{15}N , ^{31}P and ^{19}F NMR, ^{17}O NMR has received little attention [C. Rodger, N. Sheppard, in: R.K. Harris, B.E. Mann (Eds.), *NMR and the Periodic Table*, Chap.12, Academic Press, New York (1978) pp.383-400; W.G. Klemperer, *Angew. Chem. Int. Ed. Engl.* 17 (1978) 246; T.St. Amour, D. Fiat, *Bull. Magn. Reson.* 1 (1980) 118; J.-P. Kintzinger, in: P. Diehl, E. Fluck, R. Kosfeld (Eds.), *NMR-Basic Principles and Progress*, Vol. 17, Springer, Berlin (1981) pp.1-64; W.G. Klemperer, in: J.B. Lambert, F.G. Riddell (Eds.), *Multinuclear Approach to NMR Spectroscopy*, Reidel, Dordrecht (1983) pp. 245-260; D.W. Boykin (Ed.) *^{17}O NMR Spectroscopy in Organic Chemistry*, CRC-Press Inc., Boston (1991); I.P. Gerotheranassis, in: D.M. Grant, R.K. Harris (Eds.), *Encyclopedia of Nuclear Magnetic Resonance*, pp. 3430-3440, Wiley, Chichester (1996); I.P. Gerotheranassis, in: J.C. Lindon, G.E. Tranter, J.L. Holmes (Eds.), *Encyclopedia of Spectroscopy & Spectrometry*, Academic Press (1999) pp.722-729; W. McFarlane, H.C.E. McFarlane, in: J. Mason (Ed.) *Multinuclear NMR*, Plenum Press, New York (1987); S. Berger, S. Braun, H.-O. Kalinowski, *NMR Spectroscopy of Non-metallic Elements*, Wiley, Chichester (1997)]. Between the first observation of a ^{17}O nuclear induction signal in 1951 and the first comprehensive review article of all aspects of ^{17}O NMR in 1981 [J.-P. Kintzinger, in: P. Diehl, E. Fluck, R. Kosfeld (Eds.), *NMR-Basic Principles and Progress*, Vol. 17, Springer, Berlin (1981) pp.1-64] there have been only about 200 publications dealing with ^{17}O NMR. This limited interest is not surprising since of the three naturally occurring oxygen isotopes (^{16}O , ^{17}O and ^{18}O), only ^{17}O possesses a nuclear spin ($I=5/2$). It has a moderate electrical quadrupole moment ($Q = -2.63 \times 10^{-30} \text{ e m}^2$), a very small magnetogyric ratio ($\gamma = -3.688 \times 10^{-7} \text{ rad.T}^{-1} \text{ s}^{-1}$), a low natural abundance (0.037%) and an extremely low absolute sensitivity compared to that of ^1H ($\sim 1.1 \times 10^{-5}$). The ^{17}O isotope is therefore one of the more difficult nuclei to observe by NMR spectroscopy. It is however of great interest to use a nucleus, such as oxygen, that is located at strategic molecular sites and is directly involved in inter- and intra-molecular interactions. The ^{17}O NMR parameters i.e. isotropic shielding, principal elements of the ^{17}O shielding and electric field gradient tensors and transverse and longitudinal relaxation times can be considered as excellent means for probing structure, bonding and dynamics of oxygen containing compounds. Further, recent advances in instrumentation, the extremely large chemical shift scale (which aids in, several cases, in the resolution of quadrupole broadened resonances) and the availability of ^{17}O enriched compounds have alleviated some of the experimental difficulties; thus, an increased use of the ^{17}O NMR technique can be foreseen.

Rodger and Sheppard [in: R.K. Harris, B.E. Mann (Eds.), *NMR and the Periodic Table*, Chap.12, Academic Press, New York (1978) pp.383-400] presented a comprehensive review article with particular emphasis to a wide range of applications up to mid-1977; Amour and

Fiat [Bull. Magn. Reson. 1 (1980) 118] reviewed the literature up to 1980 with particular emphasis on those concepts that are most essential to the understanding of ^{17}O magnetic resonance; Kintzinger [in: P. Laszlo (Ed.), NMR of Newly Accessible Nuclei, Vol. 2, Academic Press, New York (1983) pp.79-104] reviewed the literature up to 1983 and Gerothanassis has presented brief accounts of a wide range of applications up to 1995 [I.P. Gerothanassis, in: D.M. Grant, R.K. Harris (Eds.), Encyclopedia of Nuclear Magnetic Resonance, pp. 3430-3440, Wiley, Chichester (1996).] and 1998 [I.P. Gerothanassis, in: J.C. Lindon, G.E. Tranter, J.L. Holmes (Eds.), Encyclopedia of Spectroscopy & Spectrometry, Academic Press (1999) pp.722-729]. In 1981, Kintzinger [J.-P. Kintzinger, in: P. Diehl, E. Fluck, R. Kosfeld (Eds.), NMR-Basic Principles and Progress, Vol. 17, Springer, Berlin (1981) pp.1-64] published a very comprehensive monograph which covered all aspects of ^{17}O NMR, including experimental considerations, theoretical background of characteristic parameters and a wide range of applications. In 1991, Boykin [D.W. Boykin (Ed.) ^{17}O NMR Spectroscopy in Organic Chemistry, CRC-Press Inc., Boston (1991)] edited a monograph on ^{17}O NMR in Organic Chemistry with emphasis to both principles and in depth wide range of applications. Both monographs turned out to be the standard reference textbooks in the field of ^{17}O NMR for more than a decade. Berger, Braun and Kalinowski [S. Berger, S. Braun, H.-O. Kalinowski, NMR Spectroscopy of Non-metallic Elements, Wiley, Chichester (1997)] presented a comprehensive review article with particular emphasis to a wide range of applications up to 1995.

In this review [presented in two parts: "Oxygen - 17 NMR Spectroscopy: Basic Principles and Applications (Part I)" **I.P. Gerothanassis**, *Progr. NMR Spectrosc.* 56, 95-197 (2010); "Oxygen - 17 NMR Spectroscopy: Basic Principles and Applications (Part II)" **I.P. Gerothanassis**, *Progr. NMR Spectrosc.* 57, 1-110 (2010)]. We have attempted, as in Kintzinger's and Boykin's seminal monographs, to treat both the experimental aspects and the theoretical background that is essential to the understanding of ^{17}O NMR and a wide range of applications with particular emphasis on those that most clearly demonstrate the unique potential of this nucleus. A detailed and systematic survey of the literature was carried out with the help of *Chemical Abstracts*, *The Web of Science*, and *EBSCO's Academic Premier Database* (particularly using the heading "Nuclear magnetic resonance - oxygen 17" and "oxygen properties, atomic isotope of mass 17, NMR") up to and including 2007. Emphasis will be placed on the presentation of work that has clearly demonstrated the benefits of employing ^{17}O NMR in studies of chemical and biochemical systems. Hence several older, yet classic ^{17}O NMR papers were discussed. Finally, an attempt was made to define unexplored areas where ^{17}O NMR may provide structural and dynamic information which is difficult or impossible to obtain using other techniques.

CONTENTS (PART I)

1. Introduction
2. Historical Perspective
3. ^{17}O Enrichment: Synthetic Methodologies
 - 3.1. Nucleophilic substitution reactions
 - 3.2. Addition - elimination reactions
 - 3.3. Oxidation reactions
 - 3.4. Photochemical isotopic enrichment
 - 3.5. Mono- and polynuclear oxometalates
 - 3.6. Silicates
 - 3.7. Oxides and high- T_c superconductors
4. Experimental NMR Aspects for Liquid Samples
 - 4.1. Sensitivity and resolution enhancement
 - 4.1.1. Use of high magnetic field strengths
 - 4.1.2. Comparison of Fourier transform and CW methods
 - 4.1.3. High sensitivity detection schemes
 - 4.1.3.1. Toroid vs Helmholtz cell configuration
 - 4.1.3.2. Cryogenic probe technology
 - 4.1.3.3. Parallel detection schemes using electrically isolated coils
 - 4.1.4. Optimization of experimental parameters
 - 4.1.4.1. Relationship between signal-to-noise ratio and T_2 and the line width of a ^{17}O resonance
 - 4.1.4.2. Effects of low viscosity solvents-Use of supercritical solvents
 - 4.1.4.3. Effects of temperature
 - 4.1.5. Window apodization functions: Sensitivity and resolution enhancement
 - 4.1.6. Magnetization transfer experiments
 - 4.1.7. Two dimensional ^{17}O , ^1H chemical shift correlation by polarization transfer
 - 4.1.8. Inverse detection
 - 4.2. Referencing techniques
 - 4.3. Solvent (H_2O) suppression
 - 4.4. Acoustic ringing
 - 4.5. Effects of finite pulse power
 - 4.6. Use of lanthanide shift reagents
 - 4.7. Measurement of T_1 , T_2 and $T_{1\rho}$: Effects of paramagnetic impurities
5. Chemical Shifts
 - 5.1. Experimental shielding ranges

- 5.2. Theoretical calculations of ^{17}O chemical shifts
 - 5.2.1. Basic considerations
 - 5.2.2. Gauge-independent theories
 - 5.2.3. Perturbation theory including electron correlation effects
 - 5.2.4. Inter-molecular electric field effects
 - 5.2.5. Ab initio calculations of solvent effects
 - 5.2.6. Calculation of solvent effects by a combination of density functional theory (DFT) and molecular dynamics (MD)
 - 5.2.7. Semi-empirical molecular orbital calculations
 - 5.2.8. Semi-empirical calculations of solvent and medium effects
 - 5.2.9. Scalar relativistic effects
 - 5.2.10. Absolute shielding scales
 - 5.2.11. Isotope effects on ^{17}O nuclear shielding-shielding derivatives
 - 5.2.12. Shielding surfaces: Temperature dependence of ^{17}O shieldings
- 5.3. Empirical correlations
 - 5.3.1. Correlation $\delta(^{17}\text{O})/\Delta E^{-1}$
 - 5.3.2. Correlation $\delta(^{17}\text{O})/\pi$ bond order and $\delta(^{17}\text{O})$ vs bond distance
 - 5.3.3. Correlation $\delta(^{17}\text{O})$ vs torsion and bond angle
 - 5.3.4. Correlation $\delta x/\delta o$ in X–O bonds and $\delta o/\delta c$ in X–O/X–C fragments
- 5.4. Substituent effects: Correlation analysis
 - 5.4.1. Basic background
 - 5.4.2. Selected applications
- 5.5. ^{17}O shieldings in chemical education
- 5.6. ^{17}O shieldings and the Periodic Table
 - 5.6.1. Oxygen bonded to group IA and IB elements
 - 5.6.2. Oxygen bonded to group IIA and IIB elements
 - 5.6.3. Oxygen bonded to group IIIA elements
 - 5.6.4. Oxygen bonded to group IVA elements
 - 5.6.4.1. Oxygen bonded to carbon
 - 5.6.4.2. Oxygen bonded to silicon
 - 5.6.4.3. Oxygen bonded to germanium, tin and lead
 - 5.6.5. Oxygen bonded to group VA elements
 - 5.6.5.1. Oxygen bonded to nitrogen
 - 5.6.5.2. Oxygen bonded to phosphorus
 - 5.6.5.3. Oxygen bonded to arsenic
 - 5.6.6. Oxygen bonded to group VIA elements
 - 5.6.6.1. Oxygen bonded to oxygen

- 5.6.6.2. Oxygen bonded to sulfur
- 5.6.6.3. Oxygen bonded to selenium and tellurium
- 5.6.7. Oxygen bonded to group VIIA elements
- 5.6.8. Oxygen bonded to group VIIIA elements
- 5.6.9. Oxygen bonded to transition metal elements
 - 5.6.9.1. Group 3B: The lanthanides and actinides
 - 5.6.9.2. Group 4B
 - 5.6.9.3. Group 5B
 - 5.6.9.4. Group 6B
 - 5.6.9.5. Group 7B
 - 5.6.9.6. Group 8B

Symbols and Abbreviations

Acknowledgments

References

CONTENTS (PART II)

- 6. Indirect Spin-Spin Coupling Constants
 - 6.1. Basic theoretical considerations
 - 6.2. Experimental results
 - 6.2.1. Coupling of directly bonded nuclei, 1J
 - 6.2.1.1. Coupling to protons
 - 6.2.1.2. Coupling to group IV elements
 - 6.2.1.3. Coupling to group V elements
 - 6.2.1.4. Coupling to group VII elements
 - 6.2.1.5. Coupling to group VIII elements
 - 6.2.1.6. Coupling to transition metal elements
 - 6.2.2. Coupling over two bonds, 2J
 - 6.2.3. Coupling constants to oxygen in exchanging systems
 - 6.3. Internuclear double resonance (INDOR) experiments
 - 6.4. Isotope and temperature effects on the ^{17}O , ^1H coupling constant
- 7. Nuclear Quadrupole Coupling Constants
 - 7.1. Theoretical calculations
 - 7.1.1. Basic considerations
 - 7.1.2. Ab initio calculations of field-gradients
 - 7.1.3. Semi-empirical calculations: The Townes and Dailey approximation
 - 7.2. Experimental results: Empirical correlations

- 7.2.1. Oxygen bonded to group IA and IIA elements
 - 7.2.2. Oxygen bonded to group III elements
 - 7.2.3. Oxygen bonded to group IV elements
 - 7.2.4. Oxygen bonded to group V elements
 - 7.2.5. Oxygen bonded to group VI elements
 - 7.2.6. Oxygen bonded to group VII elements
 - 7.2.7. Oxygen bonded to transition metal elements
8. Relaxation Properties for Liquid Samples
- 8.1. Quadrupolar relaxation in the extreme narrowing condition
 - 8.2. Quadrupolar relaxation outside the extreme narrowing condition
 - 8.3. Effects of relaxation mechanisms other than quadrupolar
 - 8.3.1. Chemical shift anisotropy mechanism
 - 8.3.2. Dipole-dipole relaxation mechanism: Nuclear Overhauser effect $^{17}\text{O}-\{^1\text{H}\}$
 - 8.4. Scalar relaxation
 - 8.4.1. Fast quadrupolar relaxation
 - 8.4.2. Oxygen quadrupolar effects on other nuclei
 - 8.5. Relaxation in paramagnetic systems
 - 8.5.1. Theoretical background
 - 8.5.2. Determination of coordination numbers and investigation of kinetic parameters of chemical exchange
 - 8.6. Relaxation in the gas phase
 - 8.7. Applications
 - 8.7.1. Determination of ^{17}O nuclear quadrupolar coupling constants
 - 8.7.2. Dynamic and molecular reorientation studies
9. Selected Applications
- 9.1. Dynamic and kinetic studies
 - 9.1.1. Proton and oxygen exchange
 - 9.1.2. Carbonyl ligand exchange
 - 9.1.3. Equilibrium constant
 - 9.1.4. Ionic solvation: Diamagnetic and paramagnetic cations
 - 9.1.5. Variable-temperature and variable-pressure studies of ligand substitution reactions and ^{17}O exchange studies
 - 9.2. ^{17}O NMR and steric perturbation effects
 - 9.2.1. Torsion angle effects
 - 9.2.2. Non-torsional and in-plane deformation effects
 - 9.3. Hydrogen bonding effects
 - 9.3.1. Inter-molecular hydrogen bonding effects

- 9.3.2. Intra-molecular hydrogen bonding effects
- 9.4. Polyoxometalates
- 9.5. Heme proteins and model compounds: Substrate binding to enzymes
- 9.6. Peptides
- 9.7. Nucleosides, nucleotides and biophosphates
- 9.8. ^{17}O NMR as a mechanistic probe
 - 9.8.1. Decomposition, oxidation and reduction reactions
 - 9.8.2. Rearrangement, solvolysis and reversible condensation reactions
 - 9.8.3. Photochemical and ozonation reactions
 - 9.8.4. Biosynthetic studies
- 9.9. Hydration phenomena
 - 9.9.1. Basic background
 - 9.9.1.1. Triple quantum filtered ^{17}O NMR
 - 9.9.1.2. Nuclear spin relaxation dispersion
 - 9.9.2. Hydration of proteins
 - 9.9.3. Hydration of DNA and DNA-drug complexes
 - 9.9.4. Hydration of surfactant micelles and polyelectrolytes
- 10. ^{17}O NMR in Anisotropic Media
 - 10.1. Water orientation in lyotropic phases and bilayers: ^{17}O quadrupole splittings
 - 10.2. Determination of the ^{17}O nuclear quadrupolar coupling constant (χ) and asymmetry parameter (η).
- 11. ^{17}O NMR in the Solid State
 - 11.1. Basic considerations
 - 11.2. Static first-order spectra
 - 11.3. Static spectra and cross polarization
 - 11.4. Magic angle spinning observation of the central transition: Signal enhancement via population transfer
 - 11.5. Variable angle sample spinning
 - 11.6. Magic angle spinning and cross polarization
 - 11.7. Magic angle spinning observation of satellite transitions
 - 11.8. Double rotation NMR (DOR)
 - 11.9. Dynamic angle spinning (DAS)
 - 11.10. Nutation NMR
 - 11.11. Multiple quantum NMR
 - 11.12. Multiple resonance experiments for measuring X- ^{17}O distances
 - 11.13. Two dimensional heteronuclear correlation
 - 11.14. Selected applications

11.14.1. Crystalline and amorphous materials, glasses and melts

11.14.2. Micro- and mesoporous materials

11.14.3. Transition metal carbonyl complexes and clusters

11.14.4. High- T_c superconductors and anionic conductors

11.14.5. Biological macromolecules and model compounds

12. Miscellaneous Studies

12.1. Whole cell experiments

12.2. NMR imaging – In vivo magnetic resonance spectroscopy

Symbols and Abbreviations

Acknowledgments

References

B: MULTINUCLEAR NMR STUDIES OF MOLECULES OF BIOLOGICAL INTEREST

(in bold is indicated the principal author)

- 1b. "Hydrogen Bonding Effects on ^{31}P NMR Shielding in the Pyrophosphate Group of NADPH Bound to L.Casei Dihydrofolate Reductase".
I.P. Gerothanassis*, B. Birdsall and J. Feeney, *FEBS Letters* 291, 21-23 (1991). Medical Research Institute, London.
- 2b. " ^{31}P NMR Assignment and Conformational Study of NADPH Bound to Lactobacillus casei Dihydrofolate Reductase Based on two-Dimensional ^1H - ^{31}P Heteronuclear and ^1H Detected ^1H - ^{31}P Shift Correlation Experiments".
I.P. Gerothanassis, B. Birdsall, C. Bauer and J. Feeney*, *Eur. J. Biochem.* 204, 173-177 (1992). Medical Research Institute, London.
- 3b. "NMR Detection of Bound Water Molecules in the Active Site of Lactobacillus casei Dihydrofolate Reductase in Aqueous Solution".
I.P. Gerothanassis, B. Birdsall, C.J. Bauer, T.A.Frenkiel and J. Feeney*, *J. Mol. Biol.* 226, 549-554 (1992). Medical Research Institute, London.
- 4b. " ^{31}P NMR Studies of NADPH, NADP^+ and the Complex of NADPH and Methotrexate with Lactobacillus casei Dihydrofolate Reductase in the Solid State".
I.P. Gerothanassis, P.J. Barrie, B. Birdsall and J. Feeney*, *Eur. J. Biochem.* 226, 211-218 (1994). Medical Research Institute, London.
- 5b. " ^{31}P Solid-State NMR Measurements Used to Detect Interactions Between NADPH and Water and to Determine the Ionization State of NADPH and a Protein-Ligand Complex Subjected to Low-level Hydration".
I.P. Gerothanassis*, P.J. Barrie, B. Birdsall and J. Feeney*, *Eur. J. Biochem.* 235, 262-266 (1996). University of Ioannina.
- 6b. "Observation of Large Solvent Effects on the ^{31}P Shielding Tensor of a Cyclic Nucleotide".
I.P. Gerothanassis*, P.J. Barrie* and C. Tsanaktsidis, *J. Chem Soc., Chem. Commun.* 2639-2640 (1994). University of Ioannina.
- 7b. "Ab Initio Molecular Orbital Calculations of Solvent Clusters of Trans-N-methyl-acetamide: Structure, Ring Cluster Formation and Out-of-Plane Deformation".
I.N. Demetropoulos*, **I.P. Gerothanassis***, C. Vakka and C. Kakavas, *J. Chem. Soc., Faraday Trans.* 92, 921-931 (1996). University of Ioannina.
- 8b. "Thermodynamic Origin of Cis/Trans Isomers of a Proline-Containing β -turn Model Dipeptide in Aqueous Solution: A Combined Variable Temperature ^1H -NMR, Two Dimensional ^1H , ^1H Gradient Enhanced nuclear overhauser effect spectroscopy (NOESY), One-Dimensional Steady-

State Intermolecular ^{13}C , ^1H -NOE and Molecular Dynamics Study”.

A. Troganis, **I.P. Gerothanassis***, Z. Athanassiou, T. Mavromoustakos, G.E. Hawkes and C. Sakarellos, *Biopolymers*, 53, 72-83 (2000). University of Ioannina.

- 9b. “Solvation Properties of N-Substituted Cis and Trans Amides are not Identical: Significant Enthalpy and Entropy Changes are Revealed by the Use of Variable Temperature ^1H NMR in Aqueous and in Chloroform Solutions and Ab Initio Calculations”.

A. Troganis, E. Sicilia, K. Barbarossou, **I.P. Gerothanassis*** and N. Russo*, *J. Phys. Chem. A*, 109, 11878-11884 (2005). University of Ioannina.

- 10b. “Natural Abundance ^{15}N CP MAS NMR as a Novel Tool for Investigating Metal Binding to Nucleotides in the Solid State”

K. Barbarossou, A. E. Aliev, **I.P. Gerothanassis***, J. Anastassopoulou* and T. Theophanides, *Inorg. Chem* 40, 3626-3628(2001). University of Ioannina.

- 11b. “Is the Iron-Carbon-Oxygen Moiety Linear or Bent in Heme Model Compounds? Evidence for Non-Axially Symmetric Shielding Tensors from Carbon-13 CP MAS NMR Spectroscopy”.

I.P. Gerothanassis*, M. Momenteau, G.E. Hawkes and P.J. Barrie, *J. Am. Chem. Soc.* 115, 9796-9797 (1993). University of Ioannina.

- 12b. “Solid State ^{13}C NMR Evidence for a Large Deviation from Linearity of the Fe-C-O Unit in the CO Complex with Myoglobin”.

I.P. Gerothanassis*, P.J. Barrie*, M. Momenteau and G.E.Hawkes, *J. Am. Chem. Soc.* 116, 11944-11949 (1994). University of Ioannina.

- 13b. “Measuring the ^{13}C NMR Shielding Tensor of ^{13}CO Bonded to Haemoglobin”.

P.J. Barrie*, I.P. Gerothanassis, M. Momenteau and G.E. Hawkes, *J. Magn. Reson. B* 108, 185-188 (1995). University of Ioannina.

- 14b. “ ^{13}C CP/MAS NMR Studies of Hemoprotein Models With and Without an Axial Hindered Base: ^{13}C Shielding Tensors and Comparison With Hemoproteins and X-Ray Structural Data”.

I.P. Gerothanassis*, M. Momenteau*, P.J. Barrie, C.G. Kalodimos and G.E. Hawkes, *Inorg. Chem.* 35, 2674-2679 (1996). University of Ioannina.

- 15b. "Carbon-13 Nuclear Shieldings as a Novel Method in Estimating Porphyrin Ruffling in Hexacoordinated Superstructured Heme Model Compounds in Solution"

C.G. Kalodimos and **I.P. Gerothanassis***, *J. Am. Chem. Soc.* 120, 6407-6408 (1998). University of Ioannina.

- 16b. " ^{13}C Shieldings, ^{18}O Isotope Effects on ^{13}C Shieldings, and ^{57}Fe - ^{13}C spin Couplings of the Fe-C-O Unit in Superstructured Hemoprotein Models: Comparison with Hemoproteins, C-O Vibrational Frequencies, and X-ray Structural Data"

- C.G. Kalodimos, **I.P. Gerothanassis***, A. Troganis, B. Loock and M. Momenteau, *J. Biomol. NMR* 11, 1-13 (1998). University of Ioannina.
- 17b. "The Effects of Atropisomerism and Porphyrin Deformation on ^{57}Fe Shieldings in Superstructured Hemoprotein Models"
I.P. Gerothanassis*, C.G. Kalodimos, G.E. Hawkes and P. Haycock, *J. Magn. Reson.* 131, 163-165 (1998). University of Ioannina.
- 18b. " ^{13}C and ^{57}Fe NMR Studies of the Fe-C-O Unit of Heme Proteins and Synthetic Model Compounds in Solution: Comparison with IR Vibrational Frequencies and X-ray Structural Data"
C.G. Kalodimos, **I.P. Gerothanassis*** and G.E. Hawkes, *Biospectroscopy*, 4, S57-S69 (1998). University of Ioannina.
- 19b. "Iron-57 Nuclear Shieldings as a Quantitative Tool for Estimating Porphyrin Ruffling in Hexacoordinated Carbonmonoxy Heme Model Compounds in Solution".
C.G. Kalodimos, **I.P. Gerothanassis***, E. Rose, G.E. Hawkes and R. Pierattelli, *J. Am. Chem. Soc.*, 121, 2903-2908 (1999). University of Ioannina.
- 20b. "Nitrogen-14 nuclear magnetic resonance of the amino terminal group of leu-enkephalin in aqueous solution".
I.P. Gerothanassis*, T. Karayannis, M. Sakarellos-Daitsiotis, C. Sakarellos and M. Marraud, *J. Magn. Reson.* 75, 513-516 (1987). University of Ioannina.
- 21b. "Multiple-Quantum ^1H - ^{15}N Chemical Shift Correlation Spectroscopy of the Peptide Hormone Leu-enkephalin in Solution".
I.P. Gerothanassis*, M. Bourdonneau, T. Karayannis, M. Sakarellos-Daitsiotis and C. Sakarellos, *J. Magn. Reson.* 80, 309-313 (1988). University of Ioannina.
- 22b. "On the Molecular Basis of the Recognition of Angiotensin II (AII). NMR Structure of AII in Solution Compared with the X-ray Structure of AII bound to the mAb Fab131".
A.G. Tzakos, A.M. Bonvin, A. Troganis, P. Cordopatis, M.L. Amzel, **I.P. Gerothanassis***, and N.A. van Nuland, *Eur. J. Biochem.* 270, 849-860 (2003). University of Ioannina.
- 23b. "Structure - Function Discrimination of the N- and the C- Catalytic Domains of Human Angiotensin-Converting Enzyme: Implications for Cl^- Activation and Peptide Hydrolysis Mechanisms".
A. Tzakos, S. Galanis, G. Spyroulias, P. Cordopatis, E. Zoupa, and **I.P. Gerothanassis***, *Protein Engin.* 16, 993-1003 (2003). University of Ioannina.
- 24b. "On the Structural Basis of the Hypertensive Properties of Angiotensin II: A Solved Mystery or a Controversial Issue?".

- A.G. Tzakos, A. Troganis and **I.P. Gerothanassis***, *Current Topics in Medicinal Chemistry*, 4, 431-444 (2004). University of Ioannina.
- 25b. “Domain-Selective Ligand-Binding Modes and Atomic Level Pharmacophore Refinement in Angiotensin I Converting Enzyme (ACE) Inhibitors”.
A.G. Tzakos and **I.P. Gerothanassis***, *ChemBioChem*. 6, 1089-1103 (2005). University of Ioannina.
- 26b. “The Molecular Basis for the Selection of Captopril cis and trans Conformations by Angiotensin I Converting Enzyme”.
A. G. Tzakos, N. Naqvi, K. Comporozos, R. Piarattelli, V. Theodorou, A. Husain* and **I.P. Gerothanassis***, *Bioorg. Med. Chem. Lett.*, 16, 5084-5087 (2006). University of Ioannina.
- 27b. “NMR and Molecular Dynamics Studies of an Autoimmune Myelin Basic Protein Peptide and its Antagonist. Structural Implications for the MHC II (1-A⁴) – Peptide Complex through Docking Calculations”.
A.G. Tzakos, P. Fuchs, N.A.J. van Nuland, A. Troganis, T. Tselios, J. Matsoukas, **I.P. Gerothanassis*** and A.M.J. Bonvin, *Eur. J. Biochem*. 271, 3399-3413 (2004). University of Ioannina.
- 28b. “Structure and Function of the Myelin Proteins: Current Status and Perspectives in Relation to Multiple Sclerosis”.
A.G. Tzakos, P. Kursula, A. Troganis, V. Theodorou, T. Tselios, C. Svarnas, J. Matsoukas, V. Apostolopoulos and **I.P. Gerothanassis**, *Current Med. Chem*. 12, 1569-1587 (2005). University of Ioannina.
- 29b. A Structural Charecterization of Human SCO₂”
L. Banci, I. Bertini*, S. Ciofi – Baffoni, I.P. Gerothanassis, I. Leontari, M. Martinelli and S. Wang, *Structure* 15, 1132-1140 (2007). University of Ioannina.

MULTINUCLEAR NMR STUDIES OF MOLECULES OF BIOLOGICAL INTEREST

(in bold is indicated the principal author)

Investigation of Hydrogen Bonding and Solvation Phenomena

The mode of bending of NADPH to the enzyme dihydrofolate reductase (DHFR) has been well-characterized using x-ray and NMR methods. Extensive ^{31}P NMR studies of the DHFR·NADPH and DHFR·NADPH·MTX complexes of the *L. casei* enzyme have shown that whereas the ^{31}P resonance of the nicotinamide pyrophosphate P(n) is shifted only by ~ 0.16 ppm to high frequency, the ^{31}P resonance of the adenine pyrophosphate P(a) shows a large low frequency shift (2.69-2.55 ppm). It was suggested [Feeney et al., *Nature* 257, 564-566 (1975); *Int. J. Biol. Macromol.* 2, 251-255 (1980); *Biochemistry* 20, 7186-7195 (1985); *Biochemistry* 20, 145-153 (1981)] that this shift might arise from a combination of electric field effects and charge redistribution effects accompanied by small changes in the P-O-P bond angles. In this communication [**I.P. Gerothanassis***, B. Birdsall and J. Feeney, *FEBS Letters* 291, 21-23 (1991)] we draw attention to the effects of changes in hydrogen bonding on the ^{31}P shielding of the two pyrophosphate phosphorus nuclei of NADPH in its complex with *L. casei* DHFR as deduced from the striking differences in hydrogen bonding patterns of the two phosphate groups determined by X-ray crystallography. These factors have received relatively little attention in interpreting ^{31}P chemical shifts in biomolecules. Crystallographic refinement of the ternary complex *L. casei* DHFR·NADPH·MTX [Mathews, D.A. et al. *J. Biol. Chem.* 257, 13650-13662 (1982); 13663-13672 (1982)] have revealed that the pyrophosphate oxygen O1(Pn) of the nicotinamide 5' phosphate group is at a short hydrogen bonding distance (2.7 Å) from the oxygen of the water molecule 276, Wat-276, and forms two further hydrogen bonds with enzyme residues (peptide NHs of Ala-100 and Gln-101). The oxygen O2P forms hydrogen bonds with two molecules of H₂O, Wat-301 and Wat-302, and forms a further hydrogen bond to NH1 of Arg-44. It can therefore be concluded that the solvent accessibility of the nicotinamide 5' phosphate group results in a largely aqueous-like environment similar to that of the free NADPH and therefore giving rise to similar ^{31}P NMR shieldings. By contrast the solvent accessibility of the adenine 5' phosphate group is restricted and no interacting solvation molecules of water are observed in the X-ray structure. The oxygens of the adenine 5' phosphate, O1P(a) and O2P(a) are both only hydrogen bonded to protein residues. It can therefore be concluded from the comparison of ^{31}P NMR chemical shift data and X-ray structural data for complexes of NADPH with *L. casei* dihydrofolate reductase that solvation (hydration) effects play a major role in influencing the ^{31}P shielding of the pyrophosphate nuclei whereas changes in P-O-C₅-H_{5'} torsion angle have little effect.

For any detailed NMR conformational study of a protein – ligand complex it is essential to have specific resonance assignments. We have assigned the pyrophosphate ^{31}P resonances in spectra of NADPH bound to *Lactobacillus casei* dihydrofolate reductase (DHFR) by using a combination of ^1H - ^{31}P -heteronuclear shift-correlation (HETCOR), ^1H - ^{31}P -heteronuclear multiple-quantum-coherence

correlation spectroscopy (HMQC-COSY), ^1H - ^1H COSY, homonuclear Hartmann-Hahn (HOHAHA) and NOE spectroscopy (NOESY) experiments [I.P. Gerothanassis, B. Birdsall, C. Bauer and J. Feeney*, *Eur. J. Biochem.* 204, 173-177 (1992)]. The nicotinamide pyrophosphate phosphorus, P(n), has been unequivocally assigned to a signal (-14.07 ppm) which shows a large $^3\text{J}_{\text{P-O-C-H}}$ coupling constant. Such a coupling constant when combined with the appropriate Karplus relationship provides conformational information about the P-O-C-H torsion angle. The torsion angle changes by $65^\circ \pm 10^\circ$ for the binary complex compared with the value in free NADPH. The observed coupling constants for the binary (DHFR – NADPH) and ternary (DHFR – NADPH – methotrexate) complexes (12.3 and 10.5 ± 0.6 Hz, respectively) indicate that the pyrophosphate group has a similar conformation in the two complexes.

Proton nuclear magnetic resonance spectroscopy has been used to detect two water molecules bound to residues in the active site of the *Lactobacillus casei* dihydrofolate reductase (DHFR) [I.P. Gerothanassis, B. Birdsall, C.J. Bauer, T.A. Frenkiel and J. Feeney*, *J. Mol. Biol.* 226, 549-554 (1992)]. Their presence was detected by measuring nuclear Overhauser effects between NH protons in protein residues and protons in the individual bound water molecules in two-dimensional nuclear Overhauser effect spectroscopy (NOESY), in nuclear Overhauser effect spectroscopy in the rotating frame (ROESY) and three-dimensional ^1H - ^{15}N ROESY-heteronuclear multiple quantum coherence spectra recorded on samples containing appropriately ^{15}N -labelled DHFR. For the DHFR-methotrexate-NADPH complex, two bound molecules were found, one close to the Trp5 amide NH proton and the other near to the Trp21 indole HE1 proton: these correspond to two of the water molecules (Wat201 and Wat253) detected in the crystal structure studies described by Bolin and co-workers. However, the nuclear magnetic resonance experiments did not detect any of the other bound water molecules observed in the X-ray studies. The nuclear magnetic resonance results indicate that the two bound water molecules that were detected have lifetimes in the solution state that are longer than approximately two nanoseconds. This is of considerable interest, since one of these water molecules (Wat253) has been implicated as the likely proton donor in the catalytic reduction of dihydrofolate to tetrahydrofolate.

^{31}P -NMR spectra on solid samples of NADP^+ , NADPH and NADPH bound to *Lactobacillus casei* dihydrofolate reductase have been recorded using the techniques of cross polarisation, magic angle spinning and high power proton decoupling [I.P. Gerothanassis, P.J. Barrie, B. Birdsall and J. Feeney*, *Eur. J. Biochem.* 226, 211-218 (1994)]. The isotropic chemical shifts, the principal components of the shielding tensors and the asymmetry parameters for the ^{31}P nuclei in the 2'-phosphate and pyrophosphate groups have been measured. The isotropic shifts show similar trends to the chemical shifts measured in solution. The isotropic shifts and the shielding tensors for the dianionic and monoanionic states of the 2'-phosphate group have been determined and the presence of both ionisation states has been detected in a solid sample of the lyophilised complex of *L. casei* dihydrofolate reductase with NADPH and methotrexate. This contrasts with the behaviour in solution, where only the dianionic

form is bound to the enzyme. The signals from the two pyrophosphates ^{31}P nuclei in bound NADPH were resolved and identified. The asymmetry parameters in the different ionisation states and the orientations of the shielding tensors within the molecular framework are considered in the context of previous ^{31}P studies on phosphate-containing compounds.

^{31}P -NMR spectra of NADPH and NADPH bound to *Lactobacillus casei* dihydrofolate reductase have been recorded using the techniques of cross-polarization, magic-angle spinning and high-power proton-decoupling on both lyophilized and hydrated samples [I.P. Gerotheranassis*, P.J. Barrie, B. Birdsall and J. Feeney*, *Eur. J. Biochem.* 235, 262-266 (1996)]. Previous studies on the lyophilized complex of *L. casei* dihydrofolate reductase with NADPH and methotrexate, measuring the isotropic shifts and principal components of the chemical shift tensors, have shown that the 2'-phosphate group of bound NADPH exists as a mixture of the dianionic and monoanionic states [Gerotheranassis, I.P., Barrie, P.J., Birdsall, B. & Feeney, J. (1994) *Eur. J. Biochem.* 226, 211–218]. In the present study on hydrated samples, the characterization of the isotropic shift and chemical shift tensors of the 2'-phosphate signal indicates that the 2'-phosphate is almost exclusively in the dianionic state. This is in agreement with earlier ^{31}P -NMR studies in solution [Feeney, J., Birdsall, B., Roberts, G.C.K. & Burgen, A. S. V. (1975) *Nature* 257, 564–566], In experiments examining progressively hydrated (6%, 12%, 15%, by mass) samples, the observed signals become increasingly narrower probably because the microenvironments of the ^{31}P nuclei become more homogeneous upon sample hydration. Chemical exchange between mobile water molecules and bound protons close to individual sites on NADPH has been indirectly monitored on a hydrated sample (15% water, by mass) using a pulse sequence proposed by Harbison and coworkers [Harbison, G.S., Roberts, J.E., Herzfeld, J. & Griffin, R.G. *J. Am. Chem. Soc.* 110, 7221–7223 (1988)]. In this experiment, the two diphosphate signals are totally suppressed while the 2'-phosphate phosphorus signal remains: this indicates a significant polarization of the 2'-phosphate nuclei from protons in exchange with those of mobile water molecules.

^{31}P NMR spectroscopy has been extensively used to probe the structure and dynamics of nucleic acids and nucleic acid complexes in solution. Although no single factor can rationalize the range of isotropic chemical shifts, experimental and theoretical studies indicate that the chemical shift is dependent upon both the P-O-P bond angles and the torsional angles which describe the orientation of the R-O bond relative to the plane of the O-P-O group. This has prompted many workers to interpret ^{31}P shieldings of various polynucleotide systems in solution almost entirely in terms of the conformation of the phosphodiester group [D.G. Gorenstein, *Chem. Rev.* 87, 1047 (1987); 94, 1315 (1994)]. In this communication [I.P. Gerotheranassis*, P.J. Barrie* and C. Tsanaktsidis, *J. Chem. Commun.* 2639-2640 (1994)] we reported ^{31}P shielding tensor measurements on a phosphodiester nucleotide as a powder and in frozen solutions of water and dimethylsulfoxide (DMSO). The results suggest for the first time a significant influence of hydrogen bonding on ^{31}P shielding tensor and isotropic chemical shift. The nucleotide chosen was the sodium salt of adenosine 3',5'- cyclic monophosphate (3',5'- cAMP) in

which the phosphodiester group is part of a six-membered ring in a fixed chair conformation and thus is expected to have negligible change in conformation with solvent. A significant difference in the overall anisotropy (manifested in the $\Delta\sigma$ and Ω parameters) is observed between the three different states (Table 1). The span varies from 226 ppm for 3',5'- cAMP in DMSO, which is expected to have no hydrogen bonding to the phosphodiester group and to reduce any intermolecular hydrogen bonding interactions which might persist in the solid, to 200 ppm for 3',5'- cAMP in water. This change in anisotropy is due principally to a large variation in the δ_{33} component to high frequency with increased hydrogen bonding (by ca. 18 ppm), which is only partially compensated by a smaller shift to low frequency in the δ_{11} component (by ca. 8 ppm). This results in a change greater than 1 ppm in the isotropic shift which must be due to hydrogen bonding considerations alone. Bearing in mind that the spread of ^{31}P shieldings in solution for duplex DNA fragments is generally less than 0.7 ppm, it is evident that hydrogen bonding to the phosphate group is a key factor, together with conformational changes, in determining ^{31}P isotropic chemical shifts.

TABLE 1. ^{31}P Shielding tensor results on 3',5'- cAMP^a

State	T/K	δ_{iso}	δ_{11}	δ_{22}	δ_{33}	$\Delta\sigma/\text{ppm}$	η	Ω/ppm	κ
Powder	295	-1.1	91	33	-127	189	0.46	218	0.47
	203	-1.5	89	33	-126	187	0.45	215	0.48
H ₂ O (frozen solution)	258	-1.7							
	233	-1.5	83	31	-118	175	0.45	201	0.48
	203	-1.5	83	28	-116	172	0.48	199	0.44
DMSO (frozen solution)	263	-3.0							
	233	-2.8	90	37	-135	199	0.40	225	0.53
	203	-2.9	92	34	-135	198	0.44	227	0.49

^aThe shielding tensor components are given as chemical shifts, δ , rather than shieldings, σ , which have the opposite sign, using the convention $\delta_{11} > \delta_{22} > \delta_{33}$. The other parameters given are the anisotropy, $\Delta\sigma$, defined as $0.5(\delta_{11} + \delta_{22}) - \delta_{33}$; the asymmetry parameter, η , defined as $(\delta_{11} - \delta_{22})/(\delta_{33} - \delta_{\text{iso}})$; the span, Ω , defined as $\delta_{11} - \delta_{33}$; and the skew, κ , defined as $3(\delta_{22} - \delta_{\text{iso}})/\Omega$. The isotropic chemical shift is accurate within 0.5 ppm, while the estimated error in the individual shielding tensor components (95% confidence intervals but ignoring the effect of spectral noise) is less than 2 ppm.

The solvation of *trans* amides has been investigated by the use of full gradient optimization *ab initio* quantum mechanical calculation techniques [I.N. Demetropoulos*, I.P. Gerathanassis*, C. Vakka and C. Kakavas, *J. Chem. Soc., Faraday Trans.* 92, 921-931 (1996)]. The complexes have been determined at the Hartree–Fock (HF) level with a 4-31G*/4-31G** basis set and at the second-order Møller–Plesset perturbation (MP2) level. Three NMA–water clusters were investigated: *trans*-NMA with two molecules of water forming a ring cluster at the amide oxygen; *trans*-NMA with two molecules of water at the amide oxygen forming hydrogen bonds along the direction of the lone-pair electrons; *trans*-NMA with one molecule of water at the CO group and one at the NH group. In addition, 4-31G* basis set calculations for *trans*-NMA with two molecules of acetonitrile were

performed. The C=O...H(W) hydrogen bond lengths, electron-density population analysis and molecular-orbital analysis of *trans*-NMA with two molecules of water at the amide oxygen demonstrate the importance of concurrent water–water and water–(carbonyl) oxygen hydrogen-bond interactions. The complex of *trans*-NMA with two molecules of water forming a ring cluster at the amide oxygen indicates the formation of a non-planar amide bond and the generation of a chiral centre at the amide nitrogen; this structure has a 5 % Boltzmann distribution at room temperature at the MP2 level. Vibrational-frequency analysis shows that its hydrogen-bonded water molecules are vibrationally coupled. Orbital analysis suggests that there is a considerable solute-occupied space reorganization caused by the rearrangement of the water solvent molecules. Comparisons were made with previous theoretical studies of amide–water interactions and experimental spectroscopic, X-ray and neutron-diffraction data on the hydration of amides, peptides and proteins.

The *cis/trans* conformational equilibrium of the two Ac-Pro isomers of the β -turn model dipeptide [^{13}C]-Ac-L-Pro-D-Ala-NHMe, 98% ^{13}C enriched at the acetyl carbonyl atom, was investigated by the use of variable temperature gradient enhanced ^1H -nmr, two-dimensional (2D) ^1H , ^1H nuclear Overhauser effect spectroscopy (NOESY), ^{13}C , ^1H one-dimensional steady-state intermolecular NOE, and molecular dynamics calculations [A. Troganis, **I.P. Gerothanassis***, Z. Athanassiou, T. Mavromoustakos, G.E. Hawkes and C. Sakarellos, *Biopolymers*, 53, 72-83 (2000)]. The temperature dependence of the *cis/trans* Ala(NH) protons are in the region expected for random-coil peptides in H_2O ($\Delta\delta/\Delta T = -9.0$ and -8.9 ppb for the *cis* and *trans* isomers, respectively). The *trans* NH(CH₃) proton indicates smaller temperature dependence ($\Delta\delta/\Delta T \sim -4.8$ ppb) than that of the *cis* isomer (-7.5 ppb). 2D ^1H , ^1H NOESY experiments at 273 K demonstrate significant NOEs between ProH ^{α} - AlaNH and AlaNH - NH(R) for the *trans* isomer. The experimental NOE data, coupled with computational analysis, can be interpreted by assuming that the *trans* isomer most likely adopts an ensemble of folded conformations. The C-CONH(CH₃) fragment exhibits significant conformational flexibility; however, a low-energy conformer resembles closely the β II-turn folded conformations of the x-ray structure of the related model peptide *trans*-BuCO-L-Pro-Me-D-Ala-NHMe. On the contrary, the *cis* isomer adopts open conformations. Steady-state intermolecular solute-solvent (H_2O) ^{13}C , ^1H NOE indicates that the water accessibility of the acetyl carbonyl carbons is nearly the same for both isomers. This is consistent with rapid fluctuations of the conformational ensemble and the absence of a highly shielded acetyl oxygen from the bulk solvent. Variable temperature ^1H -nmr studies of the *cis/trans* conformational equilibrium indicate that the *trans* form is enthalpically favored ($\Delta H^\circ = -5.14$ kJ mole⁻¹) and entropically ($\Delta S^\circ = -5.47$ J·K⁻¹·mole⁻¹) disfavored relative to the *cis* form. This demonstrates that, in the absence of strongly stabilizing sequence-specific interresidue interactions involving side chains and/or charged terminal groups, the thermodynamic difference of the *cis/trans* isomers is due to the combined effect of intramolecular and intermolecular (hydration) induced conformational changes.

The cis/trans conformational equilibrium of N-methyl formamide (NMF) and the sterically hindered tert-butylformamide (TBF) was investigated by the use of variable temperature gradient ^1H NMR in aqueous solution and in the low dielectric constant and solvation ability solvent CDCl_3 and various levels of first principles calculations [A. Troganis, E. Sicilia, K. Barbarossou, **I.P. Gerotheranassis*** and N. Russo*, *J. Phys. Chem. A*, 109, 11878-11884 (2005)]. The trans isomer of NMF in aqueous solution is enthalpically favored relative to the cis ($\Delta H^\circ = -5.79 \pm 0.18 \text{ kJ mol}^{-1}$) with entropy differences at 298 K ($298 \cdot \Delta S^\circ = -0.23 \pm 0.17 \text{ kJ mol}^{-1}$) playing a minor role. The experimental value of the enthalpy difference strongly decreases ($\Delta H^\circ = -1.72 \pm 0.06 \text{ kJ mol}^{-1}$), and the contribution of entropy at 298 K ($298 \cdot \Delta S^\circ = -1.87 \pm 0.06 \text{ kJ mol}^{-1}$) increases in the case of the sterically hindered tert-butylformamide. The trans isomer of NMF in CDCl_3 solution is enthalpically favored relative to the cis ($\Delta H^\circ = -3.71 \pm 0.17 \text{ kJ mol}^{-1}$) with entropy differences at 298 K ($298 \cdot \Delta S^\circ = 1.02 \pm 0.19 \text{ kJ mol}^{-1}$) playing a minor role. In the sterically hindered tert-butylformamide, the trans isomer is enthalpically disfavored ($\Delta H^\circ = 1.60 \pm 0.09 \text{ kJ mol}^{-1}$) but is entropically favored ($298 \cdot \Delta S^\circ = 1.71 \pm 0.10 \text{ kJ mol}^{-1}$). The results are compared with literature data of model peptides. It is concluded that, in amide bonds at 298 K and in the absence of strongly stabilizing sequence-specific inter-residue interactions involving side chains, the free energy difference of the cis/trans isomers and both the enthalpy and entropy contributions are strongly dependent on the N-alkyl substitution and the solvent. The significant decreasing enthalpic benefit of the trans isomer in CDCl_3 compared to that in H_2O , in the case of NMF and TBF, is partially offset by an adverse entropy contribution. This is in agreement with the general phenomenon of enthalpy versus entropy compensation. B3LY/6-311++G** and MP2/6-311++G** quantum chemical calculations confirm the stability orders of isomers and the ΔG decrease in going from water to CHCl_3 as solvent. However, the absolute calculated values, especially for TBF, deviate significantly from the experimental values. Consideration of the solvent effects via the PCM approach on $\text{NMF} \cdot \text{H}_2\text{O}$ and $\text{TBF} \cdot \text{H}_2\text{O}$ supermolecules improves the agreement with the experimental results for TBF isomers, but not for NMF.

The involvement of metal ions and their biological significance in nucleic acid processes has been well documented. The crucial role of a direct metal ion binding to N(7) of the purine residue has been emphasized by several investigators [A. Sigel; B. Song in *Metal Ions in Biological Systems*; A. Sigel, H. Sigel, Eds. Marcel Dekker: New York, Vol. 32, pp 135-205 (1996)]. However, one impediment to the definitive evaluation of the importance of the N(7) binding is the lack of effective direct spectroscopic criteria for its assessment. Nitrogen-15 NMR has the potential to provide local information about inter- and intramolecular interactions to nitrogen sites. However, no clear evidence has been given on the effect of metal binding to the ^{15}N shieldings. Natural abundance ^{15}N CP MAS was proposed as a novel tool for investigating [K. Barbarossou, A.E. Alier, **I.P. Gerotheranassis***, J. Anastassopoulou* and T. Theophanides, *Inorg. Chem.* 40, 3626-3628 (2001)] metal coordination to mononucleotides. Chemical shift changes could be correlated, at least to a first approximation, with the strength and directionality of metal to nitrogen coordination. The N(7) resonance absorption in

$\text{Cd}(5'\text{-GMP})\cdot 5\text{H}_2\text{O}$ is strongly shielded by -29.6 and -31.9 ppm compared to that of the Na^+ and Ba^{2+} complexes, respectively. This demonstrates significantly different binding modes to N(7), although X-ray structural data have been interpreted in terms of direct metal ion-N(7) interaction for Na^+ , Ba^{2+} , and Cd^{2+} complexes. Unambiguous demonstration of a direct Cd-N coordination bond was provided by the ^{113}Cd CPMAS NMR spectrum, which indicates the presence of an asymmetric 1:1:1 triplet due to (^{113}Cd , ^{14}N) indirect and residual dipolar spin-spin interaction. The effect of hydration was also investigated. This approach should be particularly valuable in studies of site specifically ^{15}N labeled DMA and RNA fragments in the solid state.

Investigation of Heme Proteins and Synthetic Models

Heme models have been widely used to understand the bonding of small molecules such as carbon monoxide to hemoproteins. The Fe-CO unit has been established crystallographically as being linear normal to the heme plane for several protein-free CO adducts of iron (II) porphyrins. By contrast crystallographic studies of several CO hemoproteins have been interpreted in favor of bent and/or titled Fe-C-O moieties. In this communication [I.P. Gerothanassis*, M. Momenteau, G.E. Hawkes and P.J. Barrie, *J. Am. Chem. Soc.* 115, 9796-9797 (1993)], ^{13}C cross-polarization magic – angle – spinning (CP/MAS) NMR spectra of several carbon monoxide (93-99% ^{13}C enriched) hemoprotein models indicated that the principal components of the ^{13}CO chemical shift tensor elements and asymmetry parameters are a novel tool for investigating whether the iron – carbon – oxygen moiety is linear or bent. An asymmetry in the shielding tensor must result either from a non-linear Fe-C-O moiety or alternatively from molecular asymmetry or crystal packing affecting the electronic distribution. However, detailed X-ray structural studies of deoxy, picket fence porphyrins show that there are no intermolecular contacts less than 3.5 Å. It can therefore be concluded that the major effect of the shielding asymmetry observed for some model compounds should be attributed to a bending of the Fe-C-O moiety.

The application of high-resolution solid-state ^{13}C NMR spectroscopy to investigate the bonding between carbon monoxide and myoglobin was explored [I.P. Gerothanassis*, P.J. Barrie*, M. Momenteau and G.E. Hawkes, *J. Am. Chem. Soc.* 116, 11944-11949 (1994)]. Selective pulse sequences (non-quaternary suppression and SELDOM) significantly reduce the problem of ^{13}CO peaks overlapping with those arising from the natural ^{13}C abundance myoglobin molecule. This enables the ^{13}CO spinning sideband manifold to be measured and, hence, the principal components of the ^{13}CO chemical shift tensor to be obtained. Results were obtained on two samples of myoglobin: one a *dry* powder and the other carefully prepared needle-like crystals containing water of crystallization. The spectra show that there is a large increase in the asymmetry of the ^{13}C shielding tensor in ^{13}CO -myoglobin compared to heme model compounds containing close to linear Fe-C-O moieties. FTIR measurements of both myoglobin samples show that the major ν_{co} stretching frequency is due to the **A3**

conformer. It can be concluded that in this particular CO-myoglobin substate there must be substantial deviation from linearity of the Fe-C-O unit, probably due to a significant polar interaction with the distal histidine. Similar studies have been extended to ^{13}C CO bonded to haemoglobin (P.J. Barrie*, I.P. Gerotheranassis, M. Momenteau and G.E. Hawkes, *J. Magn. Reson. B* 108, 185-188 (1995)).

^{13}C cross-polarization magic-angle-spinning (CP/MAS) NMR spectra of several carbonmonoxide (93–99% ^{13}C enriched) hemoprotein models with 1,2-dimethylimidazole (1,2-diMeIm) and 1-methylimidazole (1-MeIm) as axial ligands were reported [I.P. Gerotheranassis*, M. Momenteau*, P.J. Barrie, C.G. Kalodimos and G.E. Hawkes, *Inorg. Chem.* 35, 2674-2679 (1996)]. This enables the ^{13}C CO spinning sideband manifold to be measured and hence the principal components of the ^{13}C CO chemical shift tensor to be obtained. Negative polar interactions in the binding pocket of the cap porphyrin model and inhibition of Fe→CO back-donation result in a reduction in shielding anisotropy; on the contrary, positive distal polar interactions result in an increase in the shielding anisotropy and asymmetry parameter in some models. It appears that the axial hindered base 1,2-dimethylimidazole has little direct effect on the local geometry at the CO site, despite higher rates of CO desorption being observed for such complexes. This suggests that the mechanism by which steric interactions are released for the 1,2-diMeIm complexes compared to 1-MeIm complexes does not involve a significant increase in bending of the Fe–C–O unit. The asymmetry of the shielding tensor of all the heme model compounds studied is smaller than that found for horse myoglobin and rabbit hemoglobin.

The reversible binding of carbon monoxide and dioxygen has played a central role in studies of heme protein structure and function. Initial attention focused on the bent vs linear Fe-C-O unit and on the possibility that the CO binding is inhibited by steric interactions that impeded a linear geometry. More recently emphasis has been given to polar interactions in the binding pocket, ruffling distortion of the porphyrin ring, and expansion of the distal cavity. A porphyrin is ruffled when opposite pyrrole rings are counter-rotated so that the meso carbon atoms (C_{meso}) of each pyrrole ring are alternately displaced above and below the mean porphyrin plane. In this communication [C.G. Kalodimos and I.P. Gerotheranassis*, *J. Am. Chem. Soc.* 120, 6407-6408 (1998)], ^{13}C NMR shielding of the meso carbons of several carbon monoxide (99.7% ^{13}C enriched) hexa coordinated superstructured hemoprotein models are demonstrated to be a sensitive novel method for estimating porphyrin ruffling. When the average shielding of the meso carbons $\delta(^{13}\text{C}_{\text{m,av}}, \text{ppm})$, are plotted against the absolute crystallographic average displacement of the C_{meso} relative to the porphyrin core mean plane, $|C_{\text{m}}|(\text{\AA})$, then, an excellent linear correlation is observed which can be expressed as $\delta(^{13}\text{C}_{\text{m,av}}, \text{ppm}) = 115.16 - 4.0049 |C_{\text{m}}|(\text{\AA})$ with a correlation coefficient of 0.985.

^{13}C NMR spectra of several carbon monoxide (99.7% ^{13}C and 11.8% ^{18}O enriched) hemoprotein models with varying polar and steric effects of the distal organic superstructure and constraints of the proximal side were reported [C.G. Kalodimos, I.P. Gerotheranassis*, A. Troganis, B. Looock and M. Momenteau, *J. Biomol. NMR* 11, 423-435 (1998)]. This enables the ^{57}Fe - $^{13}\text{C}(\text{O})$ coupling constants,

$^1J_{\text{Fe}-^{13}\text{C}}$, ^{13}C shieldings ($\delta(^{13}\text{C})$), and ^{18}O isotope effects on ^{13}C shieldings ($^1\Delta^{13}\text{C}(^{18}\text{O}/^{16}\text{O})$) to be measured and hence comparisons with hemoproteins, C-O vibrational frequencies and X-ray structural data to be made. Negative polar interactions in the binding pocket and inhibition of Fe/ \rightarrow /CO back-donation or positive distal polar interactions with amide NH groups appear to have little direct effect on $^1J_{\text{Fe}-^{13}\text{C}}$ couplings. Similarly, the axial hindered base 1,2-dimethylimidazole has a minor effect on the $^1J_{\text{Fe}-^{13}\text{C}}$ values despite higher rates of CO desorption being observed for such complexes. On the contrary, ^{13}C shieldings vary widely and an excellent correlation was found between the infrared C-O vibrational frequencies ($\nu(\text{C-O})$) and ^{13}C shieldings and a reasonable correlation with ^{18}O isotope effects on ^{13}C shieldings. This suggests that $\delta(^{13}\text{C})$, $\nu(\text{C-O})$ and $^1\Delta^{13}\text{C}(^{18}\text{O}/^{16}\text{O})$ are accurate monitors of the multiple mechanisms by which steric and electronic interactions are released in superstructured heme model compounds. The ^{13}C shieldings of heme models cover a 4.0 ppm range which is extended to 7.0 ppm when several HbCO and MbCO species at different pH values are included. The latter were found to obey a similar linear $\delta(^{13}\text{C})$ versus $\nu(\text{C-O})$ relationship, which proves that both heme models and heme proteins are homogeneous from the structural and electronic viewpoint. Our results suggest that $\nu(\text{C-O})$, $\delta(^{13}\text{C})$ and $^1\Delta^{13}\text{C}(^{18}\text{O}/^{16}\text{O})$ measurements reflect similar interaction which is primarily the modulation of π back-bonding from the Fe d_π to the CO π^* orbital by the distal pocket polar interactions. The lack of correlation between $^1\Delta^{13}\text{C}(^{18}\text{O}/^{16}\text{O})$ and crystallographic CO bond lengths ($r(\text{C-O})$) reflects significant uncertainties in the X-ray determination of the carbon and oxygen positions.

Iron is a central element in all heme proteins and the extremely large ^{57}Fe chemical shift range offers, in principle, a very sensitive direct probe of the functionally interesting diamagnetic low spin ferrous state. The low natural abundance of ^{57}Fe (2.2%) is readily remedied by isotopic enrichment, and the shielding anisotropy is an efficient spin-lattice relaxation mechanism. In this communication [I.P. Gerothanassis*, C.G. Kalodimos, G.E. Hawkes and P. Haycock, *J. Magn. Reson.* 131, 163-165 (1998)], ^{57}Fe NMR chemical shifts of superstructured heme model compounds have been found to be extremely sensitive to atropisomerism and deformation (ruffling) of the porphyrin geometry. The ^{57}Fe chemical shifts vary by more than 50 ppm between the various models and in a seemingly regular fashion, giving an increased shielding with increased ruffling. It is concluded, in agreement with Baltzer's work [L. Baltzer and M. Landergrén, *J. Am. Chem. Soc.* 112, 2804 (1990)], that the effect of perturbation of the iron d orbital energies on ^{57}Fe shieldings is much larger than that observed upon changing the ligands in an octahedral complex.

^{57}Fe chemical shifts vary by more than 500 ppm between the various models and in a seemingly regular fashion, giving an increased shielding with increased ruffling. ^{13}C - and ^{57}Fe -NMR spectra of several carbon monoxide hemoprotein models with varying polar and steric effects of the distal organic superstructure, constraints of the proximal side, and solvent polarity were reported [C.G. Kalodimos,

I.P. Gerotheranassis* and G.E. Hawkes, *Biospectroscopy*, 4, S57-S69 (1998)]. The ^{13}C shieldings of heme models cover a 4.0 ppm range that is extended to 7.0 ppm when several hemoglobin CO and myoglobin CO species at different pHs are included. Both heme models and heme proteins obey a similar excellent linear $\delta(^{13}\text{C})$ versus $\nu(\text{C}-\text{O})$ relationship that is primarily due to modulation of π backbonding from Fe d_{π} to the CO π^* orbital by the distal pocket polar interactions. There is no direct correlation between $\delta(^{13}\text{C})$ and Fe-C-O geometry. The poor monotonic relation between $\delta(^{13}\text{C})$ and $\nu(\text{Fe}-\text{C})$ indicates that the iron-carbon π bonding is not a primary factor influencing $\delta(^{13}\text{C})$ and $\delta(^{57}\text{Fe})$. The $\delta(^{57}\text{Fe})$ was found to be extremely sensitive to deformation of the porphyrin geometry, and increased shielding by more than 600 ppm with increased ruffling was observed for various heme models of known X-ray structures.

^{57}Fe NMR spectra of several carbonmonoxy hemoprotein models (Figure 1) with varying polar and steric effects of the distal organic superstructure, constraints of the proximal side, and porphyrin ruffling were reported [C.G. Kalodimos **I.P. Gerotheranassis***, E. Rose, G.E. Hawkes and R. Pierattelli, *J. Am. Chem. Soc.*, 121, 2903-2908 (1999)]. ^{57}Fe shieldings, $\delta(^{57}\text{Fe})$, vary by nearly 900 ppm among various hemes, and an excellent correlation was found between $\delta(^{57}\text{Fe})$ and the absolute crystallographic average displacement of the meso carbon atoms, $|C_m|$, relative to the porphyrin core mean plane (Figure 2). The great variation of $\delta(^{57}\text{Fe})$ as a function of $|C_m|$ (~ 140 ppm/0.1 Å) demonstrates that iron-57 shieldings can be used in structure refinement protocols for the extraction of more accurate structures for heme rings in heme model compounds. The excellent correlation between iron-57 shieldings and the average shieldings of the meso carbons of the porphyrin skeleton of TPP derivatives suggests that the two probes reflect similar types of electronic and structural perturbations, which are primarily due to porphyrin ruffling. The present findings also emphasize the value in predicting ^{57}Fe shieldings in superstructured metalloporphyrins from ^{13}C shieldings of the meso carbons.

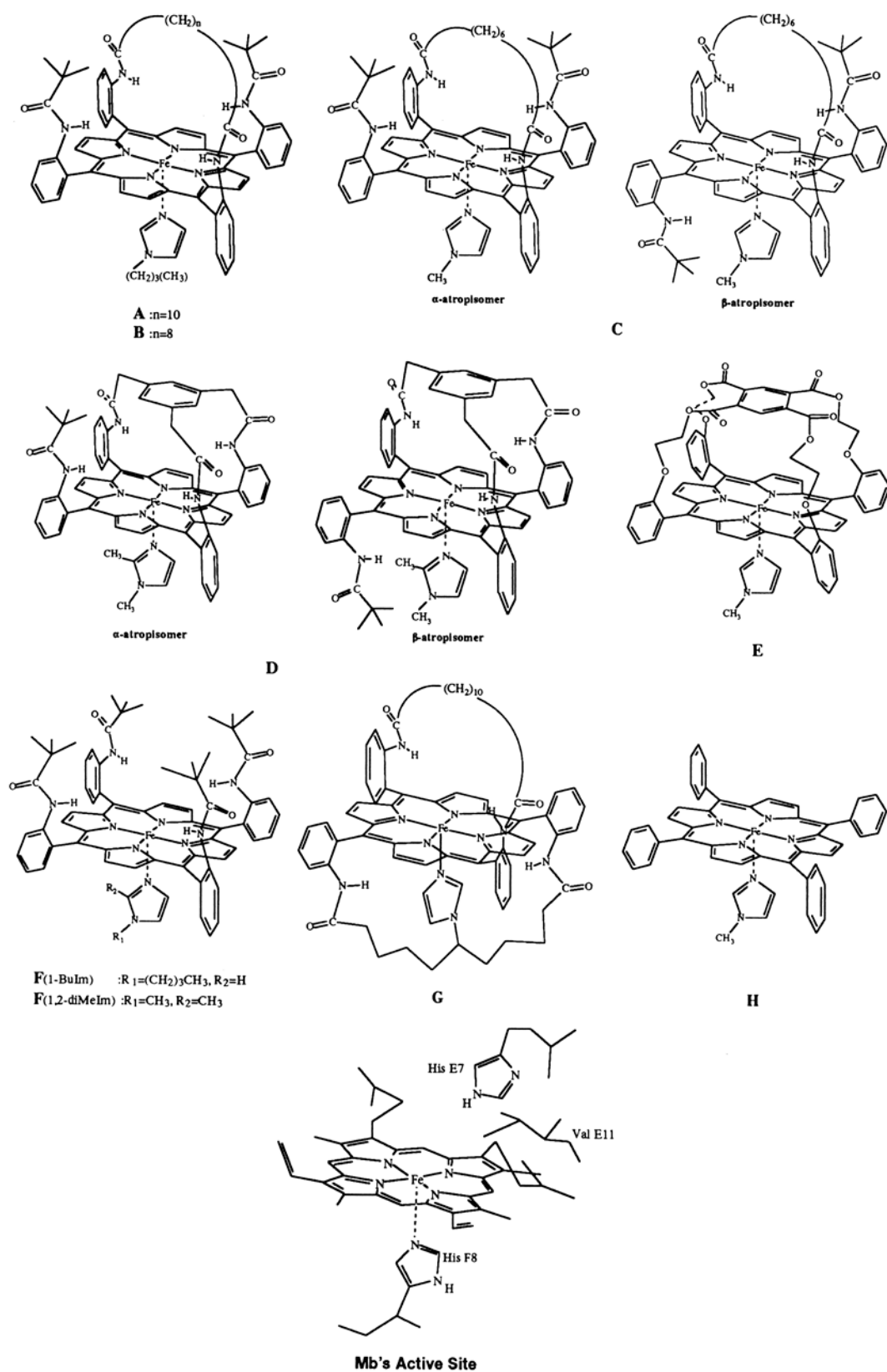


FIGURE 1. Schematic structures of the heme model compounds and the active site of (Mb) myoglobin studied by the use of ^{57}Fe NMR. [C.G. Kalodimos, I.P. Gerotheranassis*, E. Rose, G.E. Hawkes & R. Pierattelli, *J. Am. Chem. Soc.* 121, 2903-2908 (1999)].

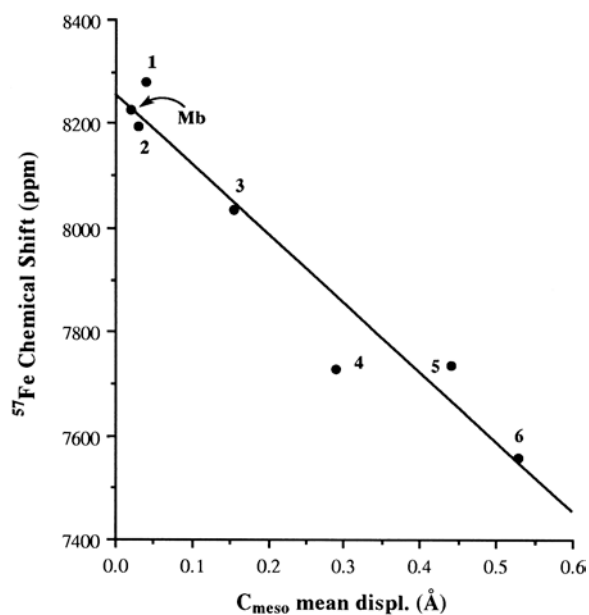


FIGURE 2. Plot of $\delta(^{57}\text{Fe})$ (ppm) vs $[C_m]$ (Å) for some of the heme model compounds of Figure 1 and Mb. Data points are as follow: 1, **E**; 2, **H**; 3, **A**; 4, **B**; 5, **C** α -atropisomer; 6, **D** β -atropisomer. [C.G. Kalodimos, **I.P. Gerothanassis***, E. Rose, G.E. Hawkes & R. Pierattelli, *J. Am. Chem. Soc.* 121, 2903-2908 (1992)] and Proteins.

Structural Investigation of Peptide Hormones and Proteins

^{14}N NMR studies [**I.P. Gerothanassis***, T. Karayannis, M. Sakarellos-Daitsiotis, C. Sakarellos and M. Marraud, *J. Magn. Reson.* 75, 513-516 (1987)] of the peptide hormone Leu-enkephalin in aqueous solution indicates the absence of head to tail intramolecular hydrogen bonding interaction between the terminal $^+\text{NH}_3$ and COO^- groups as revealed by the absence of linewidth variation upon protonation of the carboxyl group. If the amino terminal group in Leu-enkephalin became associated with the carboxyl terminal group through an intramolecular salt bridge bond, its motion (segmental and internal) would probably be restricted within the molecule. Therefore, it seems likely that the correlation time of the amino terminal group would increase by an amount related to the effective volume of the intramolecularly bonded molecule. On the other hand, an increase in the nuclear quadruple coupling constant due to partial loss of the near-tetrahedral symmetry around the nitrogen, would result in an additional line width broadening. However, the linewidths of the amino group of Leu-enkephalin in the cationic and zwitterionic state were found to be identical within experimental error (the solution viscosity was found to be independent of the pH). This result, along with the chemical shift data excludes, first, the participation of the amino terminal group in an intramolecular salt bridge bond with the carboxyl terminal group, in agreement with the ^{17}O results [T. Karayannis, **I.P. Gerothanassis***, M. Sakarellos-Daitsiotis, C. Sakarellos, M. Marraud, *Biopolymers*, 29, 423-439 (1990)] and second, the existence of conformationally dependent restrictions of its segmental and internal motions. Further ^1H – ^{15}N multiple – quantum NMR studies of Leu-enkephalin indicated that intramolecular hydrogen bonding interactions in aqueous solution between the NH and CO peptide groups should be excluded

[**I.P. Gerothanassis***, M. Bourdonneau, T. Karayannis, M. Sakarellos-Daitsiotis and C. Sakarellos, *J. Magn. Reson.* 80, 309-313 (1988)].

Angiotensin II (AII), the main effector octapeptide hormone of the rennin-angiotensin system exerts a variety of actions via specific receptors designated AT₁ and AT₂. For peptide ligand-receptor interactions there are two general approaches that can be utilized to extract structural information: a peptide (ligand)-based approach and a receptor-based approach. Structural characterization of the membrane-associated G-protein coupled receptors through which AII and most peptide hormones exert their biological activity is very difficult [W. Kuhlbrandt & E. Gouaux, *Curr. Opin. Struct. Biol.* 9, 445-447 (1999)]. In the free ligand (peptide)-based approach the key question is whether structural motifs of a flexible peptide ligand in solution can be retained during the early stages of receptor-peptide recognition processes. AII has been extensively investigated in solution during the last 40 years with a variety of techniques. The results have been interpreted in terms of various models such as an α -helix, β -turn, cross- β -forms II, γ -turn, random coil, side chain ring cluster etc. It is evident that several of the reported models are not consistent with each other and that there is no general consensus on the solution conformation of AII. The high-resolution 3D structure of the octapeptide hormone angiotensin II (AII) in aqueous solution has been obtained by simulated annealing calculations, using high-resolution NMR-derived restraints [A.G. Tzakos, A.M. Bonvin, A. Troganis, P. Cordopatis, M.L. Amzel, **I.P. Gerothanassis***, and N.A. van Nuland, *Eur. J. Biochem.* 270, 849-860 (2003)]. After final refinement in explicit water, a family of 13 structures was obtained with a backbone RMSD of 0.73 ± 0.23 Å. AII adopts a fairly compact folded structure, with its C-terminus and N-terminus approaching to within ≈ 7.2 Å of each other. The side chains of Arg2, Tyr4, Ile5 and His6 are oriented on one side of a plane defined by the peptide backbone, and the Val3 and Pro7 are pointing in opposite directions. The stabilization of the folded conformation can be explained by the stacking of the Val3 side chain with the Pro7 ring and by a hydrophobic cluster formed by the Tyr4, Ile5 and His6 side chains (Figure 3). Comparison between the NMR-derived structure of AII in aqueous solution and the refined crystal structure of the complex of AII with a high-affinity mAb (Fab131) [Garcia, K.C., Ronco, P.M., Verroust, P.J., Brunger, A.T., Amzel, L.M. *Science* 257, 502-507 (1992)] provides important quantitative information on two common structural features: (a) a U-shaped structure of the Tyr4-Ile5-His6-Pro7 sequence, which is the most immunogenic epitope of the peptide, with the Asp1 side chain oriented towards the interior of the turn approaching the C-terminus; (b) an Asx-turn-like motif with the side chain aspartate carboxyl group hydrogen-bonded to the main chain NH group of Arg2. It can be concluded that small rearrangements of the epitope 4-7 in the solution structure of AII are required by a mean value of 0.76 ± 0.03 Å for structure alignment and $\approx 1.27 \pm 0.02$ Å for sequence alignment with the X-ray structure of AII bound to the mAb Fab131 (Figure 3B). These data are interpreted in terms of a biological 'nucleus' conformation of the hormone in solution, which requires a limited number of structural rearrangements for receptor-antigen recognition and binding.

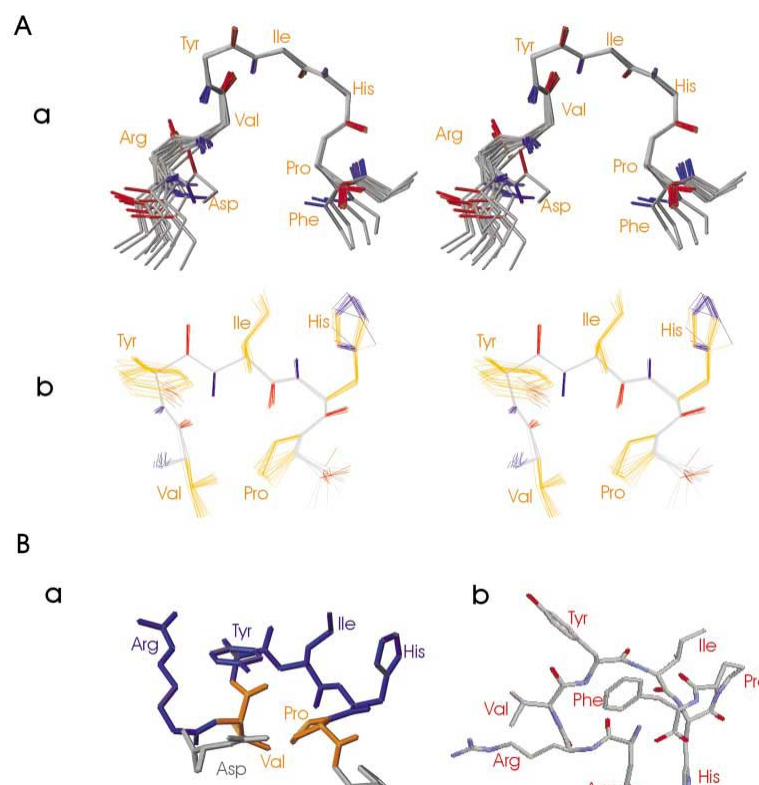


FIGURE 3. (A) Solution conformation of AII. (a) The 13 structures calculated for AII overlaid using the N, Ca and C α atoms of residues 3–7. (b) Superposition of the backbone and heavy atoms of the fragment 3–7 of AII. (B) Comparison of a representative conformer of AII with structure closest to the average co-ordinates (the blue colour denotes the side chains of Arg2, Tyr4, Ile5, His6 and the yellow the side chains of Val3 and Pro7) (a) with the the X-ray structure of AII in the Fab131–AII complex (b). [A.G. Tzakos, A.M. Bonvin, A. Troganis, P. Cordopatis, M.L. Amzel, **I.P. Gerotheranassis*** & N.A. van Nuland, *Eur. J. Biochem.* 270, 849-860 (2003)].

Human somatic angiotensin I-converting enzyme (sACE) has two active sites present in two sequence homologous protein domains (ACE_N and ACE_C) possessing several biochemical features that differentiate the two active sites (i.e. chloride ion activation. Based on the recently solved X-ray structure of testis angiotensin-converting enzyme (tACE), the 3D structure of ACE_N was modeled (A. Tzakos, S. Galanis, G. Spyroulias, P. Cordopatis, E. Zoupa, and **I.P. Gerotheranassis***, *Protein Engin.* 16, 993-1003 (2003)). Electrostatic potential calculations reveal that the ACE_N binding groove is significantly more positively charged than the ACE_C, which provides a first rationalization for their functional discrimination. The chloride ion pore for Cl2 (one of the two chloride ions revealed in the X-ray structure of tACE) that connects the external solution with the inner part of the protein was identified on the basis of an extended network of water molecules. Comparison of ACE_C with the X-ray structure of the prokaryotic ClC Cl⁻ channel from *Salmonella enterica* serovar typhimurium demonstrates a common molecular basis of anion selectivity. The critical role for Cl2 as an ionic switch is emphasized. Sequence and structural comparison between ACE_N and ACE_C and of other proteins of the gluzincin family highlights key residues that could be responsible for the peptide hydrolysis

mechanism. Currently available mutational and substrate hydrolysis data for both domains are evaluated and are consistent with the predicted model.

Angiotensin II (AII), Asp1-Arg2-Val3-Tyr4-Ile5-His6-Pro7-Phe8, the primary active hormone of the Renin- Angiotensin-System (RAS), is a major vasoconstrictor implicated in the cause of hypertension. To unravel the question of the biologically active conformation(s) of this flexible peptide hormone and to better understand the stereoelectronic requirements that lead to the molecular basis of hypertension, we analyzed research efforts in the identification of pharmacophoric groups of AII and three general approaches for structural characterisation: the free peptide - ligand approach, the receptor based approach, and approaches that target the peptide - receptor complex [A.G. Tzakos, A. Troganis and **I.P. Gerothanassis***, *Current Topics in Medicinal Chemistry*, 4, 431-444 (2004)]. The free peptide - ligand based approach can be further categorized to: (a) conformational analysis of AII and linear peptide analogues in aqueous solution; (b) the use of solvents of medium dielectric constants; (c) conformationally restricted analogues, with emphasis to cyclic analogues; (d) the use of receptor - simulating environments, and (e) non-peptide mimetics. The receptor and peptide - receptor based approaches can be categorised to: (a) The use of monoclonal antibodies and (b) the generic description of AII receptor sites through homology modelling and mutagenesis studies. These investigations, with particular emphasis to recent developments, have greatly assisted in the identification of pharmacophoric groups for receptor activation and the development of several models of AII - receptor complexes.

Somatic ACE (EC 3.4.15.1), a Zn^{II} metalloproteinase, is composed of functionally active N and C domains resulting from tandem gene duplication. Despite the high degree of sequence similarity between the two domains, they differ in substrate and inhibitor specificity and in their activation by chloride ions. Because of the critical role of ACE in cardiovascular and renal diseases, both domains are attractive targets for drug design. Putative structural models have been generated [A.G. Tzakos and **I.P. Gerothanassis***, *ChemBioChem*. 6, 1089-1103 (2005)] for the interactions of ACE inhibitors (lisinopril, captopril, enalaprilat, keto-ACE, ramiprilat, quinaprilat, peridoprilat, fosinoprilat, and RXP 407) with both the ACE_C and the ACE_N domains. Inhibitor-domain selectivity was interpreted in terms of residue alterations observed in the four subsites of the binding grooves of the ACE_C/ACE_N domains (S1: V516/N494, V518/T496, S2: F391/Y369, E403/R381, S1': D377/Q355, E162/D140, V379/S357, V380/T358, and S2': D463/E431, T282/S260). The interactions governing the ligand-receptor recognition process in the ACE_C domain are: a salt bridge between D377, E162, and the NH₂ group (P1' position), a hydrogen bond of the inhibitor with Q281, the presence of bulky hydrophobic groups in the P1 and P2' sites, and a stacking interaction of F391 with a benzyl group in the P2 position. In ACE_N these interactions are: hydrogen bonds of the inhibitor with E431, Y369, and R381, and a salt bridge between the carboxy group in the P2 position of the inhibitor and R500. The calculated complexes were evaluated for their consistency with structure-activity relationships and site-directed

mutagenesis data. A comparison between the calculated interaction free energies and the experimentally observed biological activities was also made. Pharmacophore refinement was achieved at an atomic level, and might provide an improved basis for structure-based rational design of second generation, domain-selective inhibitors.

Enzyme–inhibitor recognition is considered one of the most fundamental aspects in the area of drug discovery. However, the molecular mechanism of this recognition process (induced fit or prebinding and adaptive selection among multiple conformers) in several cases remains unexplored. In order to shed light toward this step of the recognition process in the case of human angiotensin I converting enzyme (hACE) and its inhibitor captopril, we have established a novel combinatorial approach exploiting solution NMR, flexible docking calculations, mutagenesis, and enzymatic studies. We have provided evidence [A.G. Tzakos, N. Naqvi, K. Comporozos, R. Pierattelli, V. Theodorou, A. Husain* and I.P. Gerothanassis*, *Bioorg. Med. Chem. Lett.*, 16, 5084-5087 (2006)] that an equimolar ratio of the *cis* and *trans* states of captopril exists in solution and that the enzyme selects only the *trans* state of the inhibitor that presents architectural and stereoelectronic complementarity with its substrate binding groove (Figure 4).

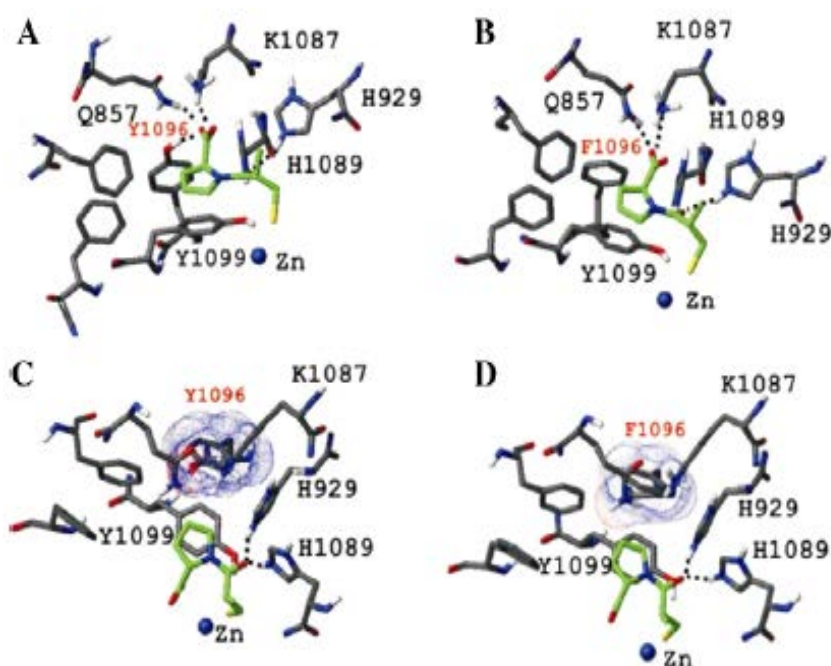


FIGURE 4. The binding of captopril *trans* conformation to the hACE (A) and Y 1096F mutant (B). The binding of captopril *cis* conformation to the hACE (C) and Y 1096F mutant (D). [A.G. Tzakos, N. Naqvi, K. Comporozos, R. Pierattelli, V. Theodorou, A. Husain* and I.P. Gerothanassis*, *Bioorg. Med. Chem. Lett.* 16, 5084-5087 (2008)].

Experimental autoimmune encephalomyelitis can be induced in susceptible animals by immunodominant determinants of myelin basic protein (MBP). To characterize the molecular features of antigenic sites important for designing experimental autoimmune encephalomyelitis suppressing

molecules, we reported structural studies [A.G. Tzakos, P. Fuchs, N.A.J. van Nuland, A. Troganis, T. Tselios, J. Matsoukas, **I.P. Gerothanassis*** and A.M.J. Bonvin, *Eur. J. Biochem.* 271, 3399-3413 (2004)], based on NMR experimental data in conjunction with molecular dynamic simulations, of the potent linear dodecapeptide epitope of guinea pig MBP, Gln74-Lys75-Ser76-Gln77-Arg78-Ser79-Gln80-Asp81-Glu82-Asn83-Pro84-Val85 [MBP(74–85)], and its antagonist analogue Ala81MBP(74–85). The two peptides were studied in both water and Me₂SO in order to mimic solvent-dependent structural changes in MBP. The agonist MBP(74–85) adopts a compact conformation because of electrostatic interactions of Arg78 with the side chains of Asp81 and Glu82. Arg78 is 'locked' in a well-defined conformation, perpendicular to the peptide backbone which is practically solvent independent. These electrostatic interactions are, however, absent from the antagonist Ala81MBP(74–85), resulting in great flexibility of the side chain of Arg78. Sequence alignment of the two analogues with several species of MBP suggests a critical role for the positively charged residue Arg78, firstly, in the stabilization of the local microdomains (epitopes) of the integral protein, and secondly, in a number of post-translational modifications relevant to multiple sclerosis, such as the conversion of charged arginine residues to uncharged citrullines. Flexible docking calculations on the binding of the MBP(74–85) antigen to the MHC class II receptor site I-A^u using HADDOCK indicate that Gln74, Ser76 and Ser79 are MHC II anchor residues. Lys75, Arg78 and Asp81 are prominent, solvent-exposed residues and, thus, may be of importance in the formation of the trimolecular T-cell receptor–MBP(74–85)–MHC II complex.

Multiple sclerosis (MS) is a chronic inflammatory disease of the central nervous system (CNS) characterized by demyelination and loss of neurological function, local macrophage infiltrate and neuroantigen-specific CD4⁺T cells. MS arises from complex interactions between genetic, immunological, infective and biochemical mechanisms. Although the circumstances of MS etiology remain hypothetical, one persistent theme involves immune system recognition of myelin-specific antigens derived from myelin basic protein, the most abundant extrinsic myelin membrane protein, and/or another equally suitable myelin protein or lipid. Knowledge of the biochemical and physico-chemical properties of myelin proteins and lipids, particularly their composition, organization, structure and accessibility with respect to the compacted myelin multilayers, becomes central to understanding how and why myelin-specific antigens become selected during the development of MS. This review [A.G. Tzakos, P. Kursula, A. Troganis, V. Theodorou, T. Tselios, C. Svarnas, J. Matsoukas, V. Apostolopoulos and **I.P. Gerothanassis**, *Current Med. Chem.* 12, 1569-1587 (2005)] focuses on the current understanding of the molecular basis of MS with emphasis: (i) on the physical-chemical properties, organization, morphology, and accessibility of the proteins and lipids within the myelin multilayers; (ii) on the structure-function relationships and characterization of the myelin proteins relevant to the manifestation and evolution of MS; (iii) on conformational relationships between myelin epitopes which might become selected during the development of MS; (iv) on the structure of

MHC/HLA in complex with MBP peptides as well as with TCR, which is crucial to the understanding of the pathogenesis of MS with the ultimate goal of designed antigen-specific treatments.

Human Sco2 is a mitochondrial membrane-bound protein involved in copper supply for the assembly of cytochrome c oxidase in eukaryotes. Its precise action is not yet understood. We reported [L. Banci, I. Bertini*, S. Ciofi – Baffoni, I.P. Gerotheranassis, I. Leontari, M. Martinelli and S. Wang, *Structure* 15, 1132-1140 (2007)] a structural and dynamic characterization by NMR of the apo and copper(I) forms of the soluble fragment. The structural and metal binding features of human Cu(I)Sco2 are similar to the more often studied Sco1 homolog, although the dynamic properties and the conformational disorder are quite different when the apo forms and the copper(I)-loaded forms of the two proteins are compared separately. Such differences are accounted for in terms of the different physicochemical properties in strategic protein locations. The misfunction of the known pathogenic mutations is discussed on the basis of the obtained structure.

C: NMR Analytical Applications of Complex Natural Extracts

(in bold is indicated the principal author)

- 1c. "Methodology for Identification of Phenolic Acids in Complex Phenolic Mixtures by High-Resolution Two- Dimensional Nuclear Magnetic Resonance. Application to Methanolic Extracts of Two Oregano Species "
I.P. Gerothanassis*, V. Exarchou, V. Lagouri, A. Troganis, M. Tsimidou and D. Boskou*, *J. Agric. Food Chem.* 46, 4185-4192 (1998). University of Ioannina.
- 2c. "Identification and Quantification of Caffeic and Rosmarinic Acid in Complex Plant Extracts by the Use of Variable-Temperature Two-Dimensional Nuclear Magnetic Resonance Spectroscopy".
 V. Exarchou, A. Troganis, **I.P. Gerothanassis***, M. Tsimidou and D. Boskou, *J. Agric. Food Chem.* 49, 2-8 (2001). University of Ioannina.
- 3c. "Towards a Consensus Structure of Hypericin in Solution: Direct Evidence for a single Tautomer and Different Ionization States in Protic and Nonprotic Solvents by the Use of Variable Temperature Gradient ^1H NMR".
 D. Skalkos*, E. Tatsis, **I.P. Gerothanassis*** and A. Troganis, *Tetrahedron*, 58, 4925-4929 (2002). University of Ioannina.
- 4c. "Antioxidant Activities and Phenolic Composition of Extracts from Greek Oregano, Greek Sage and Summer Savory"
 V. Exarchou, N. Nenadis, M. Tsimidou*, I.P. Gerothanassis, A. Troganis and D. Boskou, *J. Agric. Food Chem.*, 50, 5294-5299 (2002). University of Ioannina.
- 5c. "Do Strong Intramolecular Hydrogen Bonds Persist in Aqueous Solution? Variable Temperature Gradient ^1H , ^1H - ^{13}C GE-HSQC and GE-HMBC NMR Studies of Flavonols and Flavones in Organic and Aqueous Mixtures"
 V. Exarchou, A. Troganis, **I.P. Gerothanassis***, M. Tsimidou, and D. Boskou, *Tetrahedron*, 58, 7423-7429 (2002). University of Ioannina.
- 6c. "LC-UV-Solid Phase Extraction-NMR-MS Combined with a Cryogenic Flow Probe and its Application to the Identification of Compounds Present in Greek Oregano".
 V. Exarchou*, M. Godejohann, T.A. Van Beek, I.P. Gerothanassis and J. Vervoort, *Anal. Chem.* 75 6288-6294 (2003). University of Ioannina.
- 7c. "LC-NMR Coupling Technology: Recent Advancements and Applications in Natural Products Analysis".
 V. Exarchou*, M. Krucker, T. A. Van Beek, J. Vervoort, I. Gerothanassis and K. Albert, *Magn. Reson. Chem*, 43, 681-687 (2005) invited article. University of Ioannina.

- 8c. "Identification of the Major Constituents of *Hypericum Perforatum* by LC/SPE/NMR and/or LC/MS"
E.C. Tatsis, S. Boeren, V. Exarchou, A.N. Troganis, J. Vervoort and **I.P. Gerothanassis***, *Phytochemistry* 68 (2007) 383-393. University of Ioannina.
- 9c. "NMR Studies of Antioxidant Plant Phenols: Basic Parameters and Methodologies".
V. Exarchou and I.P. Gerothanassis, *Natural Antioxidant Phenols. Sources, Structure – Activity Relationship, Current Trends in Analysis and Characterisation*. Boskou, D., Gerothanassis, I.P. Kefalas, P. (Eds.). Research Signpost: Kerala, India, 2006, Chapter 5. p. 125-142. University of Ioannina.
- 10c. "Hyphenated Liquid Chromatography / Nuclear Magnetic Resonance Techniques".
V. Exarchou, I.P. Gerothanassis, J. Vervoort and T.A. van Beek, *Natural Antioxidant Phenols. Sources, Structure – Activity Relationship, Current Trends in Analysis and Characterisation*. Boskou, D., Gerothanassis, I.P. Kefalas, P. (Eds.). Research Signpost: Kerala, India, 2006, Chapter 6. p.143-156. University of Ioannina.
- 11c. "¹H-NMR Determination of Hypericin and Pseudohypericin in Complex Natural Mixtures by the Use of Strongly Deshielded OH Groups"
E. Tatsis, V. Exarchou, A. Troganis and **I.P. Gerothanassis***, *Anal. Chim. Acta*, 607, 219-226 (2008). University of Ioannina.
- 12c. "Phytochemicals in Olive- Leaf Extracts and their Antiproliferative Activity against Cancer and Endothelial Cells"
V. Goulas, V. Exarchou, A. N. Troganis, E. Psomiadou, T. Fotsis, E. Briasoulis and **I.P. Gerothanassis***, *Mol. Nutr. & Food Res.* 53, 600-608 (2009). University of Ioannina.
- 13c. "Rapid and Novel Discrimination and Quantification of Oleanolic and Ursolic Acids in Complex Plant Extracts using Two-Dimensional Nuclear Magnetic Resonance Spectroscopy-Comparison with HPLC Methods"
V.G. Kontogianni, V. Exarchou, A. Troganis and I.P. Gerothanassis*, *Anal.Chim. Acta* 635, 188-195 (2009). University of Ioannina.
- 14c. "Contribution of Flavonoids to the Overall Radical Scavenging Activity of Olive (*Olea Europea* L.) Leaf Polar Extracts".
V. Goulas, V.T. Papoti, V. Exarchou, M.Z. Tsimidou* and **I.P. Gerothanassis*** *J. Agric. Food Chem.* 6, 3303-3308 (2010). University of Ioannina.
- 15c. "Exploring the "Forgotten"- OH NMR Spectral Region in Natural Products".
P. Charisiadis, V. Exarchou, A.N. Troganis and **I.P. Gerothanassis***, *Chem.Commun.* (2010) 46 (2010) 3589-3591. University of Ioannina.

NMR ANALYTICAL APPLICATIONS OF COMPLEX NATURAL EXTRACTS

(in bold is indicated the principal author)

Spectroscopic methodology in analyzing two-dimensional (2D) NMR spectra of a mixture of several phenolic compounds that occur in natural products was described (**I.P. Gerothanassis***, V. Exarchou, V. Lagouri, A. Troganis, M. Tsimidou and D. Boskou*, *J. Agric. Food Chem.* 46, 4185-4192 (1998)). Particular emphasis has been given to the determination of scalar coupling connectivities by homonuclear 2D correlated spectroscopy (COSY), remote intraresidue connectivities by totally correlated spectroscopy (TOCSY), and spatially close but uncoupled ^1H nuclei by homonuclear 2D nuclear Overhauser effect spectroscopy (NOESY/ROESY). Preliminary data to identify phenolic acids in the methanolic extracts from two oregano plants are also reported.

A combination of advanced nuclear magnetic resonance (NMR) methodologies for the analysis of complex phenolic mixtures that occur in natural products was described (V. Exarchou, A. Troganis, **I.P. Gerothanassis***, M. Tsimidou and D. Boskou, *J. Agric. Food Chem.* 49, 2-8 (2001)), with particular emphasis on caffeic acid and its ester derivative, rosmarinic acid. The combination of variable-temperature two-dimensional proton-proton double quantum filter correlation spectroscopy (^1H - ^1H DQF COSY) and proton-carbon heteronuclear multiple quantum coherence (^1H - ^{13}C HMQC) gradient NMR spectroscopy allows the identification and tentative quantification of caffeic and rosmarinic acids at 243 K in extracts from plants of the Lamiaceae family, without resorting to previous chromatographic separation of the components. The use of proton-carbon heteronuclear multiple bond correlation (^1H - ^{13}C HMBC) gradient NMR spectroscopy leads to the complete assignment of the correlations of the spins of H_{2a} and H_{3a} with the ester and carboxyl carbons of rosmarinic and caffeic acid, even at room temperature, and confirms the results of the above methodology. Quantitative results are in reasonable agreement with reverse phase HPLC measurements. The ^1H - ^{13}C HMBC gradient NMR experiment provides significant resolution and structural information compared to the ^1H - ^{13}C HMQC. The principal limitation of the technique is imposed by the low natural abundance of ^{13}C and long mixing times which limit the observable signal-to-noise ratio. Furthermore, the HMBC method is more difficult to obtain on a routine basis and integration data are less reliable, compared to ^1H - ^{13}C HMQC, due to the significant variation and conformational dependence of the $^2\text{J}(^{13}\text{C}\text{-}^1\text{H})$ and $^3\text{J}(^{13}\text{C}\text{-}^1\text{H})$ couplings.

Hypericin, a meso-naphthodianthrone derivative, which is abundant in extracts of *Hypericum perforatum* displays two types of electronic spectra in organic solvents, which were attributed to the existence of two tautomeric structures. Variable temperature gradient ^1H NMR studies demonstrated [D. Skalkos*, E. Tatsis, **I.P. Gerothanassis*** and A. Troganis, *Tetrahedron*, 58, 4925-4929 (2002)] the occurrence of only one 7,14-dioxo tautomeric form, for the molecule of hypericin in protic and in nonprotic solvents, differing only in the degree of ionization of the 4-hydroxyl group in the bay region. Recording variable temperature gradient ^1H NMR spectra of hypericin at various temperatures (215-

295K) in acetone- d_6 , and at 215-295 K in MeOH- d_3 , the authors were able to unequivocally assign the acidic form of hypericin, existing in nonprotic solvents, to the neutral 7,14-diketo structure ($Q^{7,14}$, HyH), and the stable form, existing in protic solvents, to its anionic analog 7,14-diketo structure ($Q^{7,14}$, Hy $^-$). The existence of one single structure in both types of solvents, is also supported by the fact that the positions of the other groups in the aromatic skeleton of hypericin remain the same in both solvents. The singlets at 14.1 and 14.7 ppm, corresponding to the four hydroxyl groups, were recorded at the same position in both solvents, even at low temperatures. This means that the hydroxyl groups remain attached to the same carbons (at the 8,13 and 1,5 positions), regardless of the solvent in which the molecules dissolved. This conclusion might result in a consensus structure of hypericin in solution.

Oregano vulgare L. ssp. *hirtum* (Greek oregano), *Salvia fruticosa* (Greek sage), and *Satureja hortensis* (summer savory) were examined as potential sources of phenolic antioxidant compounds [V. Exarchou, N. Nenadis, M. Tsimidou*, I.P. Gerotheranassis, A. Troganis and D. Boskou, *J. Agric. Food Chem.* 50, 5294-5299 (2002)]. The antioxidant capacities (antiradical activity by DPPH $^{\bullet}$ test, phosphatidylcholine liposome oxidation, Rancimat test) and total phenol content were determined in the ethanol and acetone extracts of the dried material obtained from the botanically characterized plants. The ground material was also tested by the Rancimat test for its effect on the stability of sunflower oil. The data indicated that ground material and both ethanol and acetone extracts had antioxidant activity. Chromatographic (TLC, RP-HPLC) and NMR procedures were employed to cross-validate the presence of antioxidants in ethanol and acetone extracts. The major component of all ethanol extracts was rosmarinic acid as determined by RP-HPLC and NMR. Chromatography indicated the presence of other phenolic antioxidants, mainly found in the acetone extracts. The presence of the flavones luteolin and apigenin and the flavonol quercetin was confirmed in the majority of the extracts by the use of a novel 1H NMR procedure, which is based on the strongly deshielded OH protons in the region of 12–13 ppm without previous chromatographic separation. This significant deshielding effect may be attributed to the strong intramolecular six-membered ring hydrogen bond of the OH(5)···CO(4) moiety.

Intramolecular hydrogen bonds in crystals and in apolar media are well documented, however, the degree to which they persist in aqueous solution is controversial. We reported [V. Exarchou, A. Troganis, I.P. Gerotheranassis*, M. Tsimidou, and D. Boskou, *Tetrahedron*, 58, 7423-7429 (2002)] variable temperature gradient 1H , 1H - ^{13}C Gradient Enhanced Heteronuclear Single Quantum Correlation (GE-HSQC) and Gradient Enhanced Heteronuclear Multiple Bond Coherence (GE-HMBC) NMR studies of the abundant in extracts of natural products, flavonols quercetin and kaempferol and the flavone luteolin, in organic solvents and in mixtures of organic–aqueous solutions. It was demonstrated, for the first time, that the strong intramolecular hydrogen bond of the –CO(4) and –OH(5) moieties persists over a wide range of aqueous mixtures and, thus, provided a rare example of non-charged intramolecular hydrogen bonds, which is not overwhelmed by solvation with protic solvents, in particular in aqueous solution. The 1H NMR spectra of quercetin were recorded in mixtures

of water and acetone- d_6 in molar ratios of: (a) 0, (b) 82, (c) 88 and (d) 91% in water. With a progressive increase in water content, the highly deshielded signal at 12.3 ppm commences to broaden at room temperature. Connaturally, similar results were observed for luteolin and kaempferol. Interestingly, the OH (5) resonance of e.g. quercetin is only slightly deshielded, by about ~ 0.2 ppm, upon the addition of water. The persistence of the $-\text{CO}(4)$ and $-\text{OH}(5)$ intramolecular hydrogen bond of quercetin in solution was also investigated in water- CD_3OH mixtures with molar ratios of: (a) 0, (b) 62, and (c) 71% in water. The intramolecular hydrogen bond clearly persists up to a molar ratio of 71% in water (increasing the molar ratio of water results to an extensive broadening of OH(5) resonance and precipitation of the compound). From the above it is evident that the strong intramolecular hydrogen bond in the CO(4) and OH(5) moiety of flavonoids occurs in organic non-protic and proton solvents and in a wide range of water-acetone- d_6 and water CD_3OH solutions. The strength of this intramolecular hydrogen bond may be attributed to the greater resonance stabilization, due to the formation of a six-membered ring. A further stabilizing factor may be due to entropy reasons.

Structure elucidation of natural products usually relies on a combination of NMR spectroscopy with mass spectrometry whereby NMR trails MS in terms of the minimum sample amount required. In this study [V. Exarchou*, M. Godejohann, T.A. Van Beek, I.P. Gerotheranassis and J. Vervoort, *Anal. Chem.* 75, 6288-6294 (2003)], the usefulness of on-line solid-phase extraction (SPE) in LC-NMR for peak storage after the LC separation prior to NMR analysis is demonstrated. The SPE unit allows the use of normal protonated solvents for the LC separation and fully deuterated solvents for flushing the trapped compounds to the NMR probe. Thus, solvent suppression is no longer necessary. Multiple trapping of the same analyte from repeated LC injections was utilized to solve the problem of low concentration and to obtain 2D heteronuclear NMR spectra. In addition, a combination of the SPE unit with a recently developed cryoflow NMR probe and an MS was evaluated. This on-line LC-UV-SPE-NMR-MS system was used for the automated analysis of a Greek oregano extract. Combining the data provided by the UV, MS, and NMR spectra, the flavonoids taxifolin, aromadendrin, eriodictyol, naringenin, and apigenin, the phenolic acid rosmarinic acid, and the monoterpene carvacrol were identified. This automated technique is very useful for natural product analysis, and the large sensitivity improvement leads to significantly reduced NMR acquisition times.

An overview of recent advances in nuclear magnetic resonance (NMR) coupled with separation technologies and their application in natural product analysis was discussed [V. Exarchou*, M. Krucker, T. A. Van Beek, J. Vervoort, I. Gerotheranassis and K. Albert, *Magn. Reson. Chem.*, 43, 681-687 (2005)]. The different modes of LC-NMR operation were described, as well as how technical improvements assist in establishing LC-NMR as an important tool in the analysis of plant-derived compounds. On-flow, stopped-flow and loop-storage procedures were mentioned, together with the new LC-SPE-NMR configuration. The implementation of mass spectrometry in LC-NMR is also useful on account of the molecular weight and fragmentation information that it provides, especially when new

plant species are studied. Cryogenic technology and capillary LC-NMR are the other important recent developments. Since the plant kingdom is endless in producing potential drug candidates, development and optimization of LC-NMR techniques convert the study of natural products to a less-time-consuming task, speeding up identification.

The newly established hyphenated instrumentation of LC/DAD/SPE/NMR and LC/UV/(ESI)MS techniques have been applied for separation and structure verification of the major known constituents present in Greek *Hypericum perforatum* extracts [E.C. Tatsis, S. Boeren, V. Exarchou, A.N. Troganis, J. Vervoort and **I.P. Gerothanassis***, *Phytochemistry* 68, 383-393 (2007)]. The chromatographic separation was performed on a C18 column. Acetonitrile-water was used as a mobile phase. For the on-line NMR detection, the analytes eluted from column were trapped one by one onto separate SPE cartridges, and hereafter transported into the NMR flow-cell. LC/DAD/SPE/NMR and LC/UV/MS allowed the characterization of constituents of Greek *H. perforatum*, mainly naphthodianthrones (hypericin, pseudohypericin, protohypericin, protopseudohypericin), phloroglucinols (hyperforin, adhyperforin), flavonoids (quercetin, quercitrin, isoquercitrin, hyperoside, astilbin, miquelianin, I3,II8-biapigenin) and phenolic acids (chlorogenic acid, 3-O-coumaroylquinic acid). Two phloroglucinols (hyperfirin and adhyperfirin) were detected for the first time, which have been previously reported to be precursors in the biosynthesis of hyperforin and adhyperforin.

NMR methodologies are discussed (Exarchou, V., Gerothanassis, I.P.) in natural antioxidant phenols: sources, structure-activity relationship, current trends in analysis and characterization (Eds. Boskou, D., Gerothanassis, I.P. Kefalas, P.) that have been successfully applied for the characterization of phenolic antioxidants, such as phenolic acids and flavonoids in plant extracts, without any previous separation and isolation of the individual components. Particular emphasis has been given to two-dimensional (2D) NMR spectra of a mixture of several phenolic compounds, especially to the determination of scalar coupling connectivities by homonuclear 2D correlated spectroscopy (COSY), remote intraresidue connectivities by totally correlated spectroscopy (TOCSY), and spatially close but uncoupled ^1H nuclei by homonuclear 2D nuclear Overhauser effect spectroscopy (NOESY). In addition, the combination of the temperature dependence of the proton chemical shifts and proton-carbon heteronuclear multiple quantum coherence (^1H - ^{13}C HMQC) gradient NMR spectroscopy, which allows the identification of closely related compounds (caffeic acid and its ester, rosmarinic acid) is described. The differentiation of flavonols and flavones with proton NMR spectroscopy, based on the strongly deshielded OH protons in the region of 12-13 ppm, which provides a useful tool in the analysis of phenol antioxidants, was also discussed.

An overview was presented (Exarchou, V., Gerothanassis, I. P., Vervoort, J., Beek, T. A. van in Natural antioxidant phenols: sources, structure-activity relationship, current trends in analysis and characterization (Eds. Boskou, D., Gerothanassis, I.P. Kefalas, P.) of liquid chromatography/nuclear magnetic resonance spectroscopy and the different working modes that the commercially available

instruments can provide for plant extract analysis. LC/NMR methods have rapidly developed over the last decade and technical advancements in flow-probe design and LC/NMR interfaces supported and extended the hyphenation. On-flow, stopped-flow and loop-storage procedures were described, together with the new LC/SPE/NMR configuration. The advantages of each working mode and selected applications in the analysis of complex mixture were discussed.

The ^1H NMR spectra of the commercially available compounds hypericin and its derivative pseudohypericin in CD_3OH solutions indicate significantly deshielded signals in the region of 14–15 ppm. These resonances were attributed to the *peri* hydroxyl protons OH(6), OH(8) and OH(1), OH(13) of hypericins which participate in a strong six-membered ring intramolecular hydrogen bond with CO(7) and CO(14), respectively, and therefore, they are strongly deshielded. In this work [E. Tatsis, V. Exarchou, A. Troganis and **I.P. Gerotheranassis***, *Anal. Chim. Acta*, 607, 219-226 (2008)], we demonstrated for the first time that one-dimensional ^1H NMR spectra of hypericin and pseudohypericin, in *Hypericum perforatum* extracts show important differences in the chemical shifts of the hydroxyl groups with excellent resolution in the region of 14–15 ppm (Figure 1). The facile identification and quantification of hypericin and its derivative compound pseudohypericin was achieved, without prior HPLC separation, for two *H. perforatum* extracts from Greek cultivars and two commercial extracts: a dietary supplement, and an antidepressant medicine. The results were compared with those obtained from UV – Vis and LC/MS measurements. It should be emphasized that the low concentration of hypericins, in contrast with other secondary metabolites of *Hypericum* crude extracts, impedes the identification based on the resonance signals of the aromatic protons (Table 1). The quantitative content of hypericin and pseudohypericin in crude extracts was determined by comparing the relative integrals of the signal of the *peri* hydroxyl protons and the signal of the reference compound, sodium salt of partially deuterated 3-trimethylsilylpropionic acid ($\delta=0.00$ ppm). Linear responses were observed over the range of 0.008-0.088 mM for hypericin and 0.009-0.082 mM for pseudohypericin. The limits of detection (for $S/N=3$) were visually found to be 2.8 μM for hypericin and 3.2 μM for pseudohypericin. The broader resonances of the hydroxyl protons in commercial preparation compared to that of the *Hypericum* extracts (Figure 1(D)), could be attributed to the presence of excipients, calcium and magnesium salts which enhance the ^1H exchange rate.

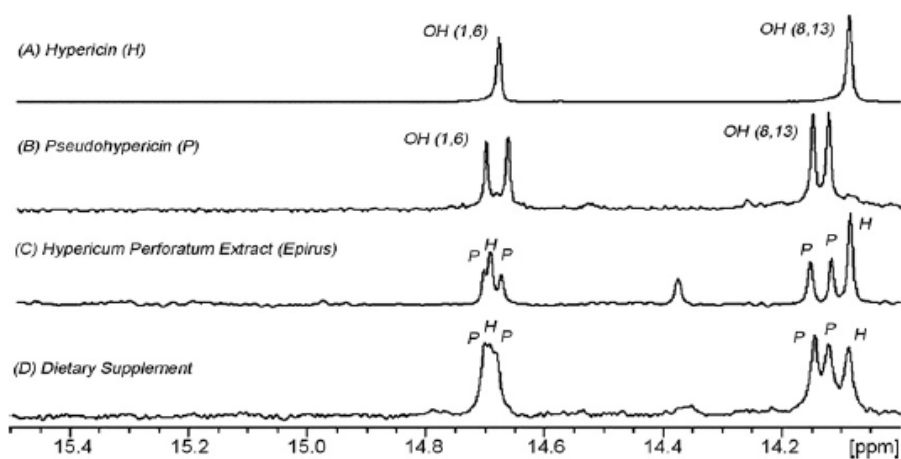


FIGURE 1. Selected region of 400 MHz ^1H NMR spectra of (A) hypericin; (B) pseudohypericin; (C) *Hypericum perforatum* extract with plant material from Epirus and (D) dietary supplement. Number of scans: 1024, acquisition time: 1.02 s, total experimental time: 102.7 min. P and H denote pseudohypericin and hypericin, respectively. [E. Tatsis, V. Exarchou, A. Troganis, & I.P. Gerotheranassis*, *Anal. Chim Acta* 607, 219-226 (2008)].

TABLE 1 – Quantitative evaluation of content of *Hypericum perforatum* extracts by the use of ^1H NMR spectroscopy and UV-vis spectroscopy (results obtained from three measurements [E. Tatsis, V. Exarchou, A. Troganis, & I.P. Gerotheranassis*, *Anal. Chim Acta* 607, 219-226 (2008)])

Sample plant extract	^1H NMR hypericin content (mg/100mg) ^a	^1H NMR pseudohypericin content (mg/100 mg) ^a	^1H NMR total hypericins content (mg/100mg) ^a	UV-vis total hypericins content (mg/100 mg) ^a
Epirus	2.71 ± 0.17	2.32 ± 0.13	5.03 ± 0.18	5.58 ± 0.09
Thrace	2.09 ± 0.15	2.83 ± 0.14	4.91 ± 0.16	4.79 ± 0.07
Dietary supplement	0.10 ± 0.02	0.22 ± 0.03	0.32 ± 0.03	0.24 ± 0.01
Antidepressant medicine	0.03 ± 0.01	0.09 ± 0.01	0.12 ± 0.01	0.16 ± 0.01

^a Mean values of three replicates ± standard deviation in 100 mg of dry extract or in 100 mg of commercial extract.

Olive oil compounds is a dynamic research area because Mediterranean diet has been shown to protect against cardiovascular disease and cancer. Olive leaves, an easily available natural material of low cost, share possibly a similar wealth of health benefiting bioactive phytochemicals. In this work [V. Goulas, V. Exarchou, A. N. Troganis, E. Psomiadou, T. Fotsis, E. Briasoulis and I.P. Gerotheranassis*, *Mol. Nutr. & Food Res.* 53, 600-608 (2009)], we investigated the antioxidant potency and antiproliferative activity against cancer and endothelial cells of water and methanol olive leaves extracts and analyzed their content in phytochemicals using LC-MS and LC-UV-SPE-NMR hyphenated techniques. Olive-leaf crude extracts were found to inhibit cell proliferation of human breast adenocarcinoma (MCF-7), human urinary bladder carcinoma (T-24) and bovine brain capillary endothelial (BBCE). The dominant compound of the extracts was oleuropein; phenols and flavonoids were also identified. These phytochemicals demonstrated strong antioxidant potency and inhibited cancer and endothelial cell proliferation at low micromolar concentrations, which is significant considering their high abundance in fruits and vegetables. The antiproliferative activity of crude extracts and phytochemicals against the cell lines used in this study was demonstrated for the first time.

A novel strategy for NMR analysis of mixtures of oleanolic (OA) and ursolic (UA) acids that occur in natural products was described [V.G. Kontogianni, V. Exarchou, A. Troganis and **I.P. Gerotheranassis***, *Anal.Chim. Acta* 635, 188-195 (2009)]. These important phytochemicals have similar structure and they are position isomers of the methyl group on the ring E. These two triterpenes may occur as free acids as aglycones of saponins. Both OA and UA are of interest as therapeutics and their antioxidant, anti-inflammatory and antitumour activities are rather well documented. Common procedures such as gas chromatography, including the necessary silylation or methylation step, liquid chromatography coupled with UV and MS spectroscopy have been used for the analysis of OA and UA. These analytes have weak chromophores, low UV absorption and the resolution by LC seems difficult on reversed phase. We reported that the combined use of proton–carbon heteronuclear single-quantum coherence (^1H – ^{13}C HSQC) and proton–carbon heteronuclear multiple-bond correlation (^1H – ^{13}C HMBC) NMR spectroscopy, might result in the identification and quantitation of oleanolic acid (OA) and ursolic acid (UA) in plant extracts of the Lamiaceae and Oleaceae family (Figure 2). The combination of ^1H – ^{13}C HSQC and ^1H – ^{13}C HMBC techniques allows the connection of the proton and carbon-13 spins across the molecular backbone resulting in the identification and, thus, discrimination of oleanolic and ursolic acid without resorting to physicochemical separation of the components. The quantitative results (Table 2) provided by 2D ^1H – ^{13}C HSQC NMR data were obtained within a short period of time (~14 min) and are in excellent agreement with those obtained by HPLC, which support the efficiency of the suggested methodology. The method, therefore, is rapid and with very promising results. Since the analysis and individual structure determination of OA and UA with the conventional chromatographic separation is problematic, the proposed method can be applied in mixtures avoiding any pre-treatment step and for rapid quality control of plant extracts.

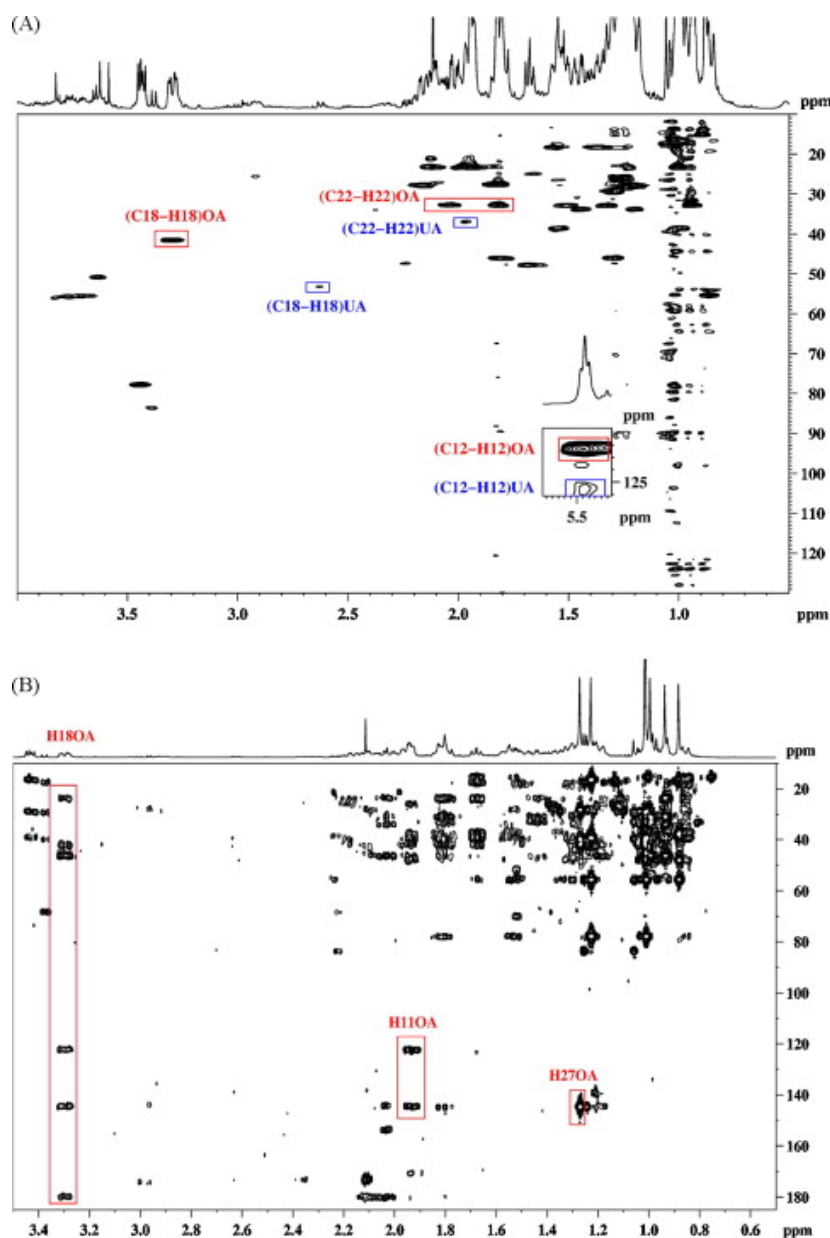


FIGURE 2. (A) 500MHz ^1H - ^{13}C HSQC spectrum of the ethyl acetate of olive leaves (ns=2, experimental time=14min); (B) the corresponding ^1H - ^{13}C HMBC spectrum (ns=16, mixing time=50ms, experimental time=1h). The cross-peaks of diagnostic importance are indicated [V.G. Kontogianni, V. Exarchou, A. Troganis & I.P. Gerotheranassis*, *Anal. Chim. Acta*, 635, 188-195 (2009)]

TABLE 2 ^1H and ^{13}C NMR chemical shifts (δ , ppm) of oleanolic and ursolic acid NMR signals and their long range connectivities that were utilized for their identification. [V.G. Kontogianni, V. Exarchou, A. Troganis & I.P. Gerotheranassis*, *Anal. Chim. Acta*, 635, 188-195 (2009)]

Oleanolic acid			Ursolic acid				
C	δ C	δ H	Long range connectivities		δ C	δ H	Long range connectivities
11		1.93	C12 (122.7), C13 (145.0)			1.93	C12 (125.8), C13 (139.4)
12	122.7	5.47			125.8	5.46	
15						2.31	C27 (24.2), C8 (40.2)
18	42.2	3.33	C16 (24.0), C14 (42.3), C19 (46.7), C17 (46.9), C12 (122.7), C13 (145.0), C28 (180.4)		53.8	2.62	C29 (17.7), C16 (25.2), C20 (39.6), C19 (39.7), C14 (42.7), C17 (48.3), C12 (125.8), C13 (139.4), C28 (180.3)
22	33.5	1.83			37.5	1.93	
27		1.25	C13 (145.0)			1.22	C13 (139.4)

The contribution of flavonoids to the overall radical scavenging activity of olive leaf polar extracts, known to be good sources of oleuropein related compounds, was examined [V. Goulas, V.T. Papoti, V. Exarchou, M.Z. Tsimidou* and **I.P. Gerotheranassis*** *J. Agric. Food Chem.* 6, 3303-3308 (2010)]. Off line and on line HPLC-DPPH' assays were employed, whereas flavonoid content was estimated colorimetrically. Individual flavonoid composition was first assessed by RP-HPLC coupled with diode array and fluorescence detectors and verified by LC-MS detection system. Olive leaf was found a robust source of flavonoids regardless sampling parameters (olive cultivar, leaf age or sampling date). Total flavonoids accounted for the 13–27% of the total radical scavenging activity assessed using the on line protocol. Luteolin 7-O-glucoside was one of the dominant scavengers (8–25%). Taking into consideration frequency of appearance the contribution of luteolin (3–13%) was considered important, too. Our findings support that olive leaf, except for oleuropein and related compounds, is also a stable source of bioactive flavonoids.

Among the most important and frequently encountered functional groups in natural products are the phenol type –OH groups. However, the ^1H NMR resonances of the –OH groups appear at room temperature as broad signals usually due to exchange of the –OH protons with protons of the protic solvents or with protons of the residual H_2O in aprotic and in protic solvents. In this communication [P. Charisiadis, V. Exarchou, A.N. Troganis and **I.P. Gerotheranassis***, *Chem. Commun.* 46, 3589-3591 (2010)] a simple NMR procedure was presented for the observation of the “forgotten” –OH NMR region in dilute acidified DMSO-d_6 solutions with significantly enhanced resolution due to elimination of fast intermolecular proton exchange. Furthermore, it was demonstrated that the significantly enriched resolution in the –OH NMR spectral region, in combination with 2D $^1\text{H} - ^{13}\text{C}$ HMBC techniques, will open new avenues in structure analysis of natural products with phenol type –OH groups in complex natural extracts without the need of laborious isolation of the individual compounds (Figure 3).

The experimental protocol for –OH resonance assignment has as follows:

- (i) Adjustment of pH values for a minimum in the –OH proton exchange rate.
- (ii) Recording of the ^1H - ^{13}C HMBC experiment optimized for $^n\text{J}(^1\text{H}, ^{13}\text{C})$ couplings in the range of 6 to 10 Hz.
- (iii) Recording of the ^1H - ^{13}C HMBC experiment optimized for weak $^5\text{J}(^1\text{H}, ^{13}\text{C})$ couplings ≤ 2.5 Hz.
- (iv) In the case of broad –OH resonance absorptions the experiments are repeated by the use of dilute solutions ($\leq 5\text{mg}$) of crude extract of natural product to minimize intermolecular proton exchange between various –OH groups and –OH and –COOH groups.

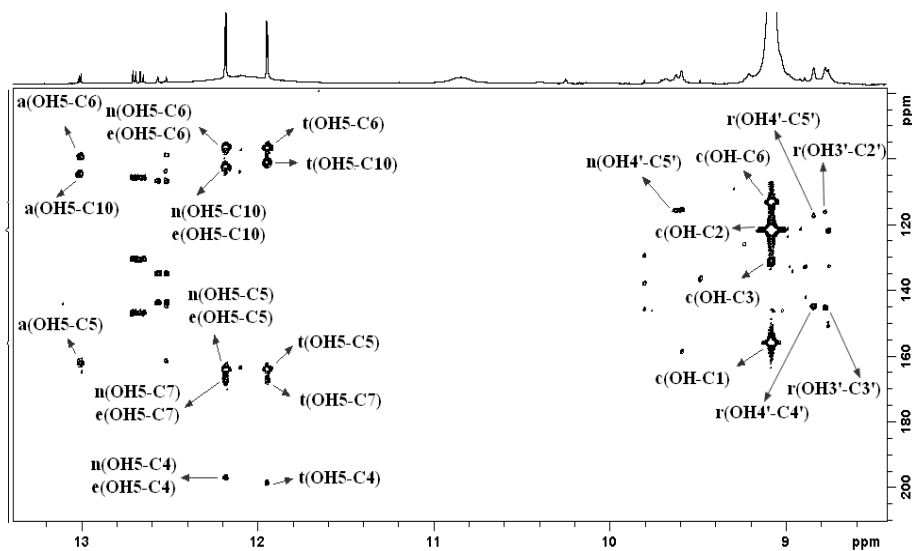


FIGURE 3. 2D ^1H - ^{13}C HMBC NMR spectrum (500MHz for ^1H) of 80 mg of acetone extract of Greek oregano in DMSO-d_6 ($T=298\text{ K}$, number of scans =72, experimental time =14h10min). The cross peaks of $-\text{OH}$ groups of apigenin (a), naringenin (n), rosmarinic acid (r), eriodictyol (e), taxifolin (t) and carvacrol (c) are indicated [P. Charisiadis, V. Exarchou, A.N. Troganis and I.P. Gerothanassis*, *Chem. Commun.* 46, 3589-3591 (2010)].